Slope Stability Evaluation of an Old Earth Fill Dam

Founded on Glaciolacustrine Clays

by

Moises Alfaro III

A Thesis submitted to the Faculty of Graduate Studies of

The University of Manitoba

In partial fulfillment of the requirements of the degree of

Master of Science

Department of Civil Engineering

University of Manitoba

Winnipeg, Manitoba

Disclaimer

1- Assumptions; analyses; and results are solely based on the author's interpretation of preliminary site investigation and laboratory testing and may not represent the existing conditions or performance of the earth fill dam being studied.

2- Conclusions are solely of the author's opinion.

3- The outcomes of this study may not be conclusive as more research is being done in that regard.

Abstract

A number of earth dams in Canada are founded on and constructed with glaciolacustrine clay deposits. This type of soil can have stability issues particularly in aging dams. Environmental loading such as wetting-drying and freezing-thawing produce fissures and can cause degradation in shear strength with time. This thesis provides an opportunity to assess the stability of an aging earth fill dam.

The author's research focused on a typical earth fill dam in Ontario. A comprehensive field investigation was conducted. Cone Penetration Test (CPTu) was carried out to determine the in-situ strength of the local materials. Shelby tubes with diameter of 102 mm and 76 mm were used to retrieve soil samples from the clay foundation, clay core and placed clay blanket. Structural and mineralogical components of the clay were examined by means of Scanning Electron Microscopy (SEM) and X-Ray Diffraction (XRD) test, respectively. A series of laboratory tests such as consolidated-undrained compression tests, direct shear tests, and 1D consolidation tests were carried out to determine the strength and the deformation parameters. Finally, seepage and stress-deformation modelling as well as slope stability analysis were performed to assess the stability of the earth fill dam.

Acknowledgements

I share the success of this research work with my advisor Dr. James Blatz, who is a great mentor and an enthusiastic supporter. He taught me not only the fundamentals of geotechnical engineering but most importantly the practicality of its application. I am so privileged to be able to work with him, and I look forward to do so in the future.

I am grateful to Dr. Marolo Alfaro for the guidance and support that he extended for the success of this research. Special thanks to Dr. Jim Graham, Dr. Alex Man, and Dr. Alfredo Camacho for their valuable inputs in this research. I look forward to continued involvement together in future works.

Thank-you to the technicians Kerry Lynch of Geotechnical Engineering Department for helping in field work preparation and laboratory test set-ups; Brendan Pachal and Chad Klowak of Structural Engineering Department and Mark Cooper of Geological Sciences Department for helping with the X-Ray diffraction testing. This research would not have been possible without their continuous assistance.

My sincere gratitude to my colleagues Irene Ubay, Alitking Anongphouth, Aron Piamsalee, and Dr. Dave Kurz; to the summer students Shobhit Varshney, Brian Wazney, Derek Drayson, Samuel Kaluzny, and Devon Adamson who helped with the field works and performed some of the tests used in this research.

I would also like to acknowledge the financial support received from the University of Manitoba International Graduate Student Entrance Scholarship, the University of Manitoba Graduate Fellowship, and the Manitoba Graduate Scholarship.

Last but certainly not the least I need to say *salamat kaayo* to my cousins Vince and Jofil , to my tita Lalaine, tita Moril, and tito Gerry , for your support and encouragement. Thank you Niloo and Eric for believing in me. I miss you Dad and Sam, I'm sure you would have been proud.

Table of Contents

List of Tables

List of Figures

List of Appendices

Chapter 1 Introduction

Aging dams constructed in the mid-1950's on glaciolacustrine clay commonly found in prairie provinces in Canada and their surrounding states in the US (Teller, 1976) are beginning to show signs of instability to different degrees associated with time-dependent strength degradation. Several stability issues were reported associated with these materials especially due to environmental loading such as wetting-drying and freezing-thawing that produce fissures and cause reduction in strength of the clay foundation (Graham and Houlsby 1983; Man and Graham 2010; Man *et al.* 2011) . Research and studies were done to characterize the properties of these clays (*e.g.* Baracos 1977; Garinger *et al.* 2004; Man *et al*. 2011), in order to understand the engineering properties and how they can be used in the analysis and design of infrastructure supported by these materials.

1.1 The study area

A number of old earth fill dams in Canada founded on glaciolacustrine clays were considered in this research. For the purpose of this thesis, the focus will be given to a particular earth fill dam *(will be referred to as Block Dam 2 henceforth)* typical in Ontario. Block Dam 2 (BD2) is an earth fill dam with an upstream sloping clay core. The embankment dam is approximately 10.7 m high *(from base of core to crest)* with a 4.6 m crest width and 360.0 m in length, concaved towards the upstream direction. BD2 is one of the largest earth fill dams constructed to impound the

upstream reservoir. Despite the acceptable performance for over 50 years, an irregular movement was observed in the upstream slope of the said earth fill dam. Two sections were considered in this study. Section A-A is representative of the western section of the embankment which is stable, and Section B-B represents the eastern section where irregular movement was observed (see Appendix A).

The local materials used in the construction of these dams are classified as lacustrine clays of high plasticity, often described as nuggetty or crumbly and highly fissured in nature, and are thought to be part of the broader Lake Agassiz deposits (MacDonald *et al.* 1961). The fill materials used in the compacted clay core and the upstream clay blanket *(on the upstream side of the eastern section)* were borrowed from nearby areas. Hence it is assumed that the fill materials shared the same properties with the local clay foundation.

Section A-A has an inclined clay core protected by a layer of filter material and rockfill on both upstream side (U/S) and downstream side (D/S). Natural clay underlies the western section of the dam, stretching from the U/S side to the D/S side of the embankment. Being the only exposed clay, the natural clay foundation became the focus of previous investigations. A thin layer of sandy silt underlies the natural clay foundation, and overlies the bedrock. Groundwater is observed at approximately 1.5 m below ground surface.

Section B-B on the other hand also has an inclined clay core, the same as Section A-A but without natural clay underlying the dam. A thick layer of highly permeable material underlies this section as part of an old creek. During construction the creek was cleaned-up and a clay

blanket was placed in the U/S of the embankment, tied to the clay core to seal the foundation and provide a longer seepage path. The bedrock is far below ground surface as compared to Section A-A. It is also worth noting that there is water ponding on the D/S of the embankment in this section due to its lower elevation.

1.2 Overview of project, objectives, and methodology

This study was undertaken in view of the lack of understanding as to why irregular movement was observed in one section of the dam (BD2) despite acceptable performance for over 56 years. This thesis study is part of a project aimed at assessing the stability condition of aging earth fill dams and at the same time determining the mechanism of the irregular movement that occurred in the specific structure examined. This particular thesis is focused on evaluating the effects of fissures on the anisotropic strength of local materials. The other components of the overall project will be undertaken by future researchers.

Field investigation using Cone Penetration Testing with pore water pressure measurement (CPTu), soil sampling, and laboratory testing were carried out to determine the properties and variation of strength and deformation characteristics of the *in-situ* materials. Vibrating wire piezometers were installed to determine the phreatic conditions within the clay core and downstream foundation of the dam. Numerical modeling of the earth fill dam was also completed using a commercially available computer program with parameters established from laboratory testing to determine the stability condition of the earth fill dam.

Although the field investigation and instrumentation were completed for at least four earth fill dams, laboratory tests done were focused on three locations at BD2; 1) the clay blanket placed on upstream side of the dam, 2) clay core, and 3) downstream clay foundation. Some tests were also done on background samples – natural clay overburden obtained from test pits removed from the dam site location. These test results are not included in this thesis.

1.3 Hypothesis

Cyclic environmental loading can cause increasing fissuring and anisotropy in the mechanical properties of clay with time that may lead to a reduction in the stability of aging earth fill dams.

1.4 Organization of thesis

This thesis comprises five chapters in total. The introduction to the study has been provided in the present chapter. Following the introduction is a review of related literature, followed by an overview of field investigation and laboratory testing completed, the details of numerical modeling, and a summary of results, conclusions drawn from this study, as well as recommendations for future work. Appendices are provided at the end of this thesis providing additional information and details of the laboratory testing and numerical modeling results.

Chapter 2 Literature Review

This chapter examines past investigations and studies related to the research elements presented in this thesis. Past investigations include geotechnical reports and observations from previous investigations completed in the study area. Related studies refer to performance of water retaining structures founded on Lake Agassiz clay deposits or other relevant foundation materials. A short discussion on factors that affect anisotropic behavior of clay will also be presented along with the effects of fissures on the mechanical behavior of clay. Further, a novel method of field investigation by means of Cone Penetration Testing with pore water measurement (CPTu) and a different approach of stability analysis *(other than what had been carried-out prior)* will be introduced briefly.

Previous geotechnical reports have been reviewed by the author which were essential to understanding the state of engineering completed at the study site to date. Understanding the limitations of previous geotechnical methodologies used as well as the implications of reported findings helped to set the direction for this research. Although this research is built upon the previous studies completed, attention in this literature review is limited to topics that are deemed relevant to the objectives of this research.

A brief discussion on the properties of Lake Agassiz Clay as well as the performance of dams in Manitoba founded on the same type of clay will also be presented. A comparison of laboratory

test results will be conducted to investigate if the clay foundation in the study area has the same behavior with those found in other areas of Manitoba. A more thorough presentation of the details of the testing program will be discussed in Chapter 3.

Strength and deformation characteristics of the clay are determined using common laboratory testing and are interpreted using a traditional Critical State Soil Mechanics (CSSM) approach. In addition, anisotropic behavior of the clay will also be interpreted using the laboratory test results. Furthermore, possible factors for the development of anisotropic behavior will be discussed in this chapter.

Clay deposits found in the study area are described to be fissured to intensely fissured. Fissures in overconsolidated clay are considered to have a significant effect on the mechanical properties of the soil particularly in the lower-stress range. The development of fissures can result in softening of the surrounding overconsolidated clay (Skempton *et al*., 1969). This effect will be further discussed in the following section.

In order to determine a more continuous profile of the *in-situ* overburden mechanical properties, the advanced method of field investigation using a CPTu with pore water pressure measurement was implemented. This section will discuss in detail the correlations between parameters obtained using CPTu and effective shear strength parameters measured using traditional laboratory methods.

Most practicing geotechnical engineers rely on Limit Equilibrium Method (LEM) for assessing the stability of slopes due to its simplicity and ease of use. However, one of the limitations in LEM is its inability to reflect appropriate stress distributions in the soil that is representative of *in-situ* stresses. To address this inaccuracy, a Finite Element Method (FEM) approach of stress distribution is incorporated in the analyses.

2.1 Previous investigations in the study area

Earth fill dams play a very important role in electricity generation in Ontario. Annually, dam safety review is carried out to evaluate the structural integrity, as well as to monitor the efficiency and maintenance, of all earth fill dams in the area.

In April 1999 a geotechnical investigation was carried-out by an independent consulting firm. Based on the investigation, several earth fill dams were identified to require further study regarding the safety criteria for these dams[1]. Further investigation was conducted which included field explorations and laboratory testing to confirm the preliminary assessment. Results of the assessment indicated that the soils are lacustrine clay of high plasticity common to the study area and to areas farther to the west in Manitoba. The report further stated that the foundation clay used in BD2 is classified as a "Fat Clay", which is cohesive and compressible clay of high plasticity. The foundation clay was described to be nuggetty or fissured in structure. Index properties showed that the liquid limit ranges from 79% - 99%; the plasticity index range

[1] Acres International Limited, 2001. Unpublished report.

is 30% - 45%; and water content of 24% - 46% that is increasing with depth. Results further indicated that the clayey foundation of the dam is part of the Lake Agassiz Clay deposits. This type of clay is associated with several stability issues in aging dams due to its relatively low shear strength. Rehabilitation of five out of eleven earth fill dams in the area was recommended based on the said assessment.

An internal review by the owner, however, maintained that the foundation clay found in BD2 is different from Lake Agassiz Clay. The review concluded that, by utilizing more realistic *in-situ* parameters of the foundation clay, all earth fill dams met the safety criteria.

In 2010, another independent consulting firm completed an independent geotechnical investigation and submitted a report associated with the earth fill dams in question. Embankment stability analyses were performed as part of their review. The assessment shows that the clay fill and the foundation clay are of the same material. Due to the fissured structure and based on the strength test results of the local materials, a bilinear strength model to be adopted in the stability analyses was suggested (Hatch Ltd. 2010). The assessment concluded that earth fill dams in the area are stable but do not meet the required factor of safety (Hatch Ltd. 2010).

It is important to note that all slope stability analysis done in the previous investigations were based on the Limit Equilibrium Method (LEM).

2.2 Performance of water-retaining structures founded on Lake Agassiz deposits

Several stability issues associated with Lake Agassiz Clay were already reported (*e.g.* Freeman and Sutherland 1974; Garinger *et al*. 2004; Graham 1979; Man *et al.* 2011) especially those related to environmental loading such as wetting-drying and freezing-thawing that creates fissures and causes reduction in strength of the clay foundation.

Rivard and Lu (1978) conducted a case study on the failures of water-retaining structures founded on highly plastic clays including the Seven Sisters Dykes and the Red River Dykes. They described the clayey foundations at Seven Sisters Dykes and Red River Dykes to have structural discontinuities. The case study concluded that embankments on highly plastic clay soils with structural discontinuities should be analyzed using the normally consolidated (also referred to as the fully softened) strength. The use of intact strength does not predict the stability condition reliably especially for fissured and highly plastic soil (Peterson *et al.* 1960). Skempton *et al*. (1969) added that the strength of highly overconsolidated fissured clays (*i.e.* effective cohesion) approached 0 due to the softening effect of fissures.

Several published papers consider different points of view on the instability of dykes at Seven Sisters Generating Station (G.S.). The effects of pore fluid chemistry on the mechanical properties of clay and in the stability of the dykes were studied by Garinger *et al*. 2004, Man and Graham 2010, and Man *et al.* 2011. It is known that proglacial Lake Agassiz clay, particularly in Southern Manitoba, Canada is smectite-rich, expansive, strain-softening, and cemented by gypsum. Garinger *et al.* (2004) identified that slow seepage beneath the dykes

may have caused depletion with time of gypsum cementing bonds in the foundation clay which further resulted in the instability of the dykes at Seven Sisters G.S. Following the works of Garinger, an investigation of the effects of the saturation state of gypsum on development of strain-softening was carried out by Man and Graham (2010). Their study shows that early straining up to 1% to 2% axial strain was a result of the presence of gypsum at near-saturation concentrations.

2.3 Anisotropy of Lake Agassiz Clays

Anisotropy is one of the factors that influence the prediction of embankment performance (Graham 1979). Anisotropy in structural composition, mechanical behavior, and shear strength of Lake Agassiz clays had been studied extensively by different researchers (*e.g.* Baracos 1977; Freeman and Sutherland 1974; Graham 1979; Loh and Holt 1974; Graham and Houlsby 1983).

Baracos (1977) examined the compositional and structural anisotropy of Winnipeg soils using Scanning Electron Microscopy (SEM) and X-ray Diffraction (XRD). Baracos (1977) reckoned that differences in composition between dark colored *(clay minerals mostly illite, interlayered smectite, some chlorite and kaolinite)* and light colored *(non-plastic, non-clay minerals such as dolomite, quartz, calcite, feldspar and gypsum)* constituents are major causes of anisotropy. Light colored and horizontally oriented varves, veins, and seams contribute to greater horizontal permeability, planes of different strength, and ease of cleavage along horizontal planes. Some layers of clay have a microstructure of mostly horizontally oriented clay particles, with much edge-to-edge bonding, which further contributes to the observed anisotropy. The

structural and compositional anisotropy further contribute to the anisotropic elastic behavior of Winnipeg clays during shearing. Winnipeg clays are also reported to have horizontal stiffness 1.8 times greater than its vertical stiffness (Graham and Houlsby 1983). Freeman and Sutherland (1974) had conducted detailed laboratory testing to assess the anisotropic strength properties of the clays by doing triaxial testing (CI$\bar{U}$ and CID) on specimens trimmed in various orientations. Test results showed that the shear strength envelopes along the layers were lower than the shear strength envelopes across the layers. Other researchers had also studied the anisotropic undrained shear strength and deformation behavior of Winnipeg upper brown clay. The study by Loh and Holt (1974) identified that anisotropic clay fabric and stratification causes anisotropy in undrained shear strength of the clay.

Cyclic expansion and contraction of clays due to wetting-drying and freezing-thawing can also cause anisotropy in clays. Environmental loading creates fissures resulting in anisotropy in its mechanical behavior. These fissures create planes with weaker strength and higher permeability (McGown and Radwan 1975). Further effects of fissures on the mechanical behavior of clay will be discussed in the following sections.

2.4 Effects of fissures on the strength of clay

The local materials in the study area are often described as being highly fissured, nuggetty or crumbly in appearance with whitish inclusions at depth. These are typical features of Lake Agassiz deposits (Graham and Shields 1985). Structural discontinuities such as fissures are believed to have been caused by cyclic expansion and contraction due to wetting and drying

and/or freezing and thawing. Fissures generated by weathering are characterized by increased fissuring with reducing depth. These fissures can be distinguished typically as having a matte surface texture. However, seldom these fissures are slickensided with polished and striated surfaces indicating a considerable degree of particle orientation (Skempton *et al*. 1969). Unlike in stiff clays, structural discontinuities in soft soils are difficult to observe and may not be noticed during initial classification. Such discontinuities may only become apparent during sample preparation for strength tests.

Terzaghi (1936) indicated that fissured clays possess decayed strength properties and are consequently more prone to instability (*e.g.* Cotecchia *et al.*, 2006). Intensely fissured clays have degraded mechanical properties resulting to the smallest state boundary surface relative to unfissured clays and to the same soil when reconstituted (Vitone *et al*. 2009). Thus, it is of practical importance to understand the effects of fissuring on the mechanical behavior of clay.

2.4.1 Shear strength of fissured clays

Fissured clay behaves like a blocky material separated by a system of fissures under low effective stresses. When sheared at a lower stress range, the shear plane passes through fissures between clay lumps within which the effect of high overconsolidation is retained. At stress levels higher than the effective overburden pressure, the shearing takes place through the hard clay lumps (Marsland, 1971), resulting in a bilinear failure envelope. Other researchers also confirmed the bimodal failure envelope for fissured glacial lake deposits particularly at

lower stress level (*e.g.* Kjartanson and Tweedie, 1978; Thomson and Kjartanson, 1985; Graham and Au, 1985).

Patton (1966) did an experimental study to describe the behavior of fissured clay. Figure 2-1 shows the shear strength model of fissured clays having a rough surface. Under low normal stress the specimen moves over the teeth *(fissured surface)* when being sheared, contributing to a higher frictional resistance and dilatancy. As the normal stress increases, the tendency of the teeth to be sheared off increases and dilatancy decreases. Under a very high normal stress, the tendency of the material to dilate will be suppressed and the shear plane will be forced to pass through the intact material resulting in a lower frictional resistance.

However, fissures also may represent planes of weakness with lower shear strength along which sliding would tend to occur (McGown and Radwan 1975). Fissured clay can soften when subjected to strain, the effect of which is to gradually reduce the cohesion. In addition, fissures can also cause shear stress concentrations that can locally exceed the peak strength of the clay and lead to progressive failure (Skempton *et al.* 1969). Bjerrum (1969) further postulated that conventional laboratory tests on small samples of fissured clay measure only the intact strength of the clay and not the field strength. A correction should be applied to laboratory strengths by assuming that the cohesion intercept would approach zero while the friction angle would remain the same as for intact clay to account for the combined effect of weakening and softening in the soil due to fissures. Additionally, Bjerrum (1969) recommended the use of this

concept to fissured clay at shallow depths where groundwater fluctuations and weathering had resulted in non-uniform straining.

Bishop *et al.* (1965) summarizes the typical characteristics of the shear strength behavior of fissured, overconsolidated clays based on a comprehensive experimental on undisturbed Blue London Clay:

(a) the stress-strain curve is of a brittle type for low to medium stress levels and changes gradually from the brittle to a ductile type as the effective confining pressure increases;

(b) the transition of the volume change from contraction to dilation occurs just before or when the peak stress is reached; and

(c) the failure envelope is markedly non-linear at low stress levels.

2.4.2 Effects of softening in fissured clays

Fissured clay tends to exhibit higher dilatancy under lower stress range. Skempton and Hutchinson (1969) studied the effects of fissures on the stability of natural slopes in overconsolidated London clay. The conclusion presented that open fissures and the softening effect facilitated by the fissures bring the strength of highly overconsolidated fissured clays to normally-consolidated value. As the softening advances, the degree and area of softening involved in shearing increases, resulting in further reduction in the shear strength. Since the clay, in reality, is under a specific effective overburden pressure, the clay at the ultimate

condition of softening - the fully softened condition - would be equivalent to normally consolidated clay (Skempton, 1970).

2.5 Evaluation of soil parameters using CPTu

Cone Penetration Testing with pore pressure measurements (CPTu) uses a modern version of electrical cone penetrometer having piezometer elements. It provides values of cone tip resistance, sleeve friction, and pore pressure as the cone is being advanced into the soil. With the advent of the piezocone, the CPTu was established as a powerful soil profiling tool for site investigation. It is an excellent method for the determination of soil stratification and the identification of soil type. It also has the potential for obtaining estimate values of *in-situ* undrained shear strength and deformation parameters in many soil types. The direct values produced by the cone test have been used as input to geotechnical formulae, usually of empirical nature to determine capacity and settlement of shallow and deep foundations (Eslami and Fellenius, 2004).

2.5.1 Correlation between shear strength and cone resistance

The CPTu measures the cone resistance, the sleeve friction resistance, and the pore pressure. These measurements can be used with empirical correlations to estimate undrained shear strength. The empirical relationships established for use with the CPTu are powerful and simple methods but must be treated carefully in unusual soil conditions.

The undrained shear strength can be evaluated from cone resistance using a cone factor and several approaches established based on total stress, effective stress and excess pore pressure. However, a generally accepted theoretical model for determination of Su has not yet been developed. Hence, the interpretation of Su is usually estimated from empirical relationship such as Eq. [1].

$$Su = \frac{q_t - \sigma_v}{N_k} \qquad \textbf{Eq. [1]}$$

where N_k is the cone factor, q_t is the cone resistance from CPT, S_u is the undrained shear strength, and σ_v is the total overburden stress.

Several studies have been conducted in order to develop more accurate cone factor values to establish a more general correlation between cone resistance and undrained shear strength of the soil (*e.g.* Eid and Stark, 1998; Larsson and Åhnberg, 2005; Rémai 2013; Shin and Kim, 2011). However, the cone factor is highly influenced by the local area where the CPTu was performed and stress state of the soil. Considerable research effort has been completed on various soil types for assessment of the cone factor.

Soil groundwater conditions can also be evaluated using the measured pore water pressure in CPTu. However, the interpretation of cone penetration pore pressures is generally limited to fine-grained soils in which penetration is essentially undrained and is generally directed towards the evaluation of undrained shear strength and stress history. The excess pore pressures during cone penetration have high positive values in clay layers, negative values in silt

layers, and values close to zero (*i.e.* equilibrium pore pressures) in coarse-grained layers (Robertson, 1990).

Effective shear strength parameters (c' and φ') can also be estimated from piezocone data. However, interpretation for overconsolidated clays is still questionable due to the complexity of the distribution of total stresses and pore pressures around the cone (Sellountou *et al.*, 2000).

2.6 Slope stability analysis of embankments with structured clays

This section is a short discussion on research addressing issues in modeling small embankments with structured clays. A more detailed discussion on numerical modeling will be provided in Chapter 4.

The global factor of safety (FOS) is a recognized criterion for slope stability assessment; conventionally, it is defined as the ratio of total stabilizing force to total destabilizing force in a given geometry. Destabilizing forces are usually governed by the shear force acting along a given plane, while stabilizing forces are *(in most cases)* dominated by the shear strength of the material along the said plane. Shear strength of structured clays are stress-dependent, (*i.e.* they exhibit dilatancy under low normal stress level). At present, the most reliable way of calculating the stability of clay mass is by using the critical state shear strength of the clay (Tavenas *et al*., 1980).

As discussed in the previous section, fissured overconsolidated clays like the one found in the study area, tend to soften with time. Yoshida *et al.* (1991) stated that the reduction of shear

strength due to softening can be represented as a lowering of the failure envelope and the reduction in the non-linearity at low stress levels. Further, the authors recognized that the finite element method, which is based on a conventional elastic-plastic formulation, can be extended to analyze softening effects.

Finite Element Method (FEM) is an alternative method that computes slope movements and stresses throughout the slope. Stress-strain relationships can be incorporated in the analysis by establishing the stress distribution in the ground using finite-element based approach. Moreover, finite element seepage analysis can also be incorporated in the evaluation to completely remove the assumptions of inter-slice forces.

Griffiths and Lane (1999) presented a study on the effectiveness of FEM in assessing slope stability of natural slopes and dams. They indicated that slip surfaces do not need to be assumed in advance; in the FEM method, failures are determined in the analysis through the zones within the modelled soil mass in which the soil shear strength is unable to sustain the applied shear stresses. Additionally, the factor of safety of a soil slope is defined as the number by which the original shear strength must be divided in order to bring the slope to the point of failure. The authors further concluded that, the FEM method in conjunction with an elastic-plastic stress-strain method has been shown to be a reliable and robust method for assessing the factor of safety of slopes. However, a pure FEM analysis is more complicated, requires more parameters and boundary conditions, and it takes time to complete an analyses due to its complexity.

2.7 Summary

Based on the reviewed literature, the evaluation of the slope stability of BD2 is highly influenced by the parameters used in the analysis. Previous completed investigations indicated that the foundation clay in the area is similar to Lake Agassiz deposits and further suggested that a fully-softened strength and a bilinear strength model should be used in the analyses due to its fissured nature. Different concerns were raised whether the use the fully softened condition in the foundation clay of these structures in the assessment of stability is appropriate. Thus, the need for further investigation of the effects of fissures on the strength of the foundation clay is warranted. Advanced field investigation by means of CPTu is carried out to determine *in-situ* parameters and establish a correlation between the measured *in-situ* data and undrained shear strength. This correlation is used to determine the undrained shear strength of the *in-situ* materials from other dams and for monitoring any future changes in strength of the local materials. Drained parameters are interpreted based on CPTu data. Further, a new approach of numerical modeling is carried-out to evaluate the current stability condition of BD2 (*i.e. in-situ* stress-distribution will be determined using FEM based approach and will be imported for a LEM slope stability analysis).

2.8 Objectives of the Research

This research is intended to evaluate the stability condition of BD2, while taking into account the effects of fissures on the strength of the foundation clays. Specifically, this research is aimed to complete the following:

1) Conduct a field investigation to determine the *in-situ* soil parameters and carry out laboratory tests including isotropically consolidated undrained ($CI\bar{U}$) triaxial tests, consolidated drained direct shear tests, oedometer tests; determine soil properties by carrying out index tests, X-ray diffraction (XRD) tests, and scanning electron microscopy (SEM) tests;

2) Establish a correlation between undrained shear strength and cone tip resistance from CPTu; and

3) Perform numerical modeling using current computer software and parameters determined from the laboratory tests to assess the current stability condition of BD2.

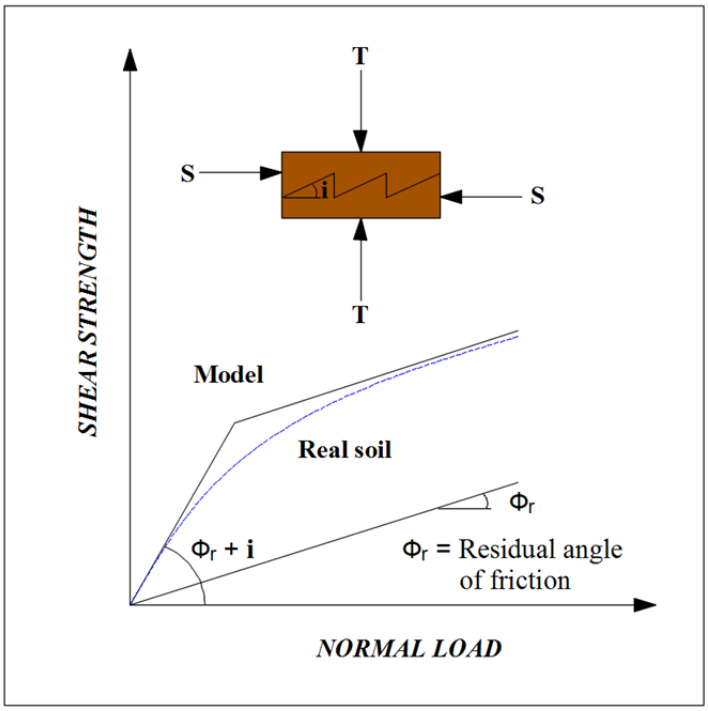

Figure 2-1. Shear strength of model specimen having rough surfaces (after Yoshida, Morgenstern, and Chan 1991)

Chapter 3 Field Investigation and Laboratory Testing

Data from the sub-surface exploration and laboratory testing program obtained from previous investigation done in 1999 were used as a basis for developing this supplementary field investigation and laboratory testing program. Field investigation was carried out primarily to assess the current *in-situ* conditions of the study area and gather new site characterization information. Instrumentation such as vibrating wire piezometers were installed to monitor the pore water pressure within the dam and at its downstream foundation. Soil samples from the clay core, foundation clay, and clay blanket were obtained for index testing and strength and deformation characterization. The program was established for all eight (8) earth fill dams, but only details of the field investigation and laboratory testing done from Block Dam No.2 will be presented in this chapter and following chapters.

3.1 *In-situ* Field Testing, Surveying, and Instrumentation

In-situ field exploration program in Block Dam No.2 includes 12 piezocone profiles with pore water pressure measurements to evaluate the *in-situ* properties of the dam; detailed topographic and bathymetric surveying to obtain general information on the surficial deformation of BD2 in the past 16 years, as well as to determine the extent of movement that occurred at Section B-B; and installation of 10 vibrating wire piezometers for long-term monitoring of pore water pressures both in the clay core and in the downstream foundation.

3.1.1 Cone Penetration Testing with Pore Water Measurement (CPTu)

CPTu was done as part of the preliminary assessment of the *in-situ* materials. All piezocone testing was done in general accordance with the ASTM D5778 standard, using a 20 ton track mounted rig, operated by ConeTec Investigations Limited. A 10 cm^2 penetrometer with net end area ratio of 0.8 and cone tip with a 60 degree apex angle, as shown in Figure 3-1, was used. The pore water pressure filter is located directly behind the cone tip in the "u_2" position (ASTM Type 2). The CPTu was conducted at a steady rate of 2 cm/s. Pore pressure dissipation (PPD) tests were also completed at selected depths in an attempt to locate the location of the phreatic surface. Profiles were conducted on the crest of the dam *(7 profiles, 4 of which were on the section with observed movement)* and along the downstream toe of the dam *(5 profiles)*. All CPTu profiles were advanced to refusal. Profiles from the crest of the dam went through 4 m of clay core and reached refusal at the downstream rockfill zone underlying the downstream filter. Profiles from the downstream toe of the dam were all terminated at refusal (most less than 3 m in depth).

Interpretation of CPTu data is based on corrected tip resistance (q_t), sleeve friction (f_s), and dynamic pore water pressure (u). Approximate interpretation of soil type is based on correlations developed by Robertson (1990 and 2009), and were confirmed from index testing done which will be discussed in the following chapter. As part of this research, a correlation between the undrained shear strength and cone tip resistance was established by determining the local cone factor, N_{kt}. Hence, locations of the profiles were strategically selected close to

borehole locations where soil samples were obtained. Other data obtained from the CPTu (*e.g.* skin friction and dynamic pore water pressure) served as a check of the condition of clay core or clay foundation (*i.e.* normally consolidated, overconsolidated, dilatant, *etc.*) as determined in the laboratory testing program. Figure 3-3 and Figure 3-4 show profiles of the clay core and clay foundation, respectively.

3.1.1.1 Drained Parameters Interpretation

The drained strength parameters (ϕ' and *c*') are estimated based on CPTu cone tip resistance (q_t) using the method developed by Senneset et al. (1989). The method requires calculation of the soil attraction, "*a*" which can be calculated from laboratory testing data. The angle of plastification was assumed to be =-30 *(for stiff and fissured soils)*, approximated from laboratory-determined ϕ' value (Senneset *et al*. 1988). Friction ϕ' are estimated using the effective stress bearing capacity factors chart shown in Figure 3-2, while the effective cohesion *c*' are calculated using the classical equation, Eq. [2].

$$c' = a\ x \tan(\phi') \qquad \textbf{Eq. [2]}$$

Drained parameters interpretation for the clay foundation (Figure 3-3) indicates a friction angle within the range of values determined from the laboratory tests. As for the clay core (Figure 3-4), the estimated friction angle is relatively higher than what was determined based on the laboratory tests. The interpreted cohesion components are relatively higher as well. The variances in strengths are postulated to be due to the following:

i. Confining stress condition in the field is anisotropic, (*i.e.* different vertical and horizontal stresses) while in the laboratory, tests were done under isotropic conditions;

ii. Samples were assumed to be fully-saturated when tested in the laboratory, resulting in lower effective strength results;

iii. Samples were assumed to be homogenous throughout the depth wherein the *in-situ* condition may not be homogeneous due to the presence of silt lenses/pockets.

iv. Samples used in laboratory testing were subjected to different disturbance *(e.g. method of soil sampling and sample handling)* to some unknown degree.

3.1.1.2 Undrained Parameters Interpretation

Undrained strength parameter interpretation is based on cone tip resistance and the undrained shear strength determined from CI$\bar{U}$ testing. However, the established correlation is only used for the clay core materials based on the stress range used in the laboratory testing (*i.e.* stress range used in the laboratory is higher than the *in-situ* stress range for the clay foundation as shown in Figure 3-5). The local cone factor was determined using 3 steps: (1) by back calculating the cone tip resistance from laboratory-based undrained shear strength varying the local cone factor, N_{kt}; (2) by calculating the undrained shear strength based on the net cone tip resistance, by varying the local cone factor, N_{kt}; (3) by determining the best fit line of the undrained shear strength and cone tip resistance for both laboratory-based and *in-situ* data, varying the local cone factor, N_{kt}. A local cone factor of N_{kt} = 35 shows the best fit line for *in-situ* and laboratory

based undrained shear strength and cone tip resistance. The correlated undrained shear strength based on CIU testing and cone tip resistance is expressed in Eq. [3] or Eq. [4].

$$Su = \frac{(qt - \sigma v)}{35} \qquad \textbf{Eq. [3]}$$

or

$$Su = 0.02857\ (qt - \sigma v) \qquad \textbf{Eq. [4]}$$

3.1.2 Topographic and Bathymetric Surveying

Topographic surveying was carried out as part of field investigation using a GTS-605AF Total Station. All surveyed points were tied to a known reference (bench mark) located at both sides or on the dam itself. Sections were surveyed along the length of the dam, with emphasis given to the section with the observed irregular movement. Bathymetric surveying and sidescan sonar were also done using HST-WSBL transducer (standard sonar) and LSS-2 StructureScan HD transducer conducted by North/South Consultants Inc. Underwater mapping was done to map the extent of movement at the upstream toe of the dam as well as to examine the possible movement mechanism observed. The topographic survey data along with the bathymetric survey data were used to generate a 3D surface model using the Civil3D software application, to show the extent of the movement that occurred, see Figure 3-7. Sections used for numerical modeling were also obtained from the 3D model. Comparison of the 3D model before and after the movement shows less or very minimal toe bulging at the upstream toe of the dam. Sidescan

images show logs accumulating at the upstream toe of the dam, see Figure 3-8. Some of the logs are sticking out of the clay blanket particularly at Section B-B, as described by the divers.

3.1.3 Vibrating Wire Piezometers

A total of ten RST vibrating wire (VW) piezometers (VW2100-DP and VW2100 models) were installed in Block dam No.2 to monitor the pore water pressure, see Appendix A. Six were installed in the clay core from the crest, and four were installed in the downstream side of the dam. All installation was completed in general accordance with the installation instructions provided by RST Instruments Ltd. Some locations have a nested installation (*i.e.* two piezometers were installed in the same location but at different layers). This is to confirm a possible differential piezometric level mostly between the downstream filter and the clay core to assess the groundwater flow direction and gradient. All VW piezometers were installed in the same boreholes where samples were obtained or where CPTu testing was conducted, and were fully-grouted the entire length. Most of the installed VW piezometers were connected to an automated data collection system, and a few were connected to a single-channel data logger. Data from the automated piezometers can be downloaded remotely, while that with single-channel data loggers requires manual readings on-site.

Piezometers installed in the clay core were used to determine the phreatic surface within the clay core to be used in the numerical modeling *(further discussed in Chapter 4)*.

3.2 Sub-surface Exploration

Following the preliminary assessment (*i.e.* cone penetration testing), two separate drilling and soil sampling programs were carried out. Maple Leaf Drilling Ltd. was contracted by the University of Manitoba to complete the drilling jobs. The first phase of the drilling was done during fall 2015, when the ground was not frozen. A continuous soil sampling of the clay core (on-shore) was carried out by means of a track-mounted Hollow Stem Auger (HSA). Shelby tubes with 102 mm (4") ID were used which are the preferred size to sample fissured clays. The second phase of drilling and soil sampling was done during winter when the upstream reservoir was frozen. Track-mounted piston sampling was used to retrieve samples from the clay blanket. Being under the water for over 50 yrs., the clay blanket was expected not to have any structural discontinuities (fissures). Hence, only 76 mm (3") ID Shelby tubes were used. All methods involved in sub-surface explorations were conducted in general accordance with the specified ASTM standards (*i.e.* ASTM D1452-09, ASTM D1586-11, ASTM D1587-08, ASTM D5784/D5784M-13, ASTM D6151/D6151M-15, ASTM D6519-15, and ASTM D4220/D4220M-14*)* and with Ontario Water Resources Act. R.R.O. 1990, Regulation 903.

3.2.1 Test Pits

Three test pits with depth no more than 3 m, were excavated in Block Dam No.2 using a Caterpillar wheel excavator operated by Maple Leaf drilling Ltd., two of which were excavated at the downstream side of the dam and one on the crest of the dam. Multi-directional (*i.e.* vertical and inclined) Shelby tube samples were obtained in the test pits downstream. A 102

mm (4”) diameter Shelby tubes were pushed vertically down to the test pit floor at different depths. Inclined samples were obtained at a 53° (*i.e.* 45° + ϕ/2) inclination from the horizontal as shown in Figure 3-11. These samples will determine the cross shear and horizontal shear strength of the clay foundation *(further discussed in following sections)*. A shallow test pit was also completed on the crest of the dam to expose the clay core and obtain vertically driven Shelby tube samples. Location of the clay core relative to the crest elevation was noted to be at 0.9 m t0 1.2 m below grade. It was assumed that the same thickness of the “topping” material (*i.e.* mixed gravel and cobbles with some boulders), overlies the clay core.

Block samples (Figure 3-12) were also obtained at different depths from test pits downstream using a 23 cm x 23 cm x 25 cm block sampler. Additional block samples were obtained following a conventional block sampling method. Samples were sealed on site with layers of cling wraps, cheese clothes and wax before enclosing them in crates for transport to avoid moisture loss. All test pits were backfilled with spoil material, levelled and compacted with the bucket of the backhoe.

Sample recovery of Shelby tubes near the surface at a depth less than 2 m was relatively “poor” (40% - 60%) and full recovery for samples was obtained from 2 m depth. This is thought to be partly due to the high compressibility of the desiccated upper soil. The clay foundation can be divided into three layers based on visual inspection from test pit walls. Underling the top soil (2’–5’) is a mottled mix of brown and grey silty clay layer, weathered, with trace of organics and medium to stiff consistency; the third layer (5’-9’) is an intensely fissured grey clay with random silt pockets, crumbly, and stiff (see Figure 3-13).

3.2.2 On-shore Undisturbed Soil Sampling

Continuous undisturbed soil sampling was carried-out using a track mounted Hollow Stem Auger (HSA). A 102 mm (4") ID Shelby tubes was used to retrieve continuous samples from five boreholes in the clay core and three boreholes in the clay foundation as shown in Appendix A. Drilling from the crest of the dam was challenging. Coring through 3 m to 5 m of riprap (with average $D_{50} \approx 0.4$ m) and rockfill was necessary to avoid alteration of the upstream slope of the dam and to be able to sample the clay core. The first Shelby tube of clay core sample is often slightly disturbed to very disturbed with trace of rockfill and gravel near the top of the tube. Determination of soil stratigraphy was not possible due to the method of sampling (*i.e.* HSA). Boreholes from the crest of the dam were advanced down to 5 m – 7 m depth, while boreholes at the downstream toe of the dam were advanced to refusal at 2.1 m – 3.4 m deep. All boreholes were backfilled with cement-bentonite grout to the ground surface or to the top of clay core and topped with bentonite chips. Retrieved Shelby tube samples were all sealed with paraffin wax at both ends and were transported to the University of Manitoba Geotechnical Engineering Laboratory to be stored in a temperature-controlled environmental chamber.

3.2.3 Off-shore Undisturbed Soil Sampling

Off-shore drilling and soil sampling was done to retrieve samples from clay blanket and natural clay located upstream of the dam (under water) using a 76.2 mm (3") ID piston tube sampler. A 20 ton track mounted rig had to drill through at least 45 cm (18") of blue ice or equivalent

thickness of white ice before the piston sampler can be advanced to sample the clay blanket. A total of 18 boreholes were drilled for this drilling program. Borehole locations were predetermined based on the 3D model and the sidescan images presented in a previous section. Since some of the logs are sticking out from the lake bed, it is necessary to ensure that the borehole locations are clear from randomly oriented logs to avoid disturbance of the clay blanket. Divers were involved in the process to properly locate these boreholes. All boreholes were backfilled with bentonite grout/pellets and topped with bentonite chips and sand with the aid of the divers.

During soil sampling, the natural clay foundation on Section A-A (wet side) was noted to be fissured with random silt pockets. The clay blanket on the other hand was noted to be soft in the upper layer and had medium consistency at depth (see Figure 3-15).

3.3 Laboratory Testing

Samples obtained from four boreholes (*i.e.* BH3, BH5, BH8, and PS13) and one test pit (TP2) were used for laboratory testing, representing specimens from clay core (both from section A-A and section B-B), clay foundation and clay blanket. The laboratory testing program was established to determine the properties of the soil necessary to understand the behavior of the *in-situ* materials. Soil properties tests included index testing and soil classification, scanning-electron microscopy (SEM) testing, and x-ray diffraction (XRD) testing. The testing program was also designed to identify the strength and deformation parameters needed for numerical modeling to assess the stability condition of the dam. Soil parameters tests included

isotropically-consolidated undrained (CIŪ) triaxial compression testing, consolidated-drained direct shear testing, and oedometer testing.

3.3.1 Index Properties and Soil Classification

All index testing was completed in accordance to the specified ASTM standards. Tests done on selected samples included determination of specific gravity *(ASTM D854-02),* unit weight *(ASTM D 4254-00)*, Atterberg limits *(ASTM D4318-00)*, and particle-size analysis of soils *(ASTM D433-63).* Individual specimens were classified in accordance with Unified Soil Classification System (USCS).

Extruded clay core samples can be described to have a mottled mix of grey and brown in color as shown in Figure 3-16, matted texture with presence of random silt lenses generally with horizontal orientation (Figure 3-17) and silt pockets, and had a medium to stiff consistency. Random polished fissures with varying sizes were also observed in clay core samples and more in clay blanket samples (see Figure 3-18). Clay foundation samples had similar characteristics as the clay core but had more frequent silt pockets (Figure 3-16) and had more intense fissuring with mostly stiff consistency. The clay blanket samples on the other hand seemed to be more uniform in appearance, soft and brown clay in the upper half layer *(approximately the upper 0.6m)* and mottled mix of brown and grey (mostly grey) with soft to medium consistency in the bottom half layer. Figure 3-20 shows the plasticity chart of the samples tested. All samples are classified as “fat clay” with high plasticity. Plasticity indices range from 50 to 58, and liquid limits range from 79 to 87. Hydrometer analysis (Figure 3-19) shows clay fraction ranging from

73% to 80%. Average moisture content ranges from 38% to 40%. Table 3-1 summarizes the results of index testing and soil classification. The results show that the fill materials (*i.e.* clay core and clay blanket) appear to be the same material as the local clay foundation.

3.3.2 Scanning Electron Microscopy Testing (SEM)

Twelve rectangular specimens manually trimmed to about 1 cm x 1 cm in cross-section and 2 cm in length, see Figure 3-21. Specimens were obtained from Shelby tubes samples from the clay foundation, clay core, and clay blanket. Air-dried specimens were brought to the Microbeam Laboratory in the University of Manitoba for examination of the structural compositions of fine grains. Carbon coated specimens were examined using FEI Inspect S50 Scanning Electron Microscope (SEM) with back-scattered electron and Energy Dispersive X-ray (EDX) system. Images were obtained from the top of the specimens. Regions along or at the cracks were selected to be able to examine the edges of the soil particles.

3.3.2.1 Clay Particle Identification

Identification of clay minerals present under Scanning Electron Microscope is possible as presented by reference to structural descriptions of usual clay particles examined under SEM (Deer *et al*. 1966; Baracos 1977; Welton, 1984), smectite (S) clay particles are often described to be “crenulated or flaky” in structures such as shown in Figure 3-22(b) and Figure 3-23(b) and also observed in most specimens; Illite (I) clay particle appears to be like a “soap flakes nibbled by mice”, such as shown in Figure 3-24(a) and Figure 3-25(a); Kaolinite (K) and chlorite (C) clay particles appear to have “hexagonal shapes”, which were not observed to be present in the

examined specimens. Non-clay particles observed to be present are quartz (Q) and dolomite (D) seen in Figure 3-22(a). Random point analysis using EDX shows that the dominant elements present are Oxygen (O), Silicon (Si), Aluminum (Al), some Magnesium (Mg) and Sodium (Na), and trace of Potassium (K) and Iron (Fe). These are mostly the chemical formulation for Mica group of silicate sheets minerals, mostly for clays. An example of EDX point analysis in Figure 3-31 shows what seem to be smectite particles. EDX is not a definitive means of identifying clay and non-clay minerals present, but will however aid in understanding the SEM images. Better identification of minerals is done by X-ray diffraction testing which will be discussed in the following chapter.

3.3.2.2 Particle Shape and Orientation

Images of clay particles from the clay foundation show predominantly edge-to-edge contacts with random non-clay particles for specimens at lower depths *(Figure 3-22)* and not much of a preferred alignment or orientation. Specimens obtained from the upper layer of the clay foundation *(Figure 3-23)* show micro-fissures between flocs. Specimens from the clay core show a more flocculated structure such as in Figure 3-24 and often times these flocs or flakes are separated by micro fissures as shown in Figure 3-25. A specimen with polished fissures such as the one shown in Figure 3-18 was also examined; Figure 3-26 shows a strong alignment of clay particles when examined under scanning electron microscope. Clay blanket specimens from the top layer *(Figure 3-27, at depth <0.3 m from top of the clay blanket)* shows more edge-to-edge contact and slight particle alignment; specimens from the bottom layer *(Figure 3-28, at*

depth >1.0 m from top of the clay blanket) shows most clay particles forming broad overlapping sheets. The difference in colors (*i.e.* light brown and dark brown), corresponds to differences in the shapes of clay particles and the presence of non-clay minerals; light colored streaks shows more flocculated clays with the presence of non-clay minerals such as quartz and dolomite as in Figure 3-29; dark colored constituents show more uniform shape of clay particles with less or no non-clay minerals present and had a slightly preferred orientation of clay particles.

3.3.3 X-Ray Diffraction Testing (XRD)

Sizes, shapes, and surface characteristics of soil particles are controlled by its mineralogy. Mineralogy also determines interactions with fluid phases. These factors further define the plasticity, swelling, compression, strength and permeability of clays.

X-ray diffraction (XRD) testing was carried-out to determine the mineralogical composition of the clay and non-clay constituents of the samples. Samples were obtained adjacent to SEM specimens to ensure similarities of materials examined. Dry powder specimens were prepared following the procedure described by Mitchel (1956). All specimens for XRD testing were air dried and pulverized using mortar and pestle. Due to the presence of whitish silt pockets, pulverized samples were not sieved to include non-clay minerals in the analysis. Samples were tested using Rigaku MiniFlex600 diffractometer within 2°-70° range of diffraction angle (2). The machine uses a copper K $_1$ radiation at an operating voltage of 41 kV and 15 A. Results were interpreted in two ways, interpretation using JADE software and by calculating the d-

spacing of each peaks using Bragg`s law and determining the corresponding minerals from published literatures (*e.g*. Mitchell, 1993; Tan, 2005).

Figure 3-32 shows some of the XRD results from the clay core, clay foundation, and clay blanket. X-ray diffraction charts of other samples are included in the appendix. All samples show similar mineralogical composition, regardless of the difference in color, and intensity of fissuring. Clay minerals present are mostly interlayered smectite and illite with some kaolinite and some mica, and trace of attapulgite. Non-clay minerals present are quartz, feldspar, and trace of dolomite. The dominant clay mineral smectite is generally expansive, weak, and with low hydraulic conductivity (Mitchell, 1993). Observed non-clay minerals such as quartz and feldspar are main mineralogical composition of silt, consistent with visual observation of the samples. These non-clay minerals are typical in the area with granitic bedrock outcrops[2]. Previous geological report has also identified the bedrock in the local area as granite, granite gneiss and grandiorite gneiss (Hatch Ltd. 2010). The presence of non-clay minerals were thought to produce higher effective strength under the normally consolidated condition (Graham and Shields 1985). To some degree, similar findings were reported by Baracos (1977) and by Loh and Holt (1974) in their extensive study on properties of Winnipeg clays (Lake Agassiz clay).

[2] *A. Camacho, personal communication, May 2016.*

3.3.4 Oedometer Testing

One-dimensional consolidation testing was done in accordance with ASTM D2435-96 standards on select samples from each location. A twenty-four hour loading cycle was implemented with a load increment ratio of 2.0. Incremental loading started at 50 kPa and was increased up to 1600 kPa. Swelling of samples was not permitted by adding water 2 minutes after the first loading. Samples were unloaded after 800 kPa loading to 200 kPa. Figure 3-33 shows results from oedometer testing. Pre-consolidation or apparent pre-consolidation pressures were calculated using the Cassagrande method. An apparent pre-consolidation of 150 kPa and 170 kPa was observed from the clay core and clay blanket specimens, respectively. The apparent pre-consolidation pressure from the clay core is suggested to be due to the mechanical compaction of the fill material during construction of the dam. Higher apparent pre-consolidation pressure was observed from the clay blanket, it is most likely because the clay blanket had already been consolidated under the weight of the rockfill shell. No sample outside the rockfill zone has been tested yet for 1D consolidation test. Compression and recompression indices were determined from the slope of the normally consolidated line (NCL) and unload-reload line (URL), respectively, in *e* vs. log σ_v' plot. Table 3-2 summarizes the deformation parameters determined from oedometer test.

3.3.5 Isotopically Consolidated Undrained Triaxial Testing (CI$\bar{U}$)

Reviewed literature reckoned that the clayey materials of Lake Agassiz deposits are anisotropic. Visual observations noted the presence of silt pockets or silt lenses, laminations, and fissures in

the clay foundation and clay core samples. These can cause anisotropy in strength properties (Baracos 1977; Graham and Houlsby 1983; Loh and Holt 1974). To assess the anisotropy in strength of the clay materials, multi-directional shearing was carried out. Cross-shear strengths were determined from isotropically-consolidated undrained triaxial compression tests (CI$\bar{U}$) on vertical samples. Strength determined from CI$\bar{U}$ testing done on inclined samples from clay foundation however, correspond to the horizontal shear strength of the clay foundation. Since no inclined samples were obtained from the clay core, the horizontal shear strength was determined by means of consolidated-drained direct shear test that is presented in a following section. Further, fissured clays tend to soften when strained, hence cross-shear and horizontal shear strength parameters were interpreted using a Critical State Soil Mechanics (CSSM) approach. A linear trendline regression with no intercept was used in interpreting the critical state strength of most specimens. Coefficient of determination (R^2) was also checked to be at least 0.7 or higher (indicative of a reasonable model).

3.3.5.1 Procedure

Triaxial compression tests were performed in accordance with the ASTM D4767-95 standard. As part of the experimental investigation on the effects of fissures to anisotropy in strength, all specimens prepared for CI$\bar{U}$ testing are 71.12 mm in diameter with specimen height to diameter ratio of 2:1. Specimens were carefully trimmed down to 71.12 mm (2.8”) diameter on a trimming pedestal using a thin wire-cutter. Most specimens have two-phase consolidation. The first phase was to consolidate the specimen under a high pressure. The second phase was to unload it to about half of the confining pressure and allowing it to re-consolidate, before

shearing. The idea was to simulate the *in-situ* overconsolidation of the sample before shearing (*i.e.* Ro ≈ OCR). A B-test was performed on each specimen, and B value of at least 0.98 was required before shearing was initiated.

Effective strength parameters were interpreted using a Critical State Soil Mechanics (CSSM) approach and were calculated based on the slope of the critical state line, Eq. [5] and cohesion intercept as interpreted in q-p space, Eq. [6].

$$M = \frac{6sin\phi'}{3 - sin\phi'} \qquad \textbf{Eq. [5]}$$

$$c'oc = c'pq\ x\ \frac{3 - sin\phi'}{6cos\phi'} \qquad \textbf{Eq. [6]}$$

where, M is the slope of critical state line in q-p space, c'_{oc} is the cohesion, c'_{pq} is the cohesion intercept at q-p space.

3.3.5.2 CI$\bar{U}$ test results from clay core

Figure 3-36 shows the stress-paths for the clay core samples in q-p space during undrained shearing. It shows an isotropic elastic behavior (*i.e.* m p ≈ u) for specimens sheared between 100 kPa to 300 kPa mean effective stress. However, a slight elastic anisotropy was observed on specimens sheared under low confining stress level (m p ≠ u). This could be attributed to the tendency of the material to dilate due to its fissured nature. The stress path of the specimen sheared at higher stress levels is typical for a normally consolidated behavior of the specimen

sheared beyond its pre-consolidation pressure (Graham and Houlsby 1983). Figure 3-38 shows the stress-strain behavior of clay core samples during CI$\bar{U}$ testing. The plot shows trends typical for normally consolidated (NC) or lightly overconsolidated clay (LOC) under low confining stress, at higher stress levels, trends show slight strain softening. Figure 3-39 confirms the dilatant behavior of specimens sheared under low confining stress with decreasing trend of generated excess pore water pressure. It is thought that the NC behavior of the stress-strain plots (shown in Figure 3-38) under low confining stress is actually influenced by the effect of dilatancy during shearing. Peak and post peak (or large strain) data points from each test are plotted in Figure 3-37. The best fit line defines the peak and post peak strength envelopes.

3.3.5.2 CI$\bar{U}$ test results from clay foundation

Both vertical and inclined specimens show elastic anisotropy to some degree during undrained shearing. Inclination of the stress paths towards the left (*i.e.* m>1) indicates that the sample has higher horizontal stiffness than its vertical stiffness (*e.g.* Graham and Houlsby 1983). Figure 3-41 and Figure 3-42 shows the stress-strain behavior and generation of excess pore water pressure of specimens, respectively, during undrained shearing. Results show that the clayey foundation has higher tendency to dilate as compared to the clay core. Effective strength envelopes for both vertical and inclined samples are shown in Figure 3-43 and Figure 3-44, respectively.

3.3.6 Direct Shear testing

Consolidated drained direct shear testing was also done to determine the shear strength of the samples along its horizontal plane. Testing was performed in accordance with ASTM D3080-98 standard. Residual strengths were achieved by the 'multiple reversal' method. It was noted that the clay blanket samples squeezed out of the shear box during the consolidation phase particularly under higher normal stresses (*i.e.* σ_n >200 kPa). Excessive clay had been squeezed out of the shear box under 400 kPa normal stress hence, the test result was not included. Figure 3-45 shows the stress-strain behavior of samples from the clay foundation, clay core and clay blanket, normalized by the applied normal stress. All three samples exhibit brittle behavior under low normal stress and behave more ductile as the normal stress increases. It is also interesting to note that the clay foundation and the clay blanket show more tendency to undergo strain softening as compared to that of the clay core. These are typical behaviors of fissured clay (Yoshida *et al.* 1991). The same can also be said for cemented clays. The fully softened strength was attained after 15%-20% of straining for most of the samples. The observed residual strengths are relatively low and seemed to be fairly consistent for all specimens between 7°-9°. This low residual strength is typical for smectite-rich soil as reported by Graham and Shields (1985) in their study on Lake Agassiz clays. Results from direct shear testing on clay foundation, clay core, and clay blanket are shown in Figure 3-46, Figure 3-47, Figure 3-48, respectively.

3.4 Summary and Discussion

3.4.1 Field Investigation

Based on *in-situ* filed investigation, the clay foundation is classified into three identifiable layers: weathered top soil, weathered mottled mix of brown and grey clay layer, and intensely fissured grey clay with random silt pockets. The same fissured grey clay layer with random silt pockets is also found in the upstream side of the dam (wet side) at Section A-A; it is suggested that the upper layer was stripped-off when the dam was constructed. The clay core is weathered on top (roughly above the phreatic surface), and has random silt lenses with traces of fissures with polished surfaces that are horizontally oriented. These fissures may be due to alignment of clay particles to some degree when water flows through the gaps in between clay nuggets[3]. Alignment of platy particles and particle groups can also be caused by anisotropic consolidation stresses (Mitchell, 1993). The clay blanket on the other hand is more uniform as compared to the clay core and clay foundation, with soft upper layer (depth < 0.6 m) and medium to stiff consistency at depth. During sample preparation, the clay blanket was observed to have some fissures with polished surfaces. Further, it was also noted that samples easily break along the fissured planes. Fell *et al.* (2015) suggested that the strength along these types of fissures can be as low as its residual strength due to the alignment of microstructure – examination under SEM has confirmed the alignment of clay particles.

[3] *J.Graham, personal communication, January 2016.*

The CPTu profile on the section with the observed movement shows a relatively weaker zone in the upper part of the clay core. *In-situ* cone tip resistance from CPTu were interpreted in terms of drained (ϕ' and c') and undrained parameters (Su). Interpreted drained parameters are found to be higher than what is determined from the laboratory tests. Results are shown in Figure 3-3and Figure 3-4. The difference is suggested to be mainly due to the difference of *in-situ* conditions and conditions simulated in the laboratory during testing (*e.g.* anisotropic vs. isotropic stress conditions), sample disturbance, and pore water pressure conditions. Undrained shear strength parameters were interpreted by establishing a correlation between the laboratory-based undrained shear strength and *in-situ* cone tip resistance (see Figure 3-6). An N_{kt} value of 35 was found to have a best fit line of the undrained shear strength and cone tip resistance. However, the established correlation is only true for the clay core materials and not for the clay foundation due to insufficient testing done under very low stresses corresponding to *in-situ* stress range of the clay foundation.

Survey data shows minimal toe bulging at the upstream toe of the dam at section with observed movement. This could mean that the observed movement might be more of a translational rather than of a rotational movement. This is true of most movement that involves fissured clays (Fell *et al.* 2015; Stark and Eid 1997).

3.4.2 Laboratory Testing

Index properties and soil classification results show that the clay foundation, clay core, and clay blanket are the same materials. Examination of the structural and mineralogical composition of the clayey materials shows dominant interlayered smectite-illite. Smectite contents are

suggested to be Montmorillonite with exchangeable Na^{+}or Ca^{+} cations. The content of smectite in the clay samples has significant engineering implications. These flaky minerals are swelling and/or expansive and have a very low inter-particle friction resulting in a low residual strength (Baracos 1977; Graham and Shields 1985; Loh and Holt 1974). Non-clay minerals are found to be mostly quartz, feldspar, and include traces of dolomite and calcium commonly in a form of silt pockets. No trace of sulfur was noted during SEM testing which could mean no gypsum (or gypsum residue) is present in the examined samples unlike Lake Agassiz clays in Winnipeg which is cemented with gypsum. Further, a quick acid test on whitish silt pockets/inclusions shows the presence of carbonates.

Fissures in microstructure level were also observed under SEM, particularly on specimens from the clay core. The presence of fissures in clay plays a significant role on why post peak strength governs over peak strength. The flow under the dam saturates these fissures which causes softening of the overconsolidated clay foundation. In addition to softening effects shear stress concentration in fissures also increases the stress where it exceeds the yield and shares the stress to its neighboring intact soil making it overstressed (Skempton *et al*. 1969)[4].

Laboratory based drained and undrained shear strengths at critical state (post peak) condition are summarized in Table 3-3. Based on the CI$\bar{U}$ triaxial testing and CD direct shear testing, results show that the clay core has anisotropic strength with horizontal shear strength less than its cross-shear strength, and that both strengths are independent of stress range. The clay

[4] *Also J.Blatz, personal communication, April 2016.*

foundation on the other hand shows anisotropic strength and a bilinear failure envelopes in both cross-shear and horizontal shear. Based on CI$\bar{U}$ test results under low confining stress, shear strengths are higher for both directions which subsequently decreases as the confining stress increases. Results also show a decrease in strength anisotropy as confining stress increases. Strength anisotropy is common for postglacial clays[5]. The bilinear failure envelope of the clay foundation is a typical trend for intensely fissured clays due to its dilatancy effect, as discussed in Chapter 2. As for the clay blanket, anisotropy in strength wasn't evaluated. The cross-shear strength of the clay blanket is unlikely to be mobilized based on the possible shape of slip surface, or if it would be, it would have less contribution. Under fully-softened (post peak) condition, a value of *c'=9 kPa* was calculated; however, to take into account the presence of fissures in the clay blanket the cohesion component is neglected (Rivard and Lu 1978; Skempton *et al.* 1968; Skempton *et al*. 1969; Stark and Eid 1997). Results also show that the horizontal drained shear strength of the clay blanket is relatively higher as compared to clay core and clay foundation, even its residual strength. The difference in horizontal shear strength could be attributed to different stress required to mobilize the strength along the uneven surface of the fissured clay, this is shown in the brittle strength behavior of the clay blanket. The low residual strength of the clay foundation (ϕ_r = 7°) relative to the residual strength of clay blanket (ϕ_r = 9°) could be directly related to its smectite content as determined from XRD testing.

[5] J.Graham (2015). "Understanding Clay Behavior in Modern Geotechnical Practice." *2015 CGS Manitoba Short Course.* Lecture 2b.

Table 3-1. Summary of classification results.

Location	Clay Foundation	Clay Core	Clay Blanket
Moist unit weight (kN/m^3)	17	17	17
Moisture Content (%)	38	38	40
Liquid limit (%)	85	80	84
Plasticity index (%)	54	58	56
Specific gravity, *Gs*	2.72	2.75	2.69
Minus #200, <0.075mm (%)	100	100	100
Clay fraction, <0.002mm (%)	76	80	73
Activity	0.71	0.73	0.77

Table 3-2. Summary of deformation characteristics.

Location	Clay Foundation	Clay Core	Clay Blanket
Pre-consolidation/apparent pre-consolidation pressure (kPa)	85	150	170
OCR/ OCR $_{apparent}$	4.6	2	1.5
Compression index , Cc	0.1235	0.1252	0.1448
Recompression index, Cr	0.0275	0.0243	0.0420

Table 3-3. Summary of drained and undrained shear strengths at critical state condition.

	Clay Core		Clay Foundation		Clay Blanket
Stress range	*Φ′* (°) *cross shear*†	*Φ′* (°) *horizontal shear*‡	*Φ′* (°) *cross shear*†	*Φ′* (°) *horizontal shear*†	*Φ′* (°) *horizontal shear*‡
Stress <110 kPa	19	12	24	29	15
Stress > 110 kPa	19	12	18	16	15
Residual strength‡	-	8	-	7	9

†*Undrained triaxial test* ‡*Drained direct shear test*

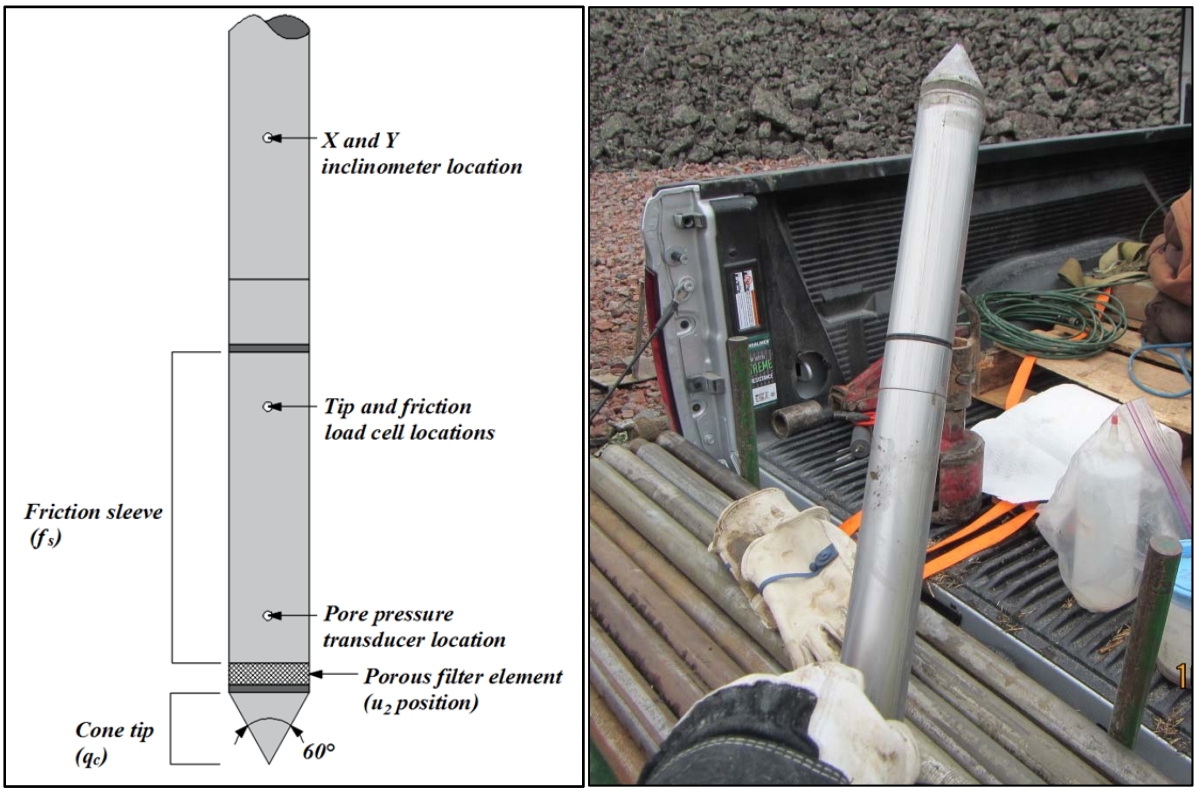

Figure 3-1. Piezocone Penetrometer (10 cm^2).

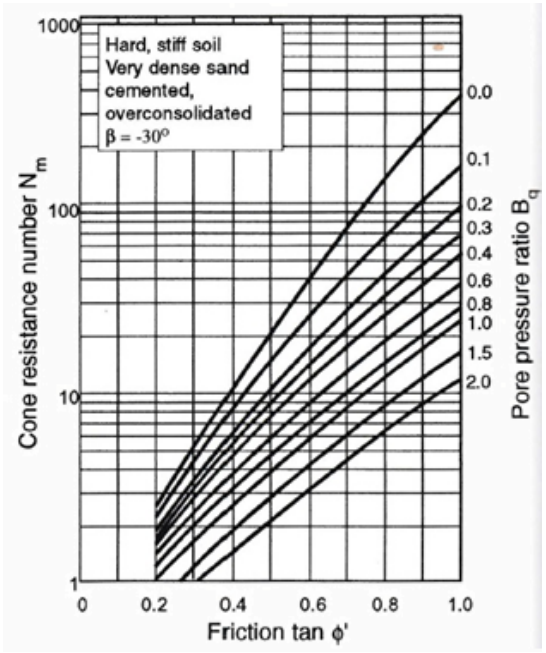

Figure 3-2. Effective stress bearing capacity factors (after Senneset *et al.*, 1988). (Used with permission)

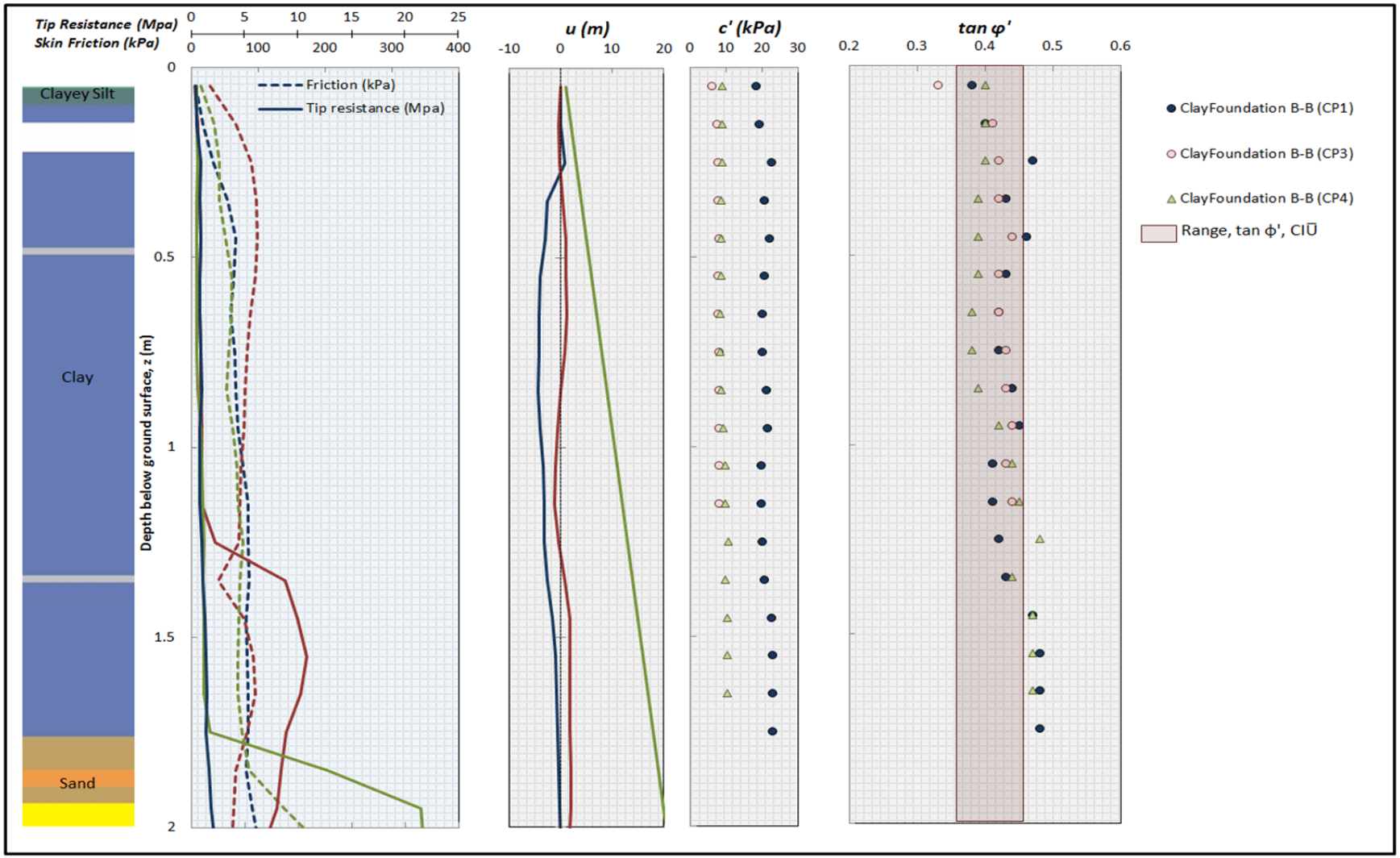

Figure 3-3. CPTu data and correlated drained parameters (ϕ' and c') from clay foundation.

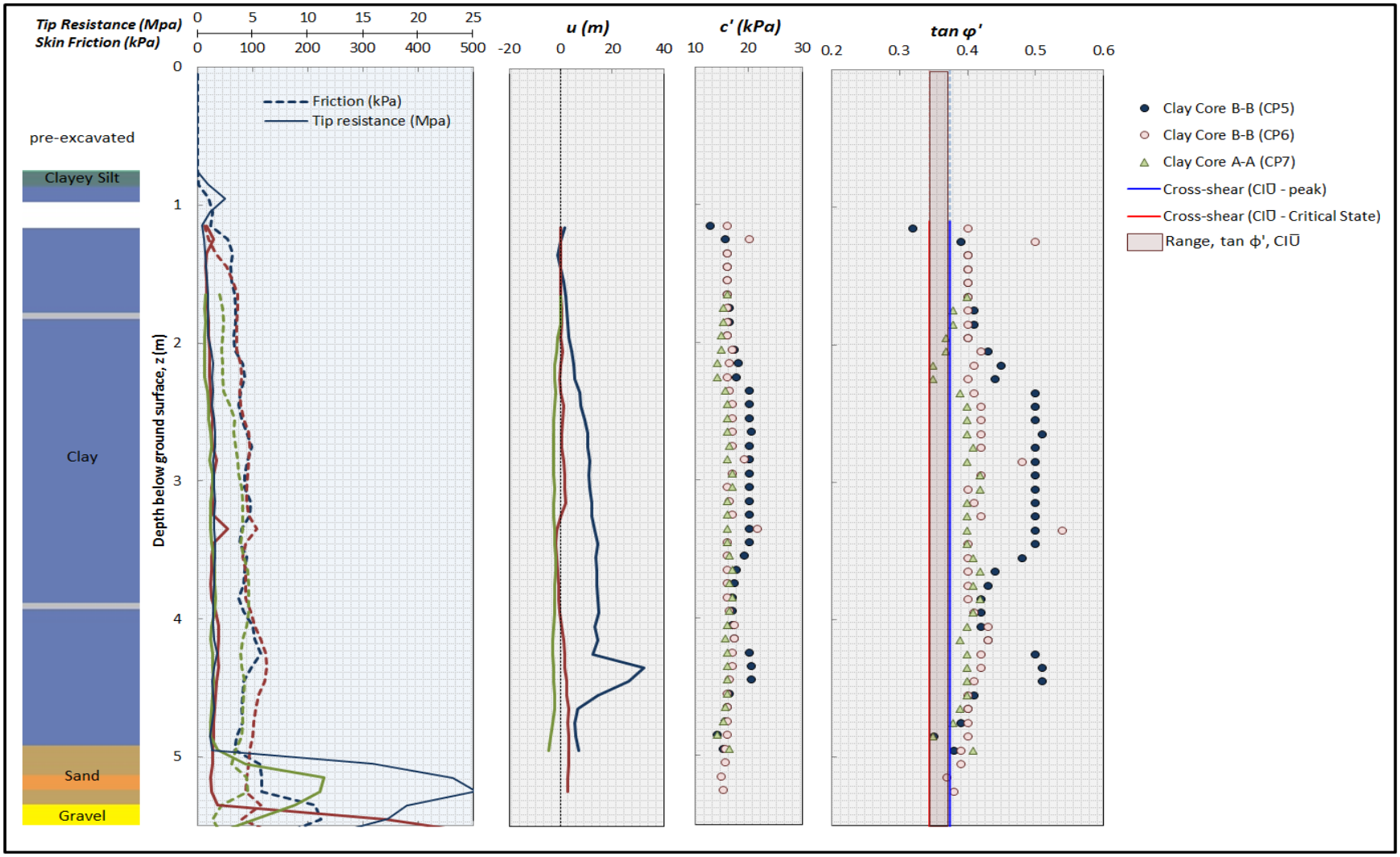

Figure 3-4. CPTu data and correlated drained parameters (*φ' and c'*) from clay core.

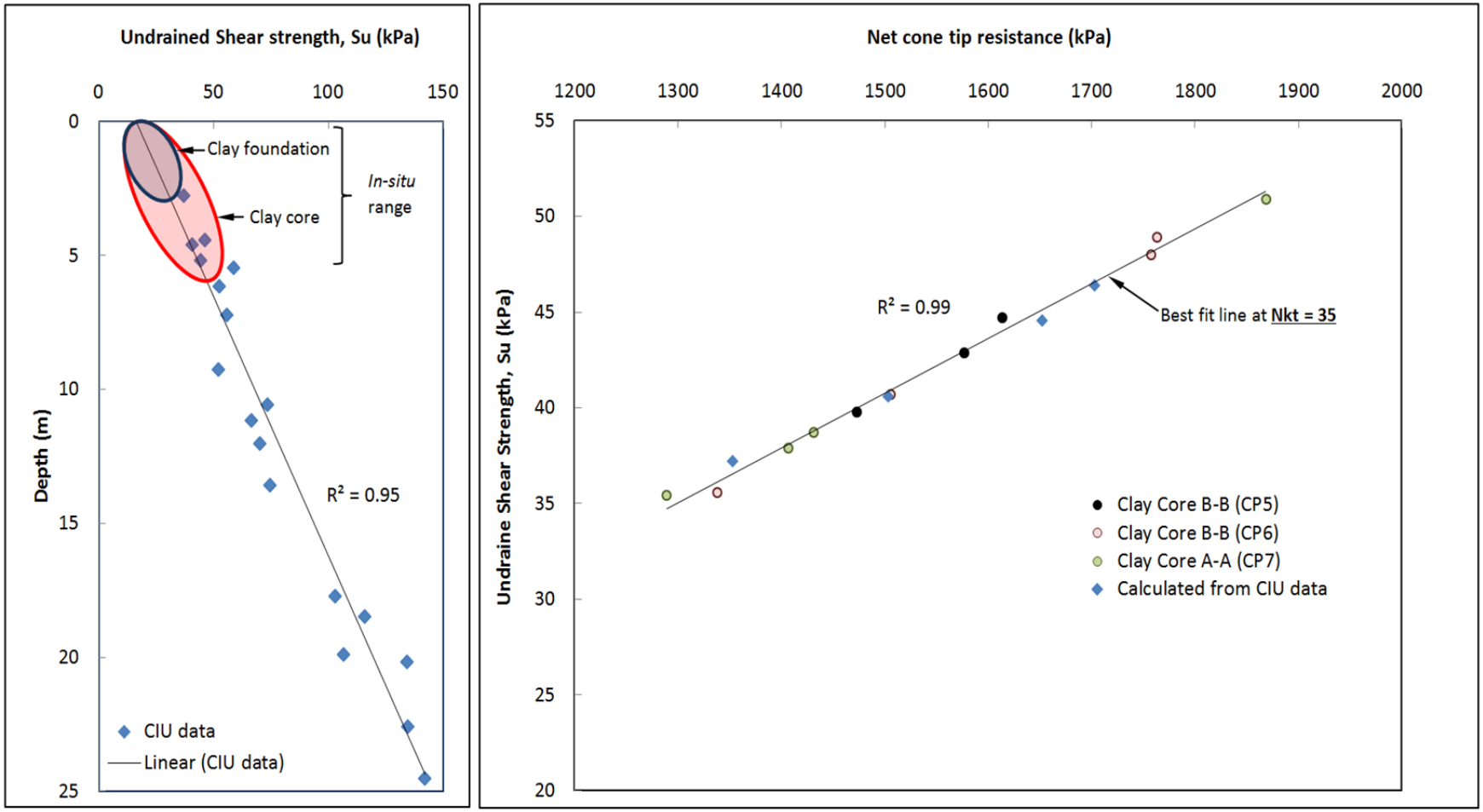

Figure 3-5. Undrained strength with depth based on CIU testing (left); best fit line of *in-situ* and laboratory based undrained shear strength, with Nkt =35 (right).

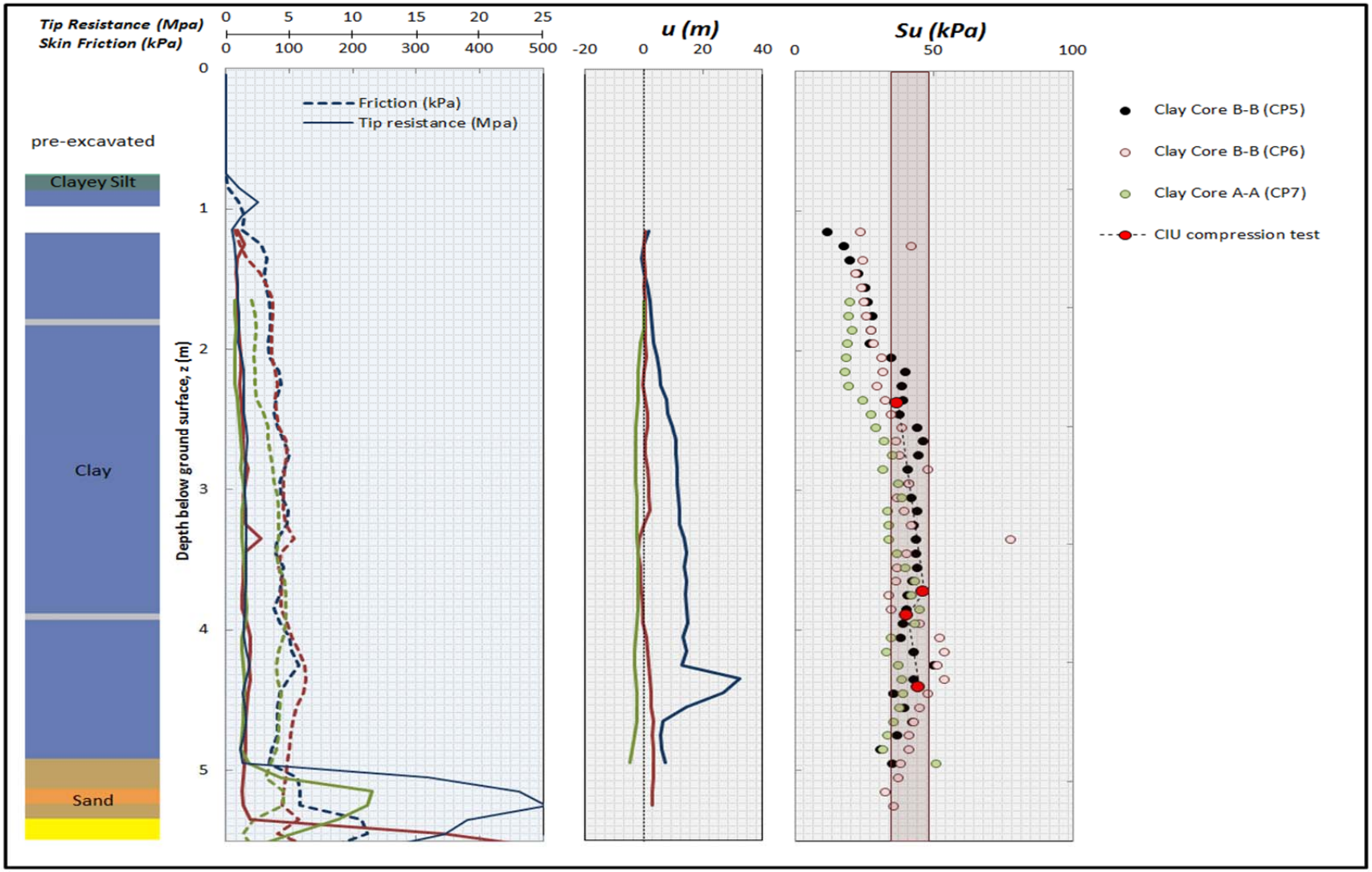

Figure 3-6. CPTu data and correlated undrained strength (Su) from clay core.

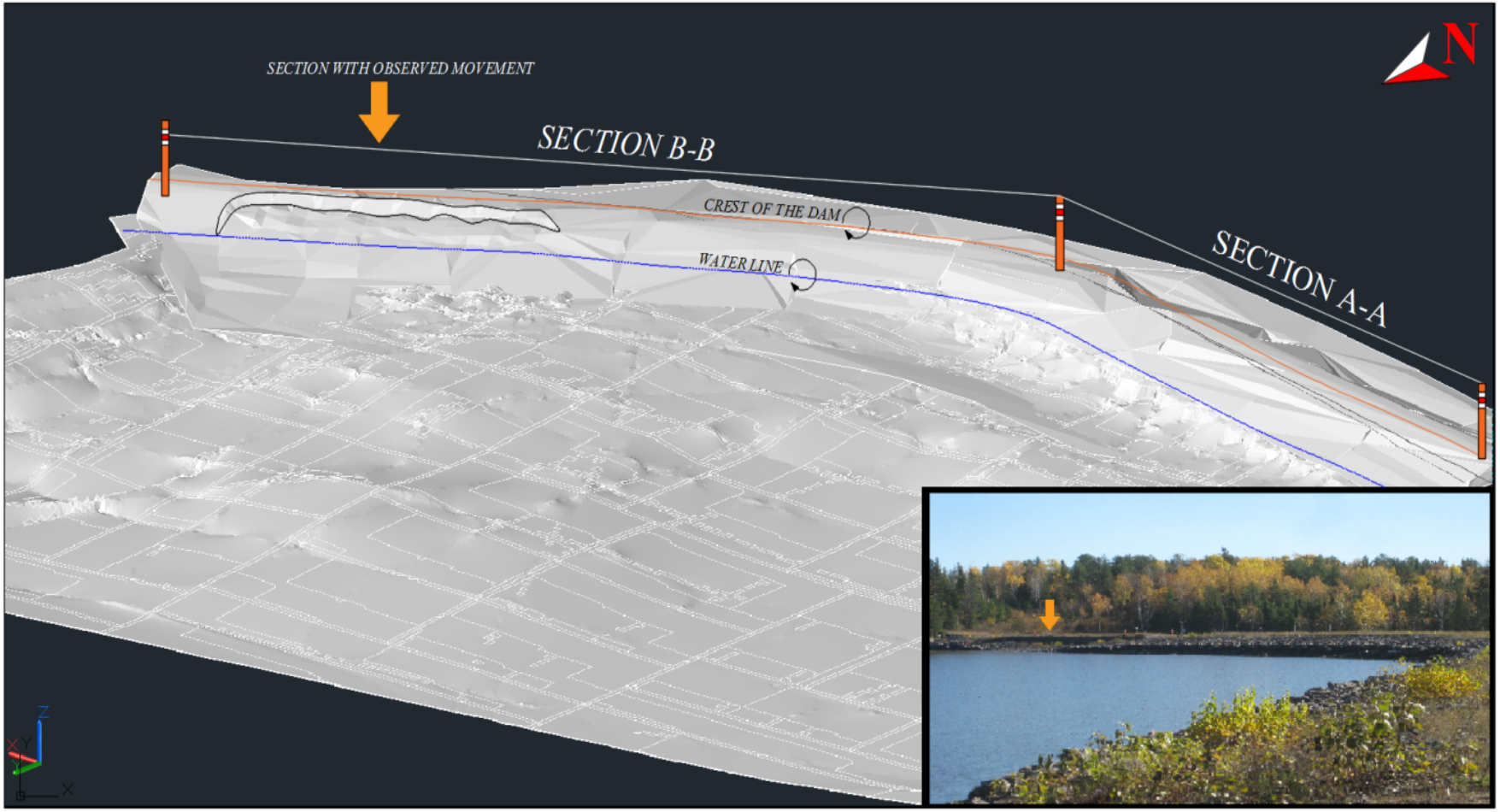

Figure 3-7. 3D model of Block Dam No.2.

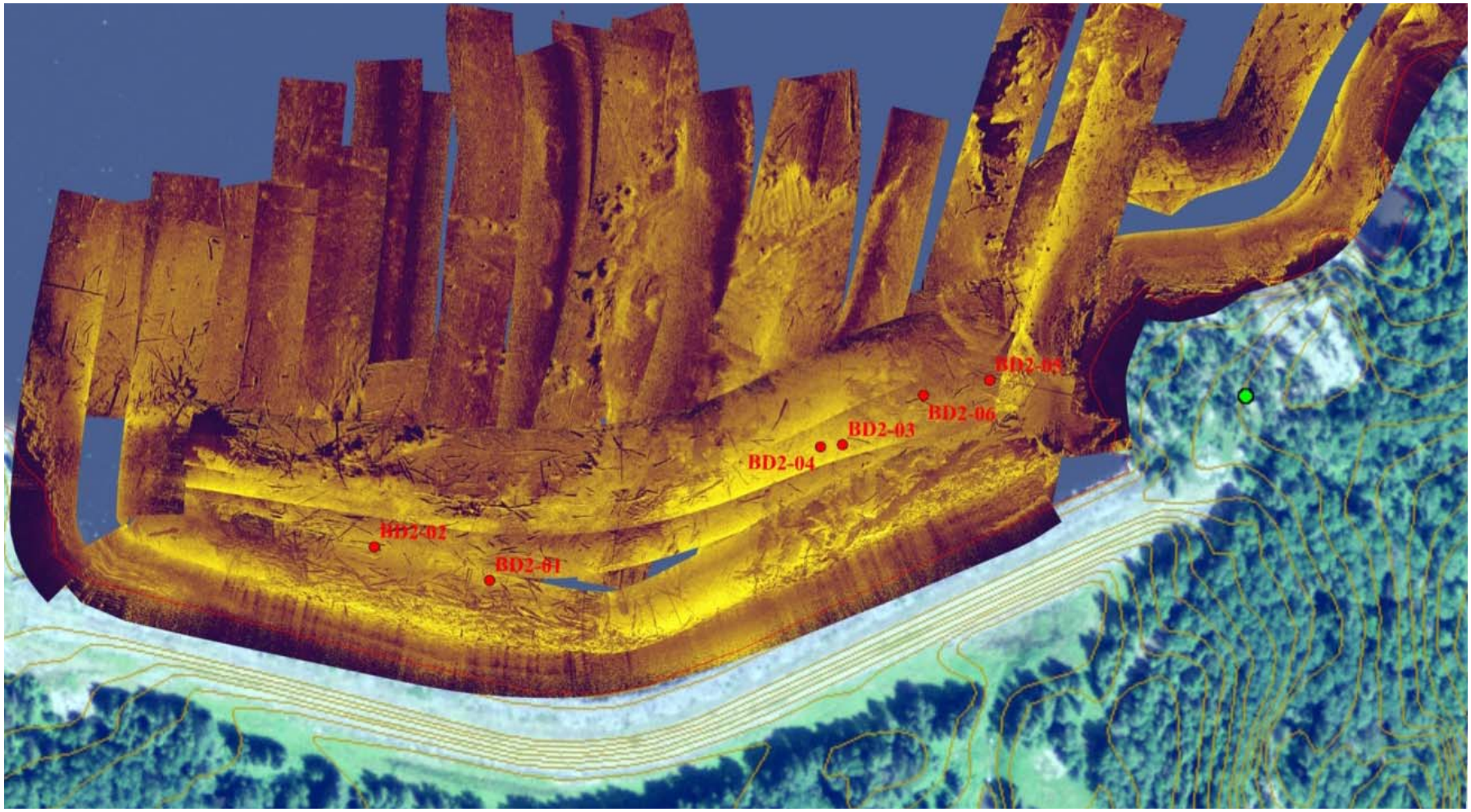

Figure 3-8. Sidescan image showing randomly oriented logs and locations of ponar grabs.

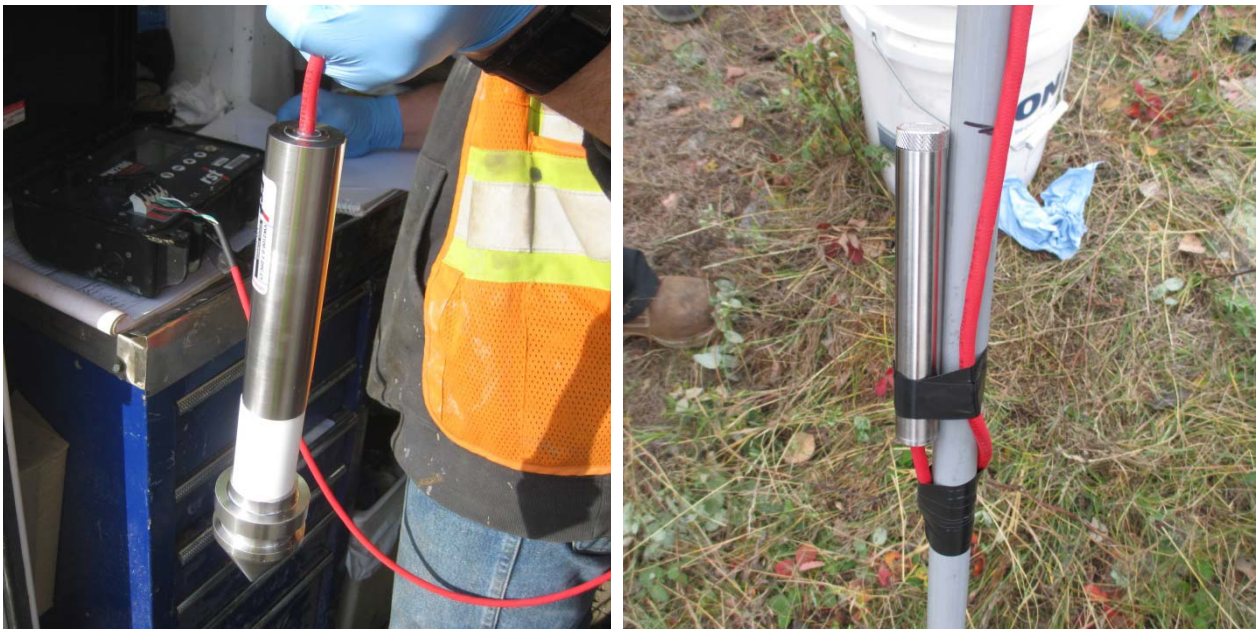

Figure 3-9. VW2100-DP (left) and VW2100 (right) piezometers.

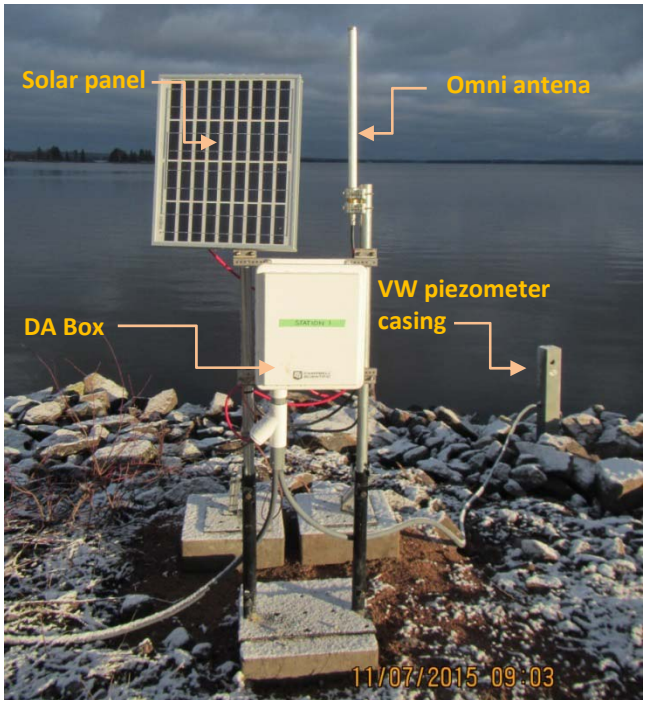

Figure 3-10. Automated data collection for VW piezometers.

Figure 3-11. Inclined samples pushed into the test pit walls.

Figure 3-12. Block samples obtained using block sampler (left) and conventional method (right).

Figure 3-13. Soil profile from Test Pit 2 in Block Dam No.2.

Figure 3-14. Fissured clay foundation from Test Pit 2 at depth = 7 ft.

Figure 3-15. Off-shore samples. Fissured clay foundation at Section A-A (left), and soft clay blanket at Section B-B (right).

Figure 3-16. Clay core (left) and clay foundation (right) samples.

Figure 3-17. Clay core sample breaks easily along horizontal planes with silt lenses.

Figure 3-18. Polished fissures from clay core (left) and clay blanket (right) samples.

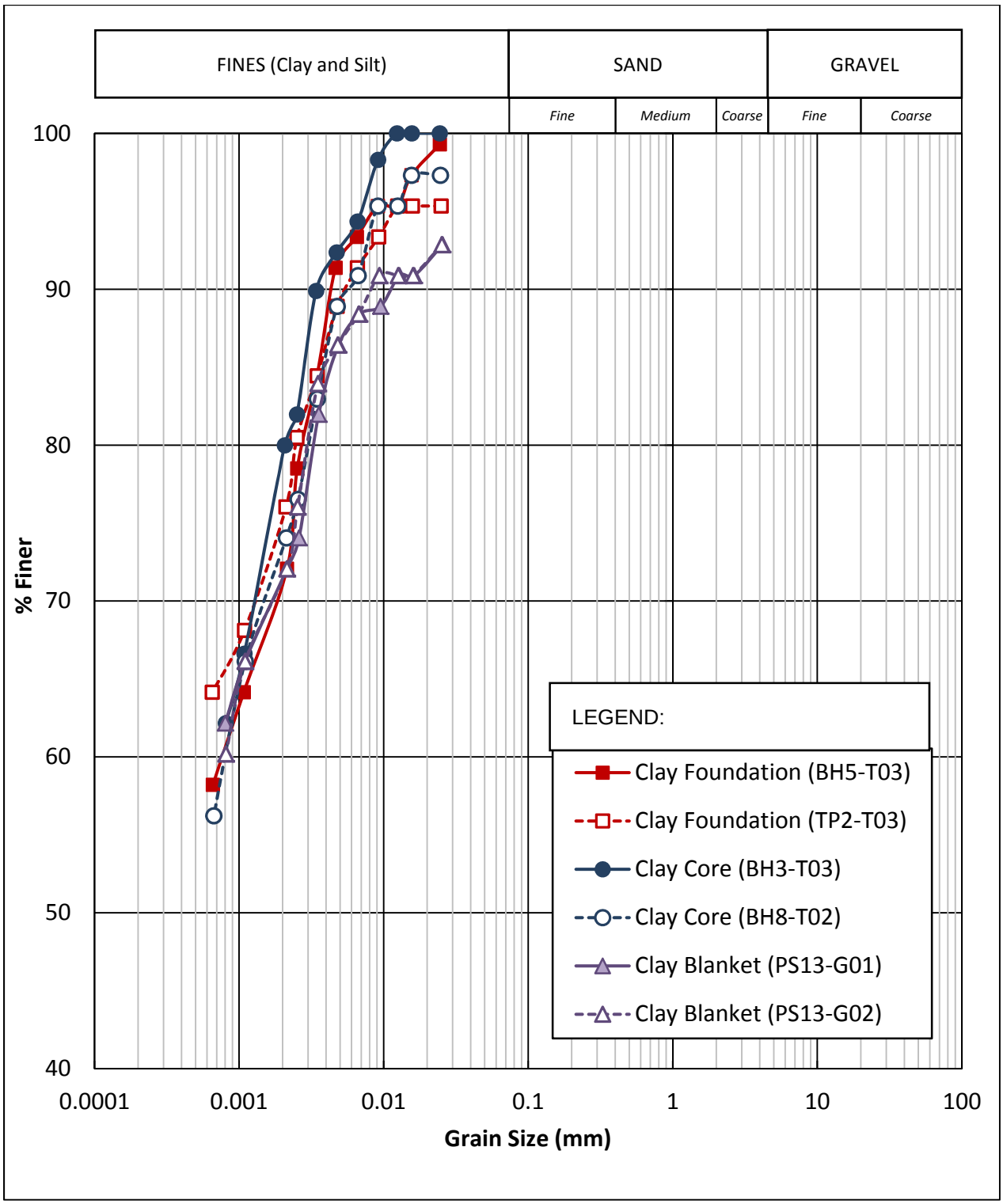

Figure 3-19. Particle size distribution curve.

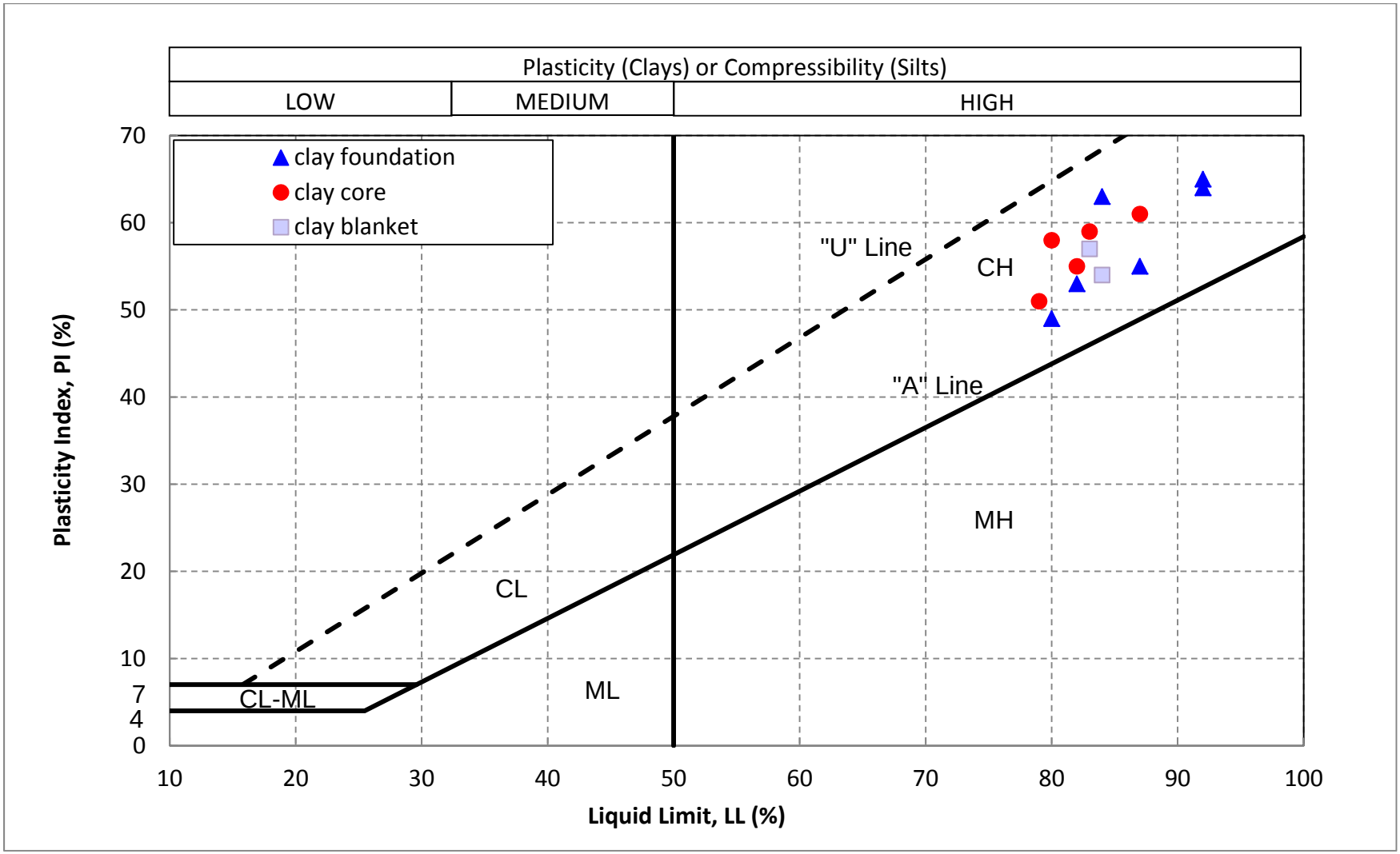

Figure 3-20. Plasticity chart.

Figure 3-21. 2 cm x 1 cm specimens for SEM testing.

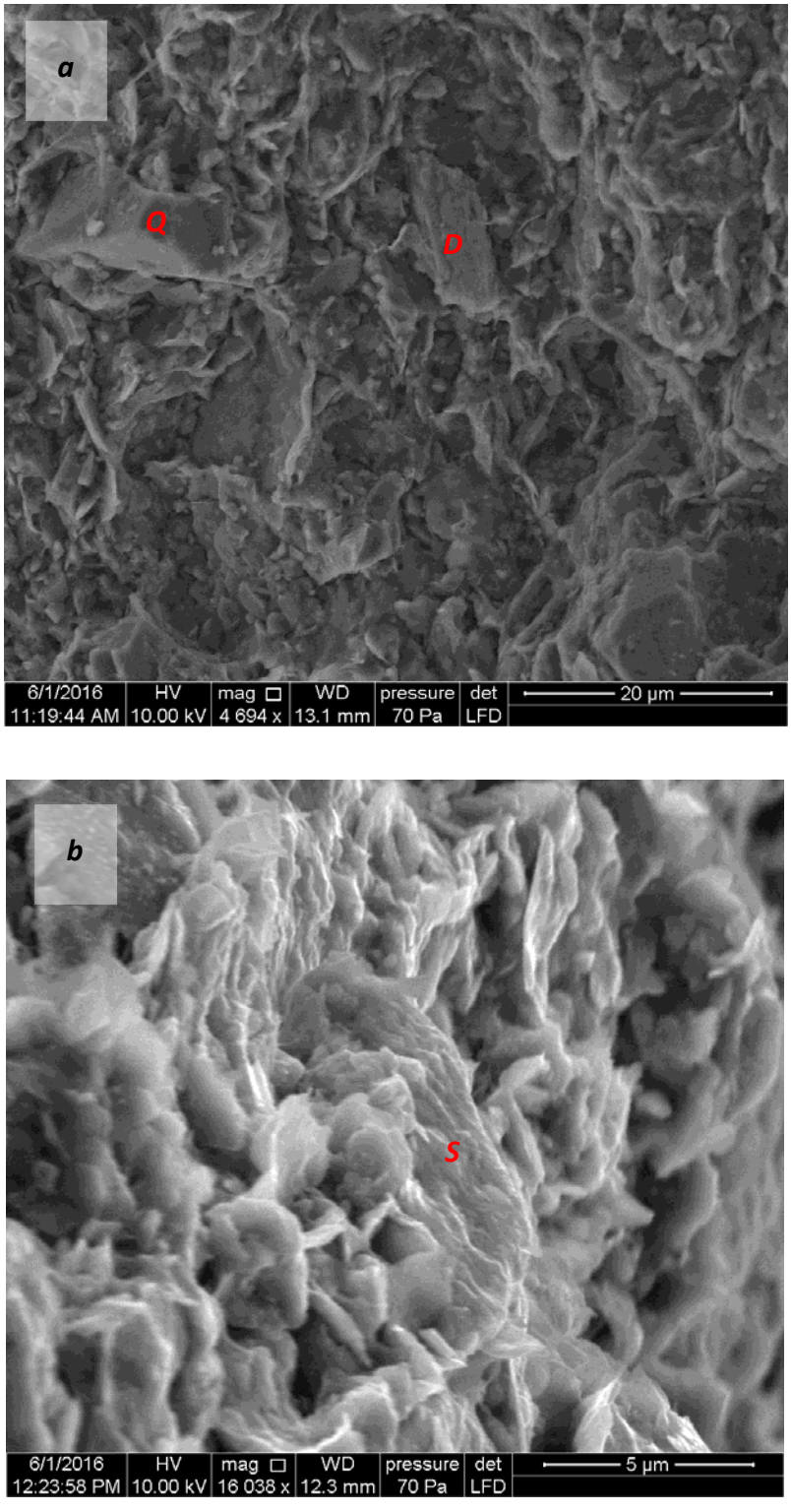

Figure 3-22. Clay foundation specimen at depth> 2 m (a) under 4 694 magnification, 20 µm (b) under 16 038 magnification, 5 µm.

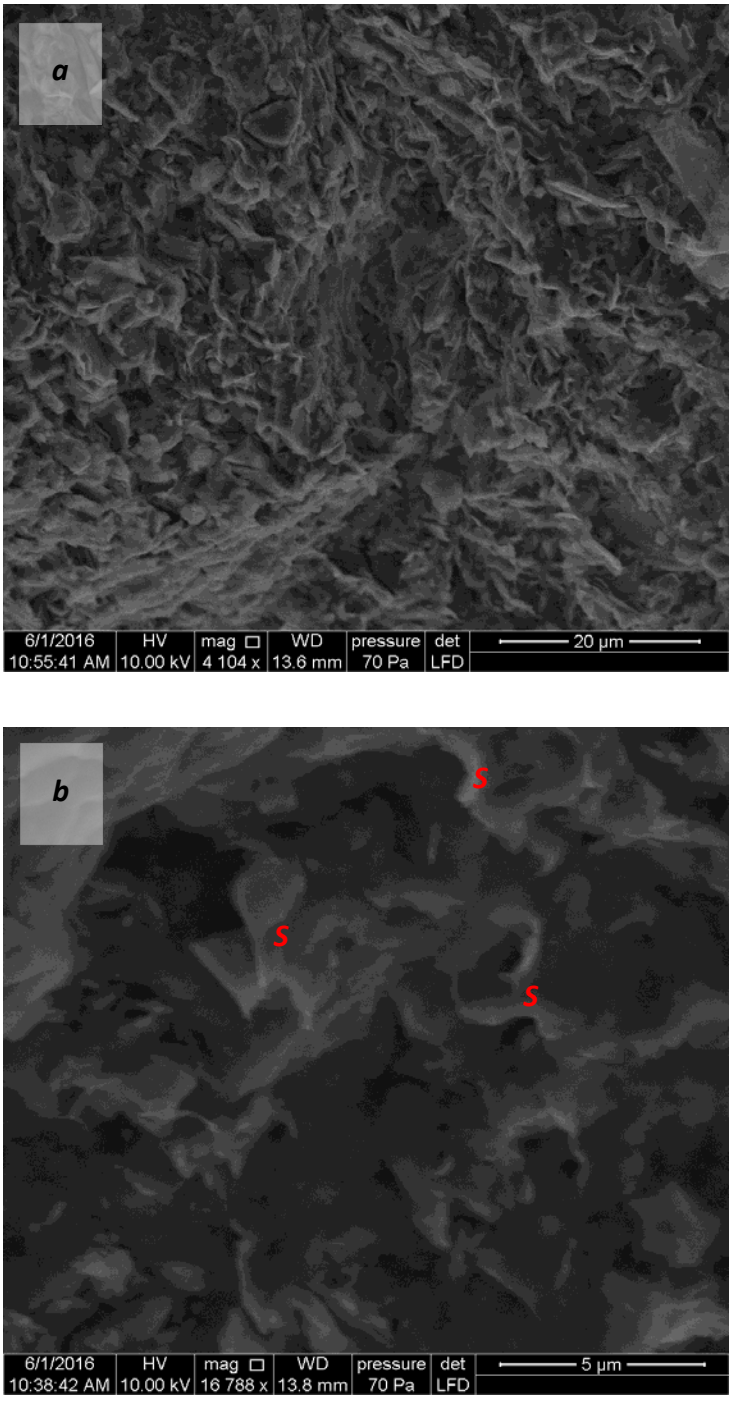

Figure 3-23. Clay foundation specimen at depth < 0.7 m (a) under 4 104 magnification, 20 µm (b) under 16 788 magnification, 5 µm.

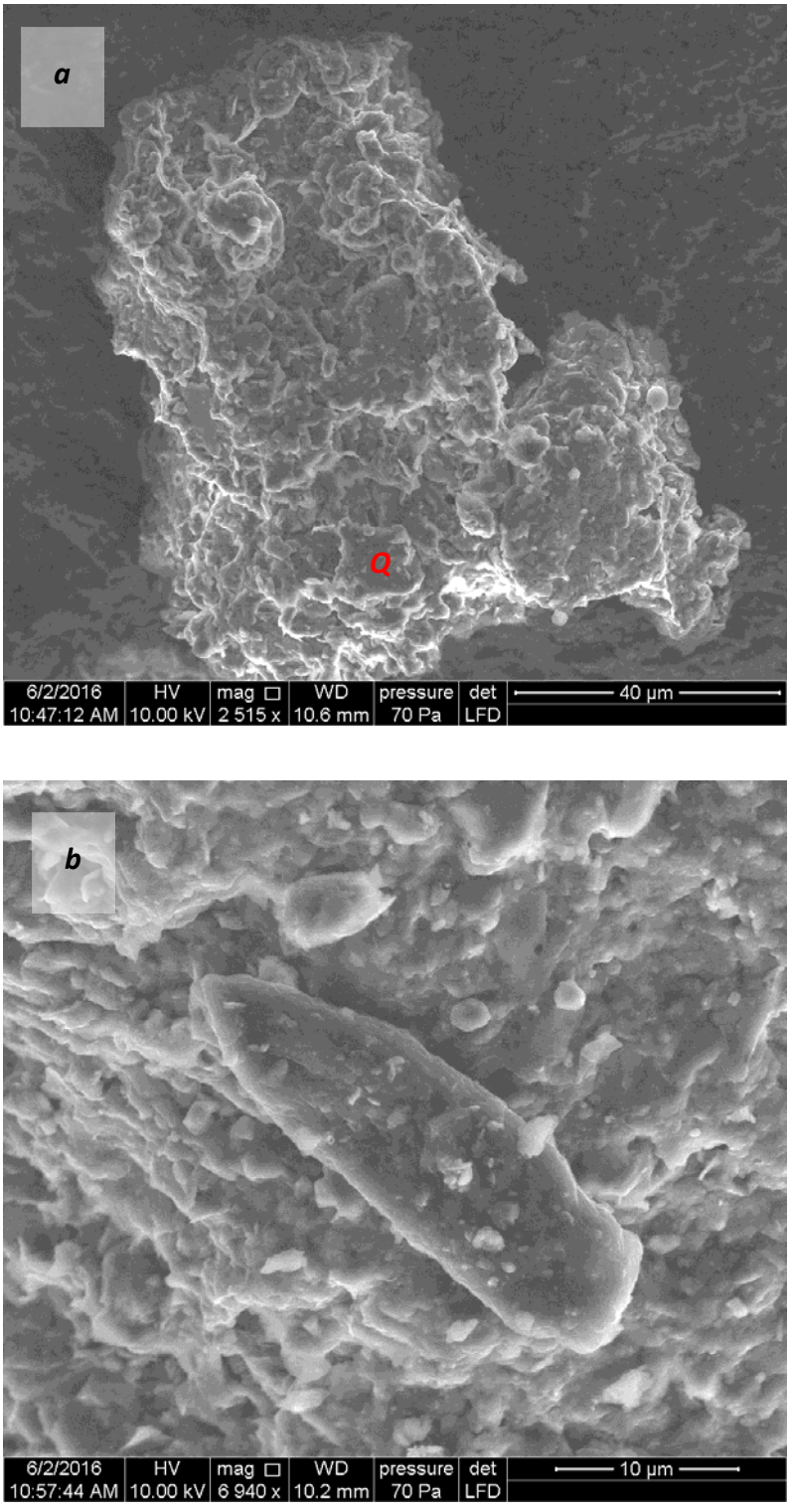

Figure 3-24. Clay core specimen obtained below the phreatic surface (a) under 2 515 magnification, 40 µm (b) under 6 940 magnification, 5 µm.

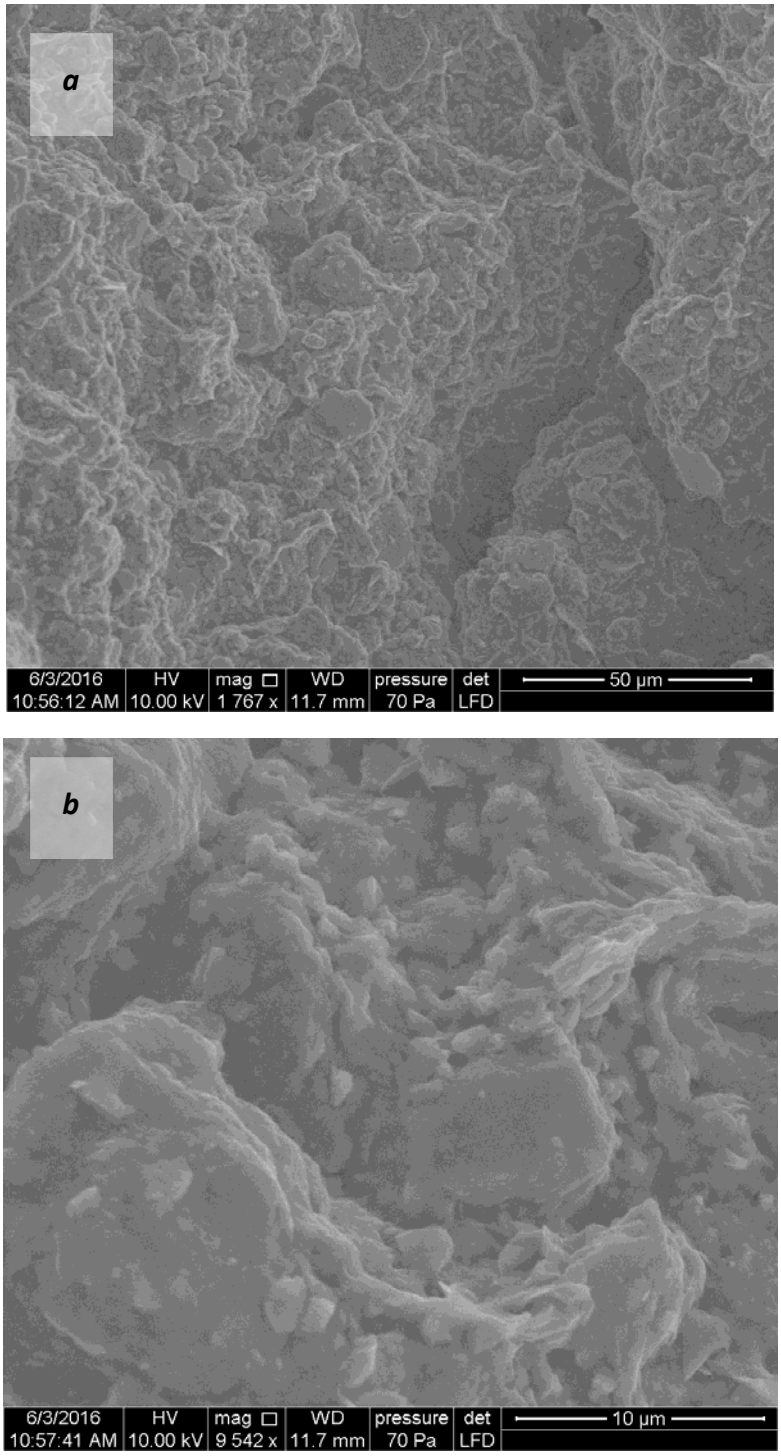

Figure 3-25. Clay core specimen obtained above the phreatic surface (a) under 1 767 magnification, 50 µm (b) under 9 542 magnification, 10 µm.

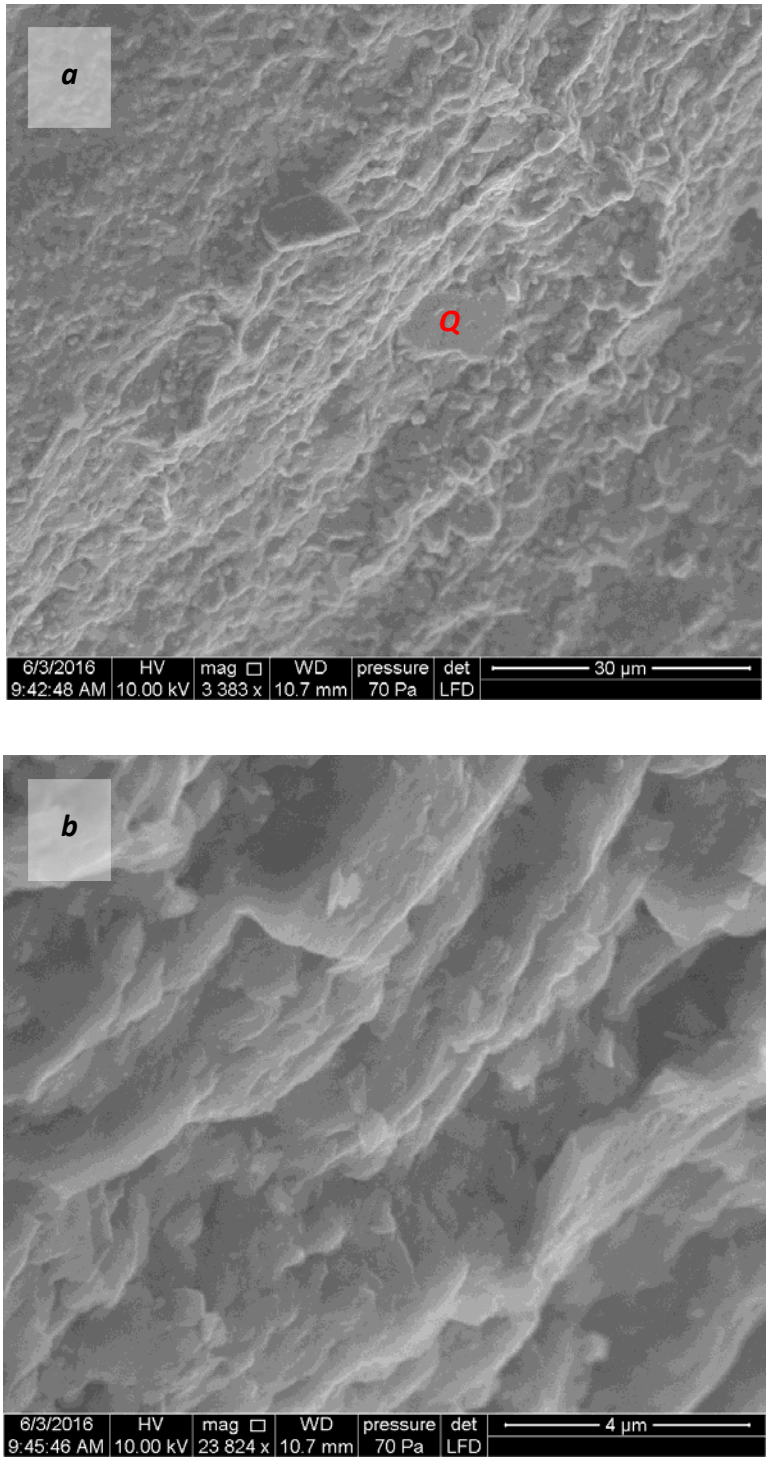

Figure 3-26. Clay core specimen with observed polished fissures (a) under 3 383 magnification, 30 µm (b) under 23 824 magnification, 4 µm.

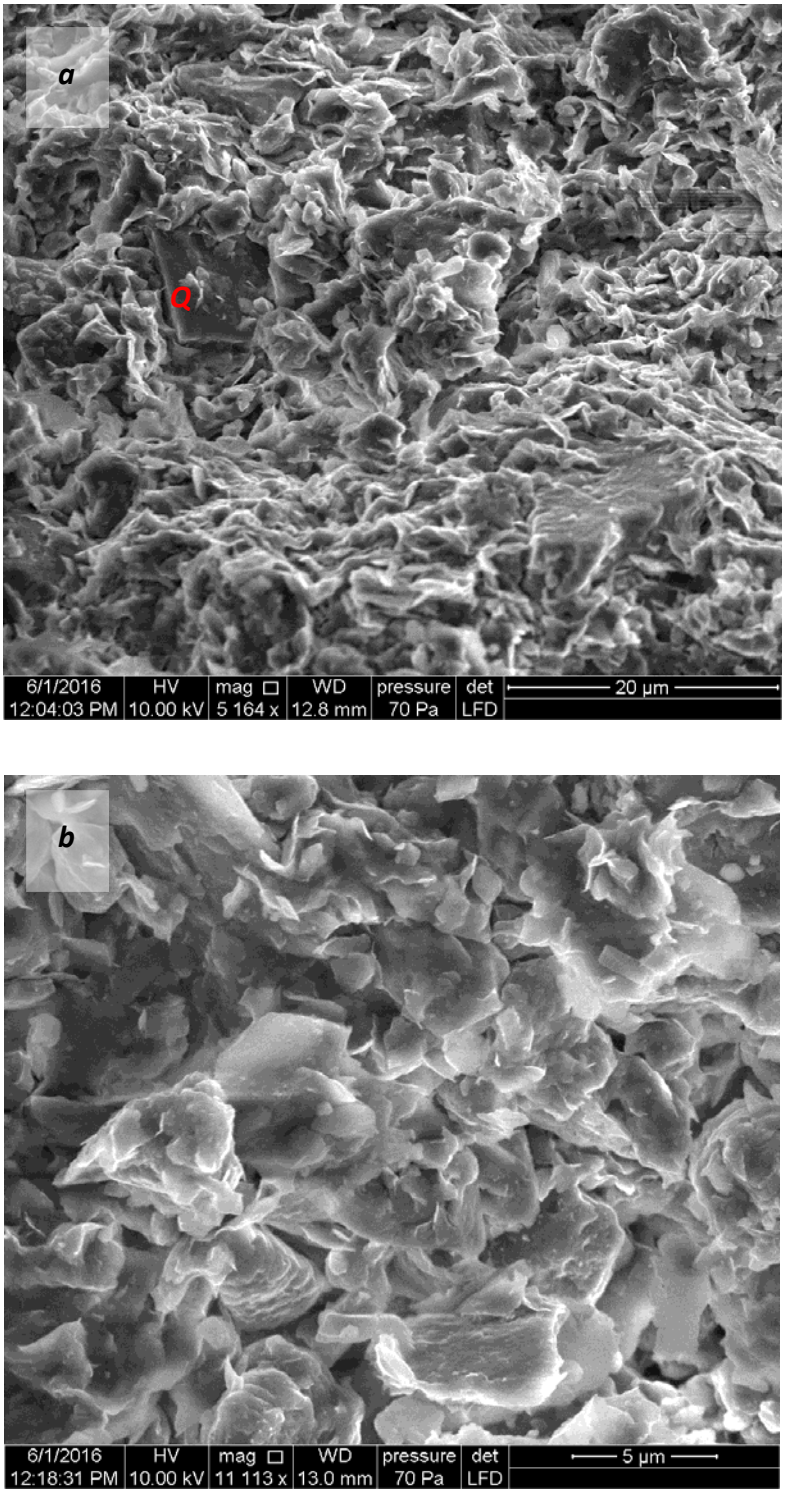

Figure 3-27. Specimen from top layer of clay blanket (a) under 5 164 magnification, 20 µm (b) under 11 113 magnification, 5 µm.

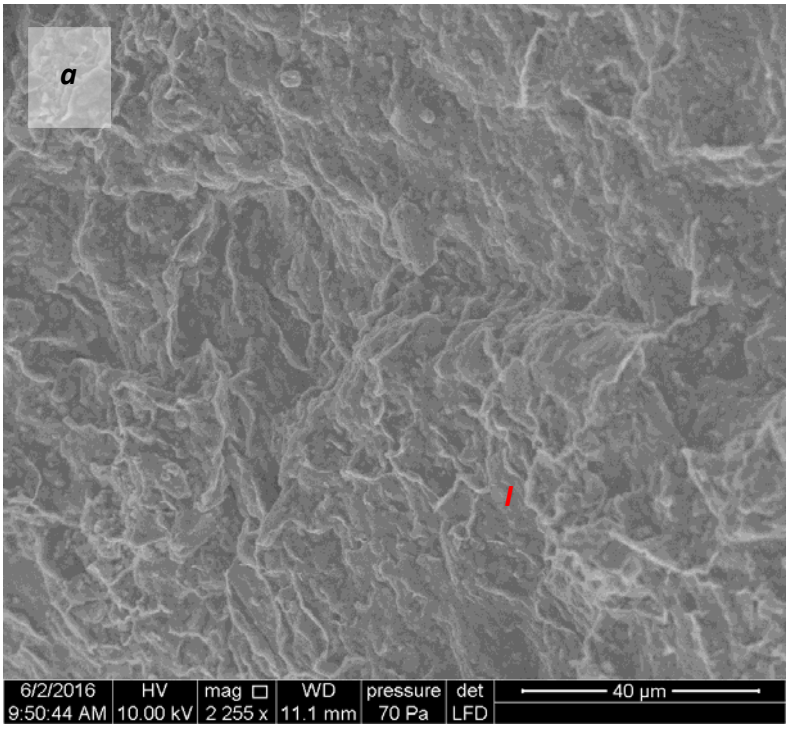

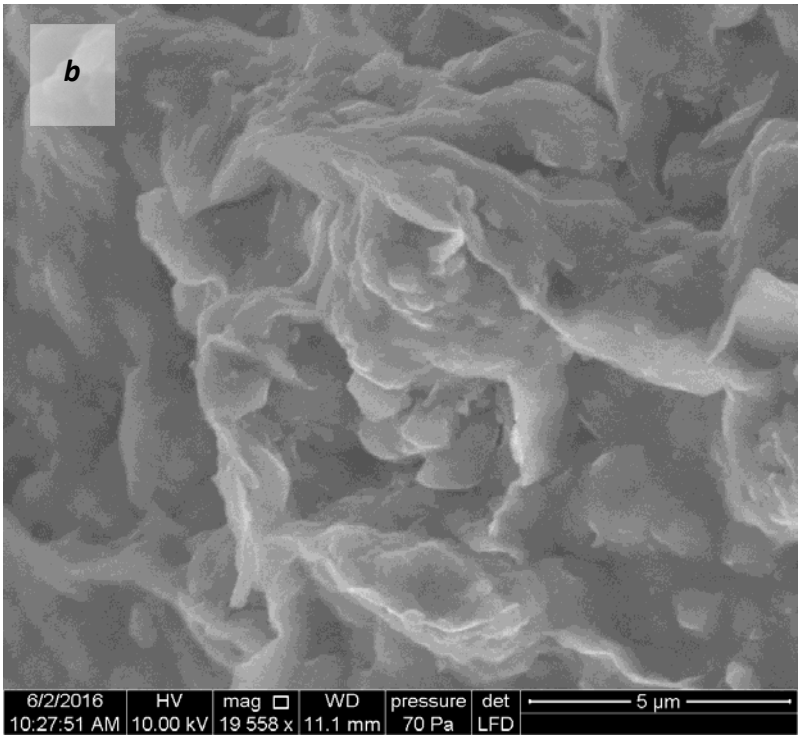

Figure 3-28. Specimen from bottom layer of clay blanket (a) under 2 255 magnification, 40 µm (b) under 19 558 magnification, 5 µm.

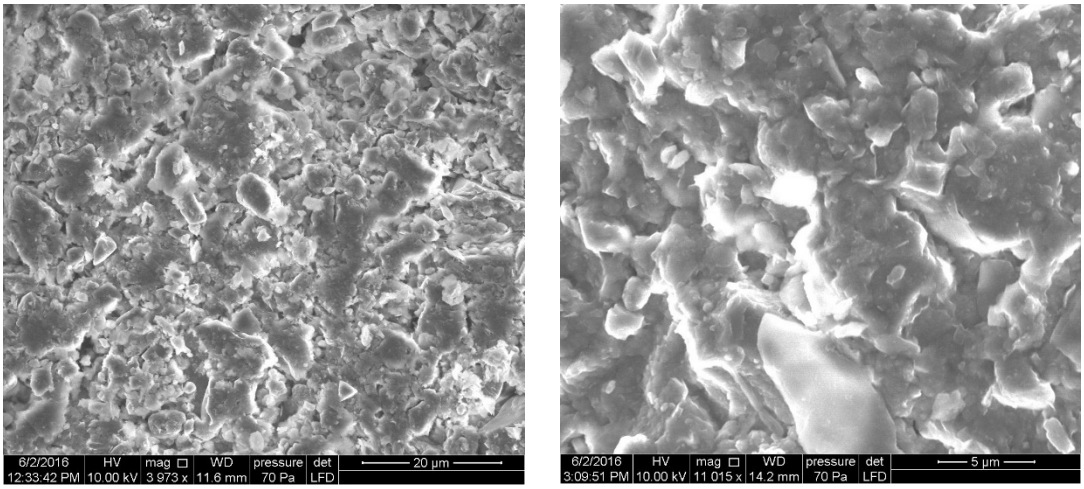

Figure 3-29. Light colored patches in the specimen under (a) 3 973 magnification, 20 µm, (b) 11 015 magnification, 5 µm.

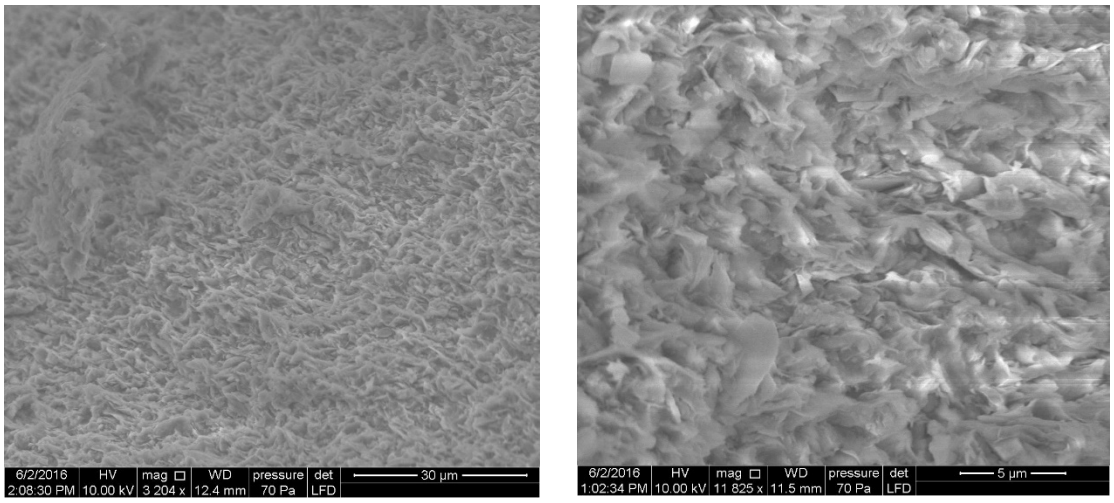

Figure 3-30. Dark colored patches in the specimen under (a) 3 204 magnification, 30 µm, (b) 11 825 magnification, 5 µm.

Energy Dispersive X-ray Spectrum (EDX)

Smectite $(\frac{1}{2}Ca, Na)_{0.7}(Al, Mg, Fe)_4[(Si, Al)_8O_{20}](OH)_4 \bullet nH_2O$

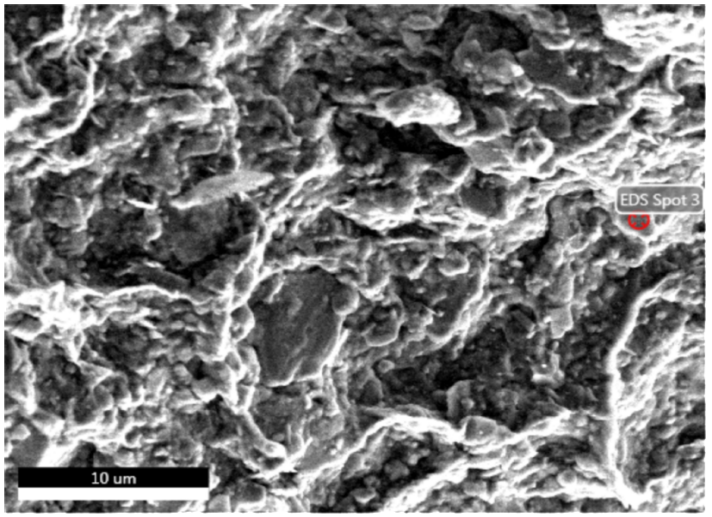

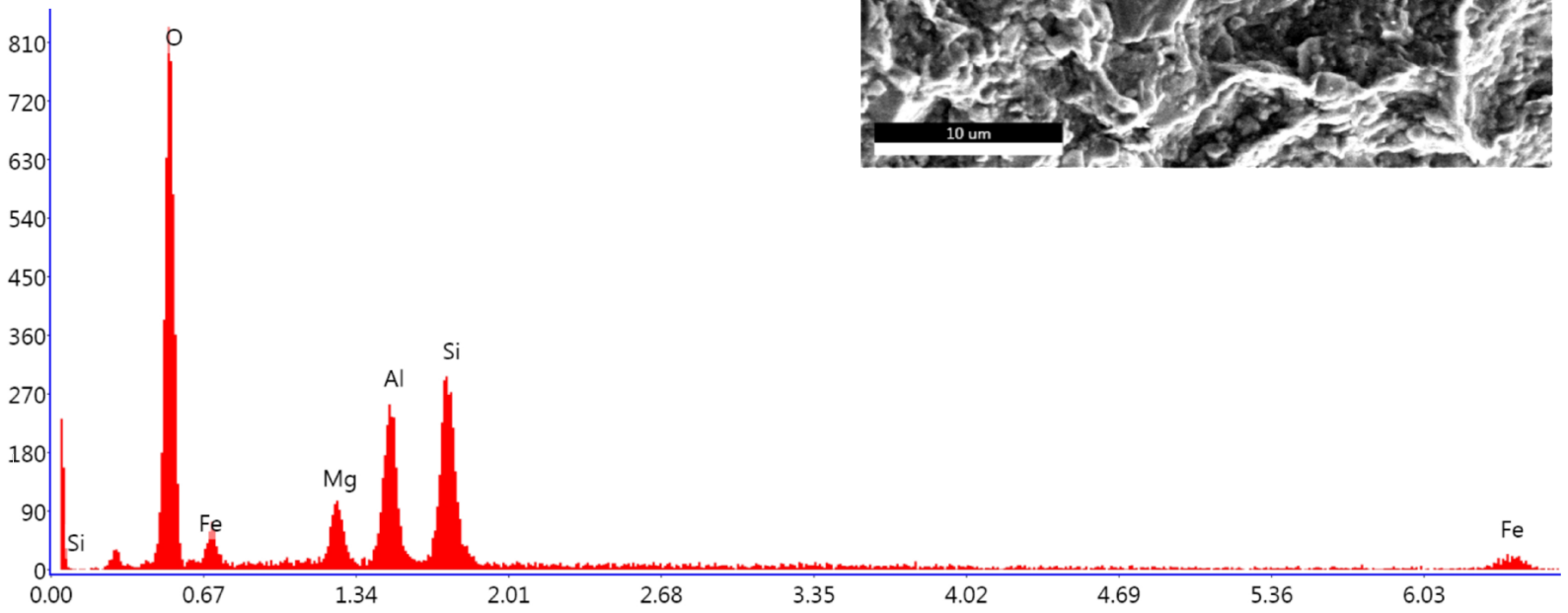

Figure 3-31.Energy Dispersive X-ray Spectrum (EDX) from clay foundation.

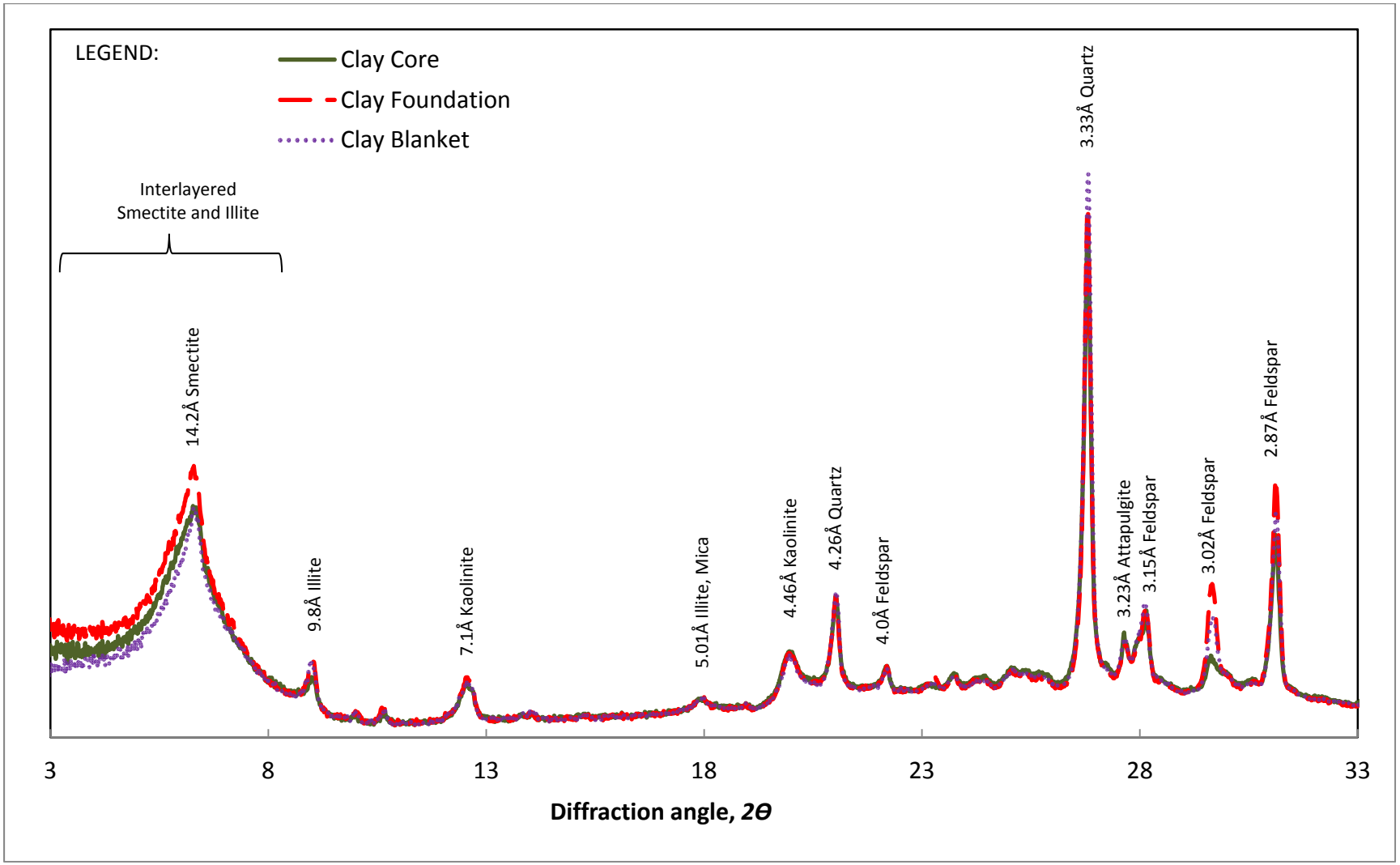

Figure 3-32. X-ray diffraction patterns of air dried powder specimens.

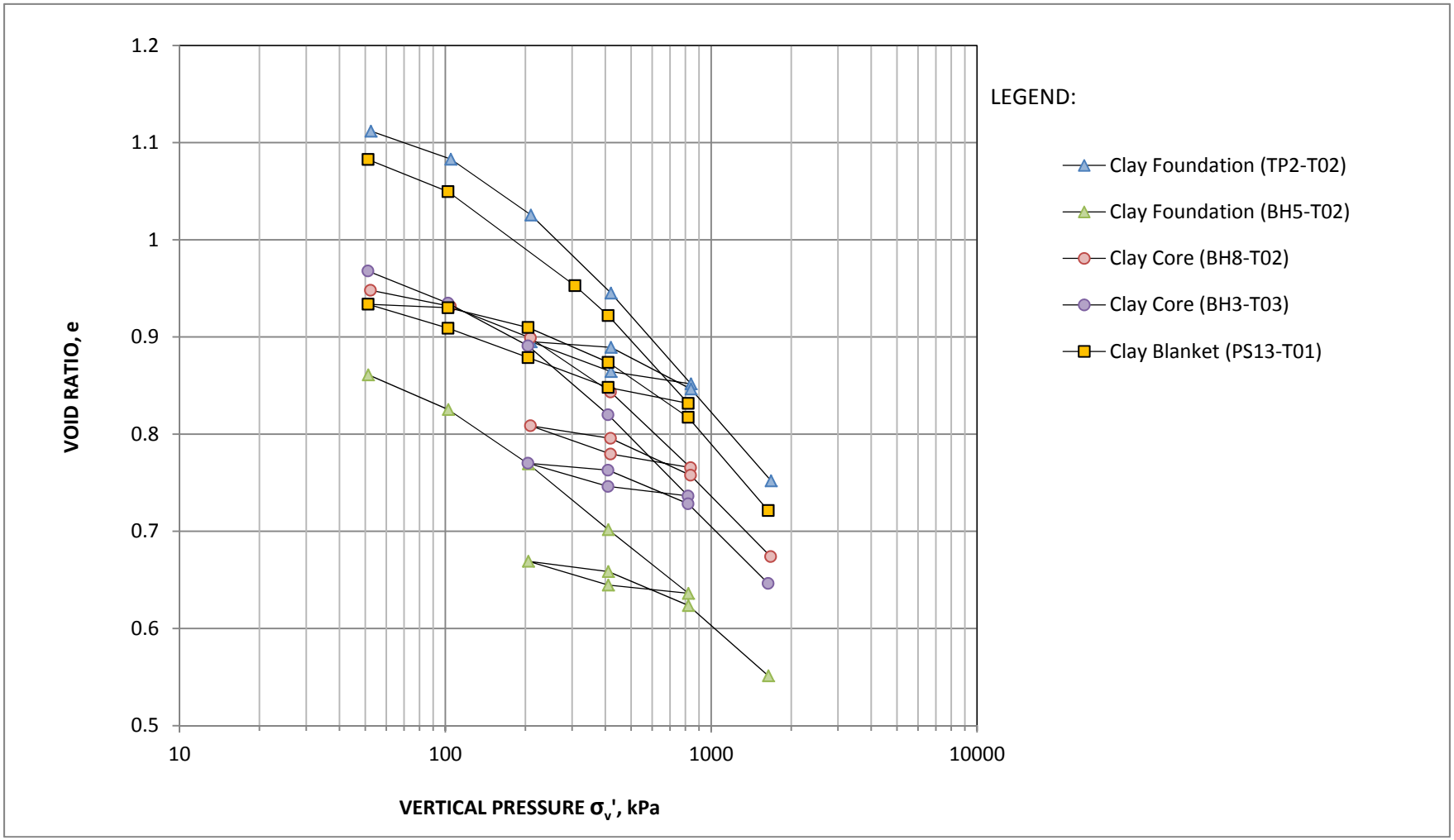

Figure 3-33. 1D consolidation results.

Figure 3-34. 71.12 mm diameter triaxial specimen with shown silt pockets from clay foundation.

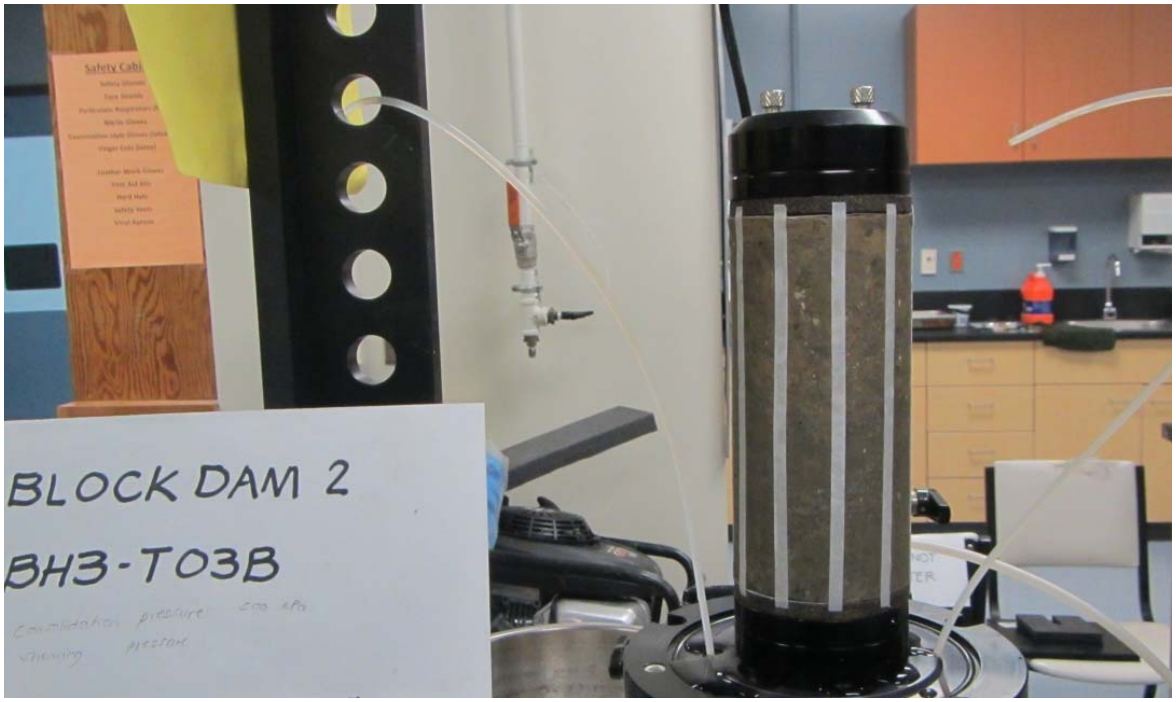

Figure 3-35. 71.12 mm diameter triaxial specimen from clay core.

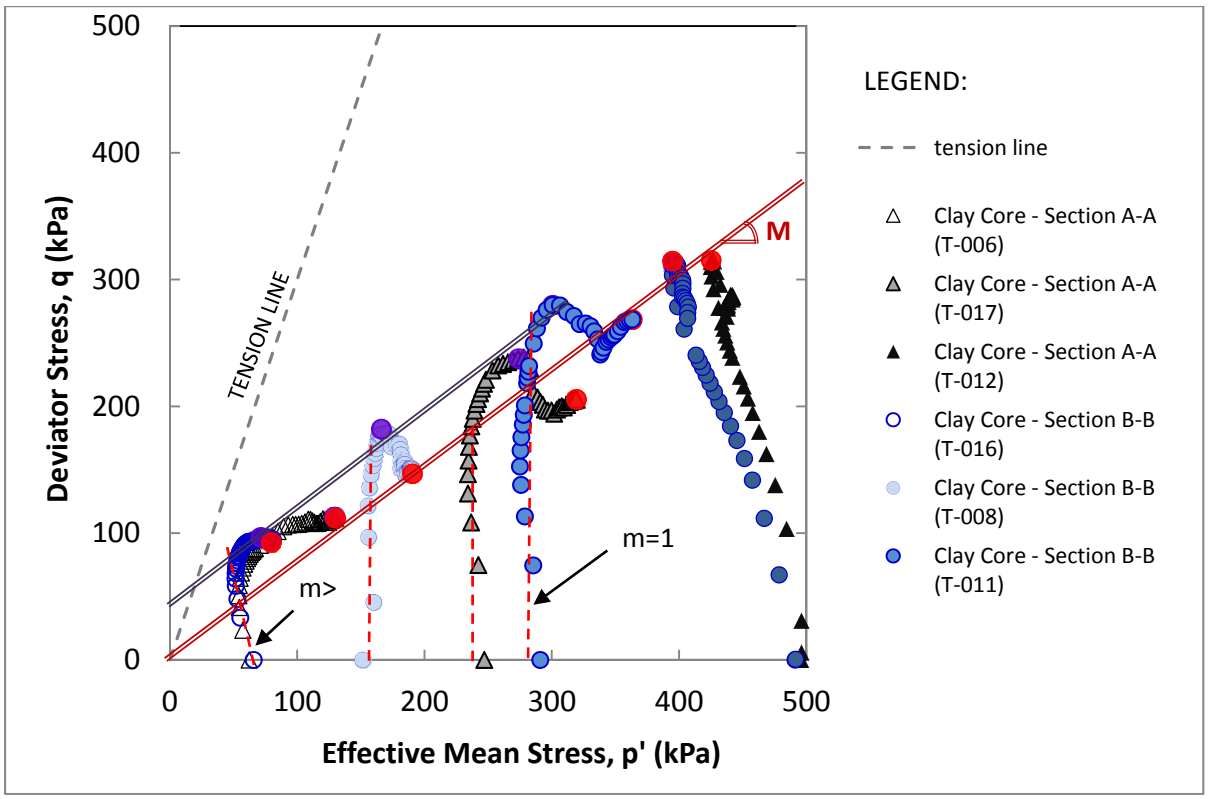

Figure 3-36. Stress paths in q-p space for clay core samples.

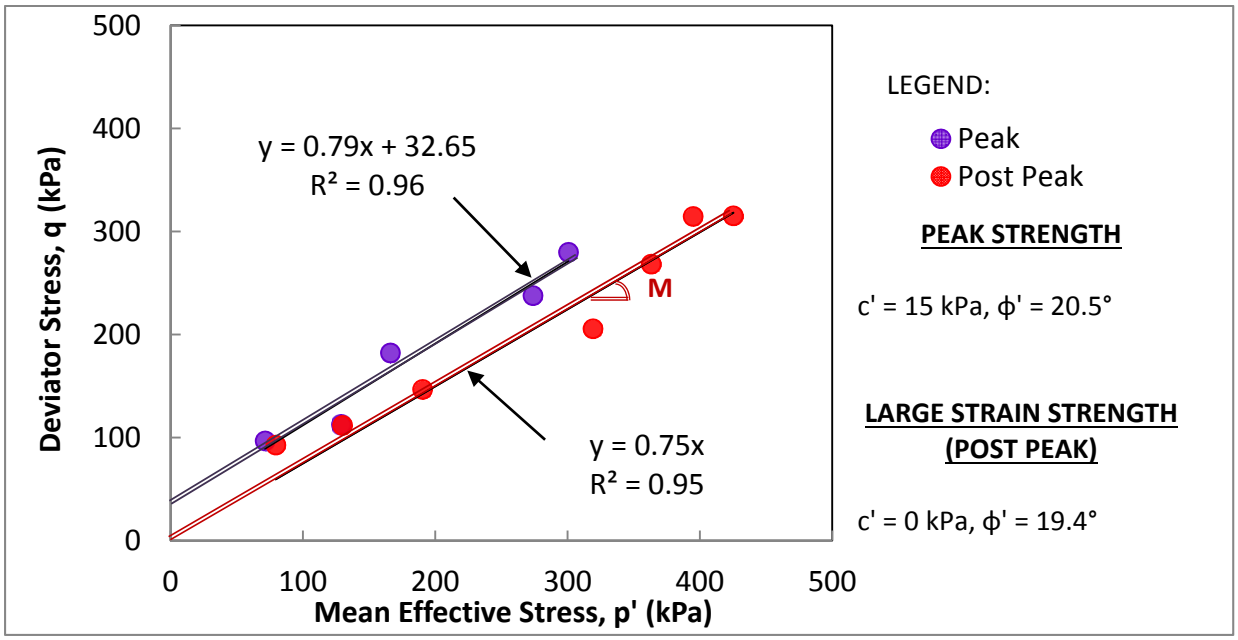

Figure 3-37. Peak and large strain (or post peak) effective strengths from clay core.

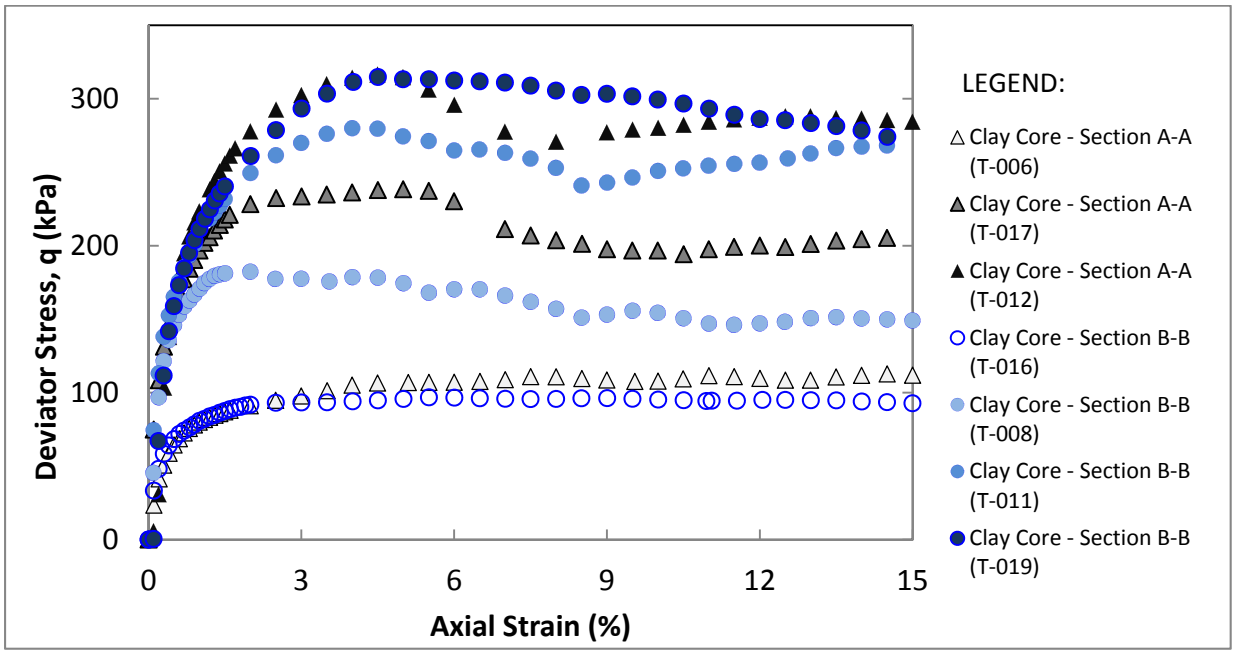

Figure 3-38. Stress-strain results from clay core.

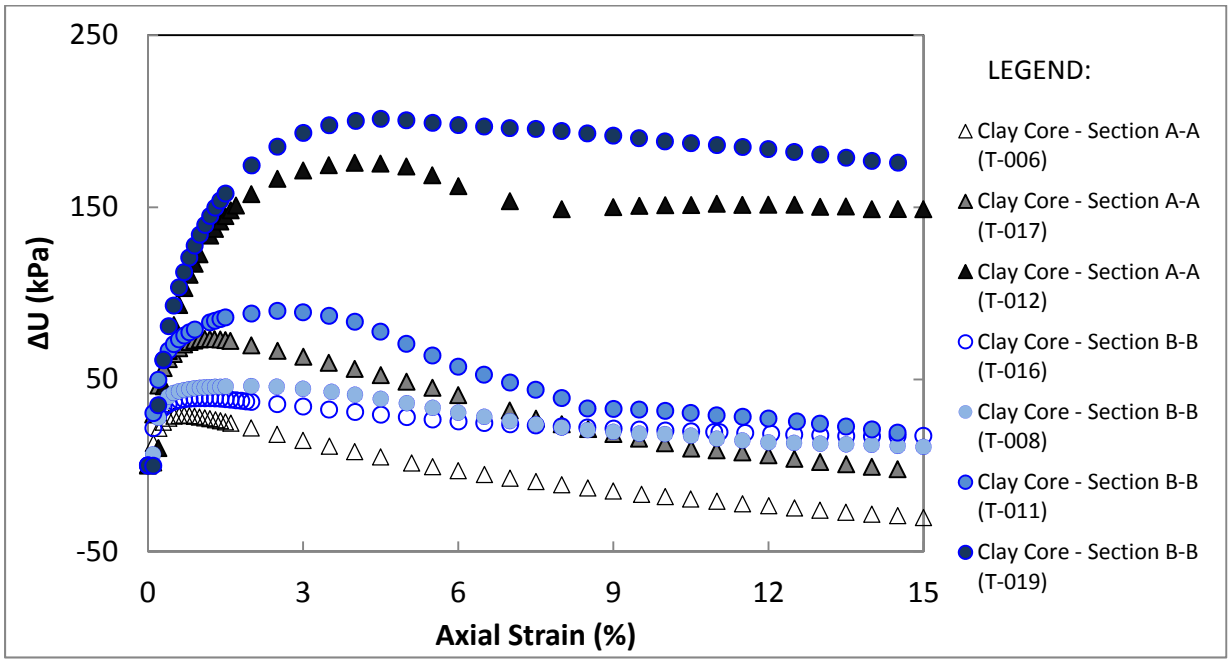

Figure 3-39. Pore-water pressure measurements from clay core during undrained shearing.

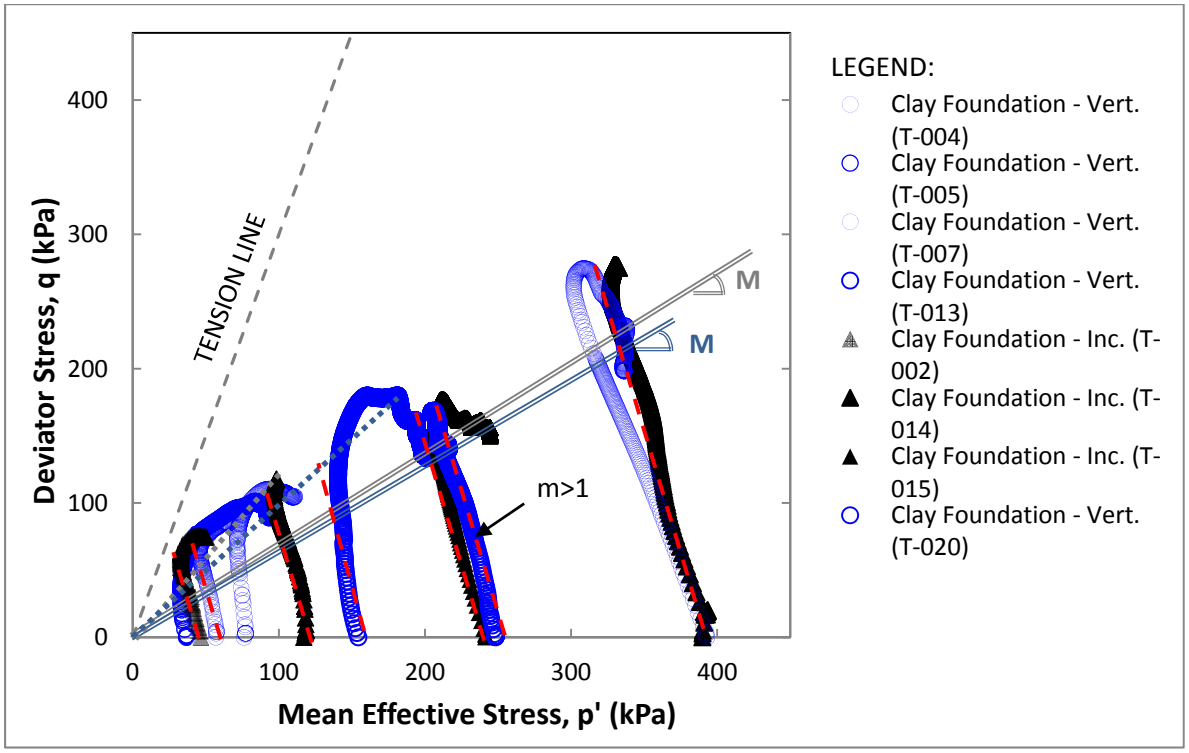

Figure 3-40.CIU triaxial test result from clay foundation samples.

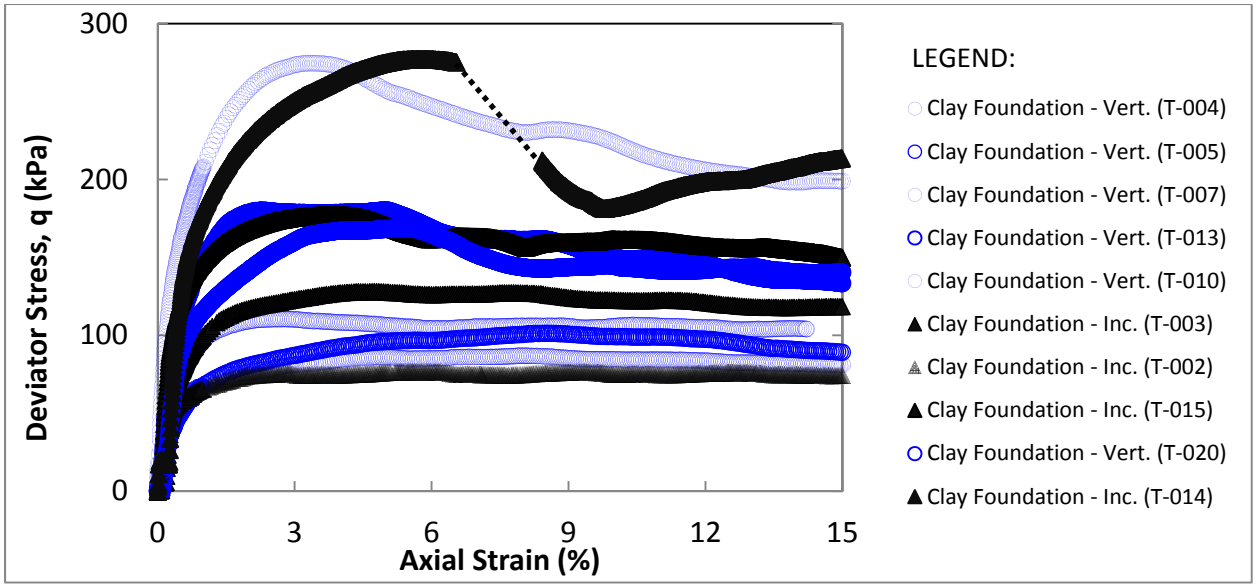

Figure 3-41. Stress-strain results from clay foundation.

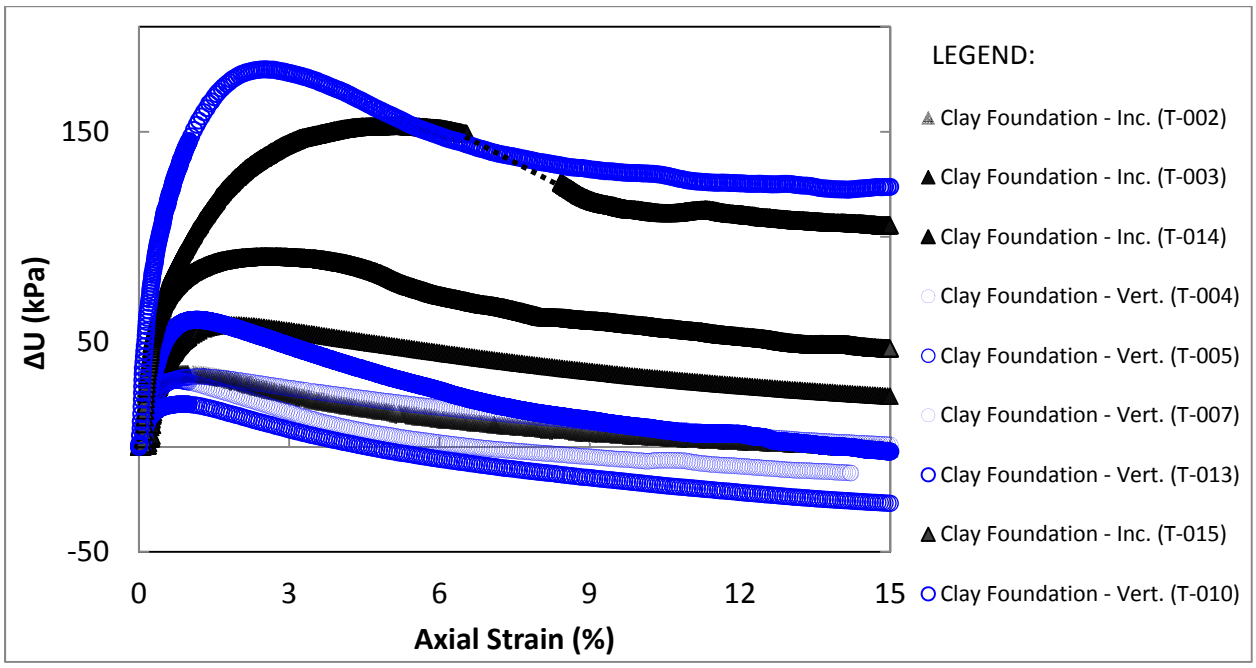

Figure 3-42. Pore water pressure measurements from clay foundation during undrained shearing

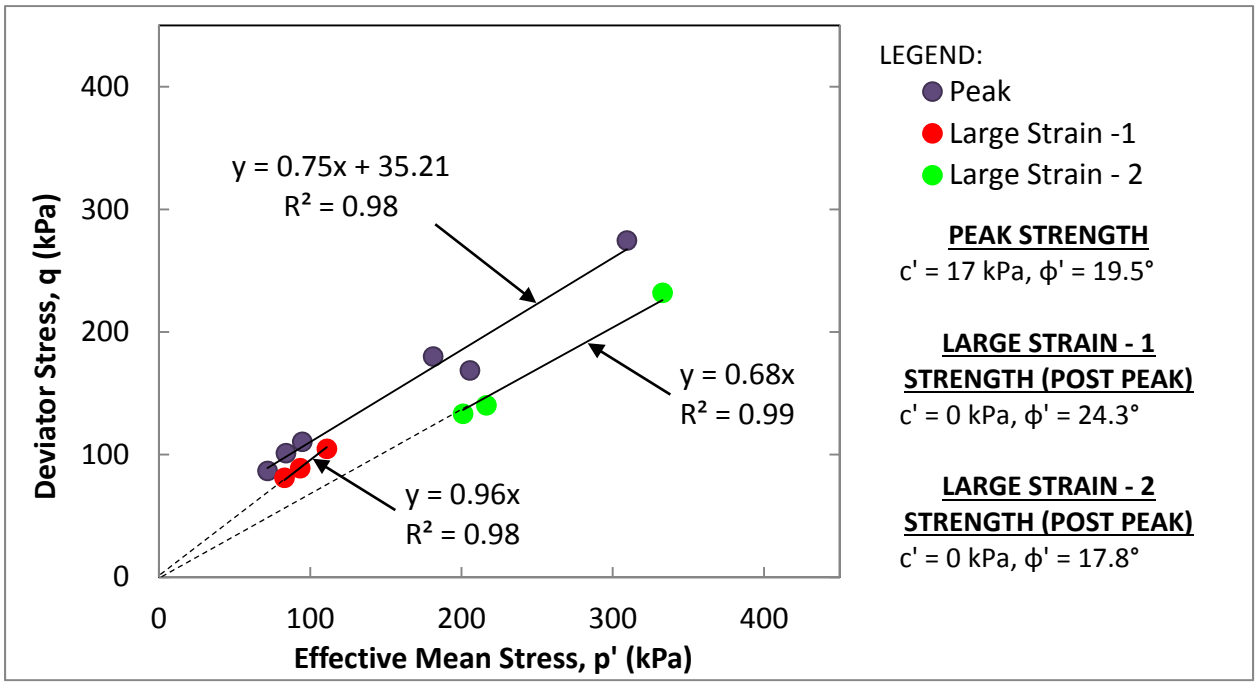

Figure 3-43.Peak and large strain (or post peak) effective strengths from clay foundation (vertical specimens).

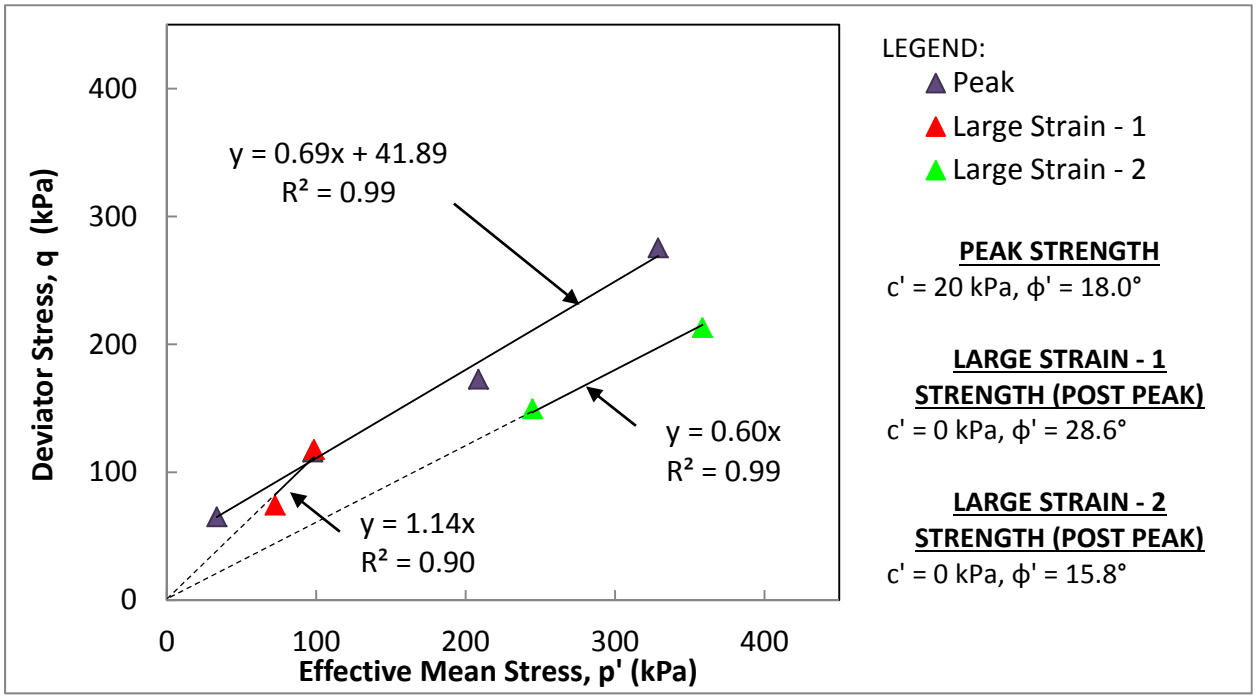

Figure 3-44. Peak and large strain (or post peak) effective strengths from clay foundation (inclined specimens).

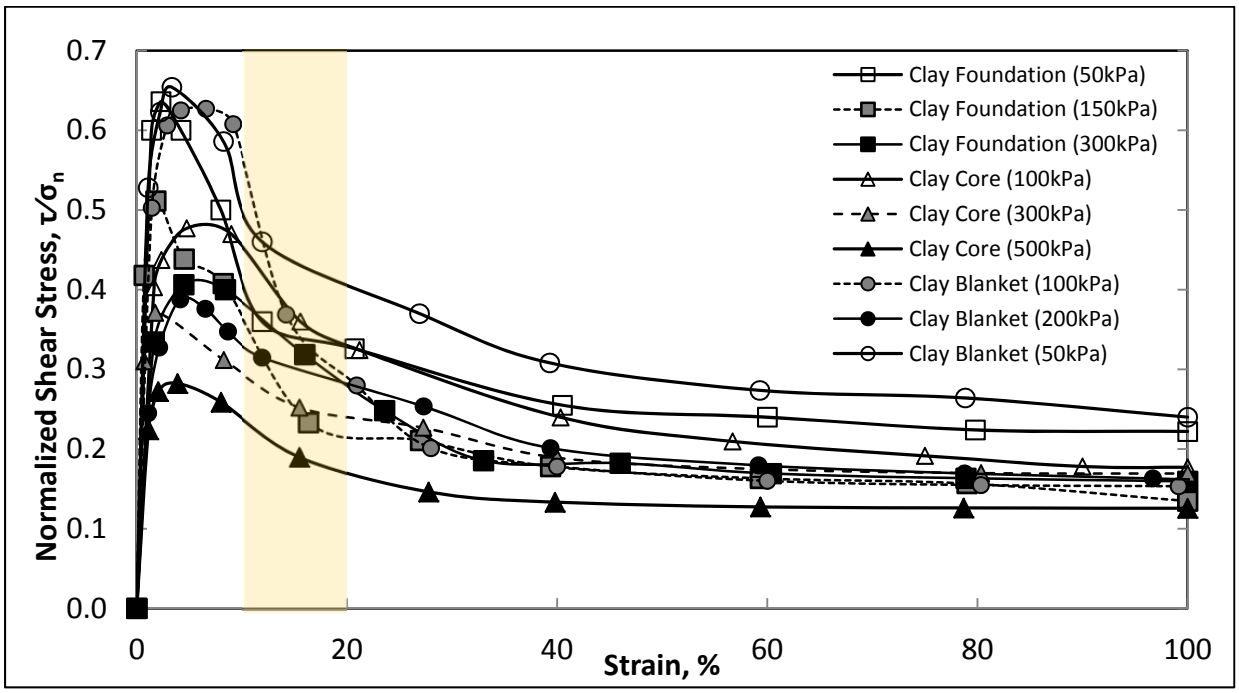

Figure 3-45. Stress-strain behavior from consolidated-drained direct shear tests.

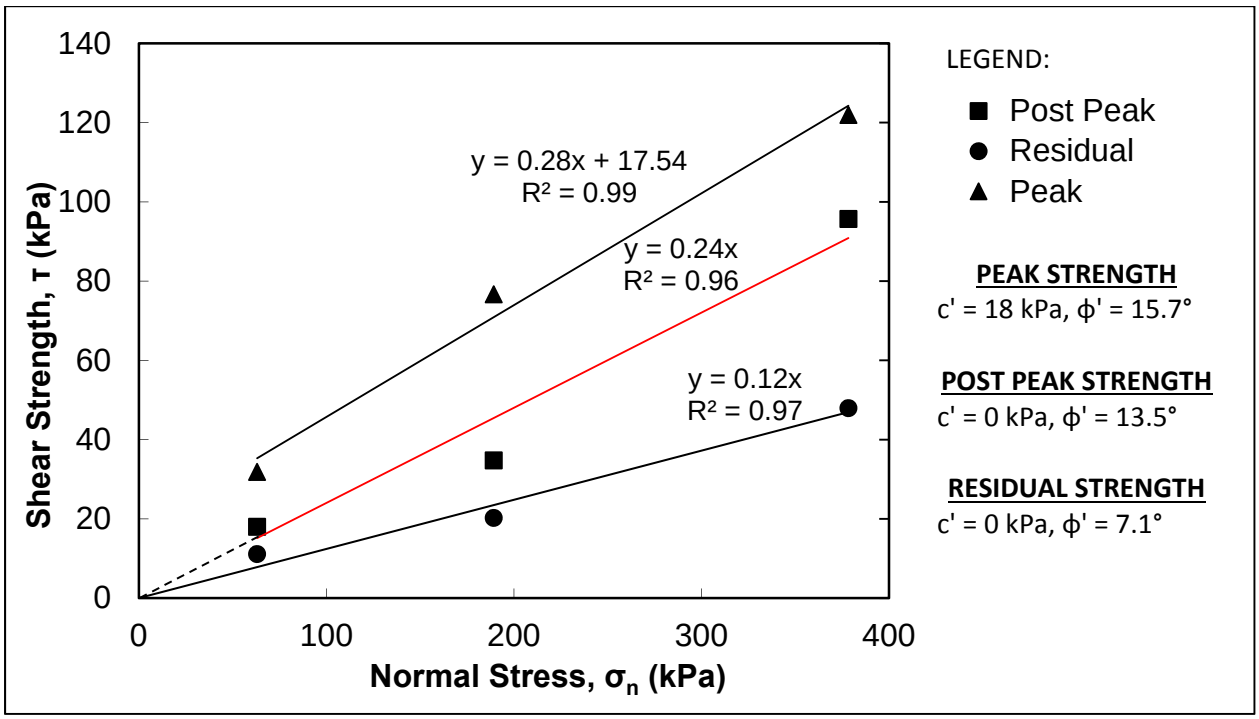

Figure 3-46. Horizontal drained shear strength envelope from clay foundation.

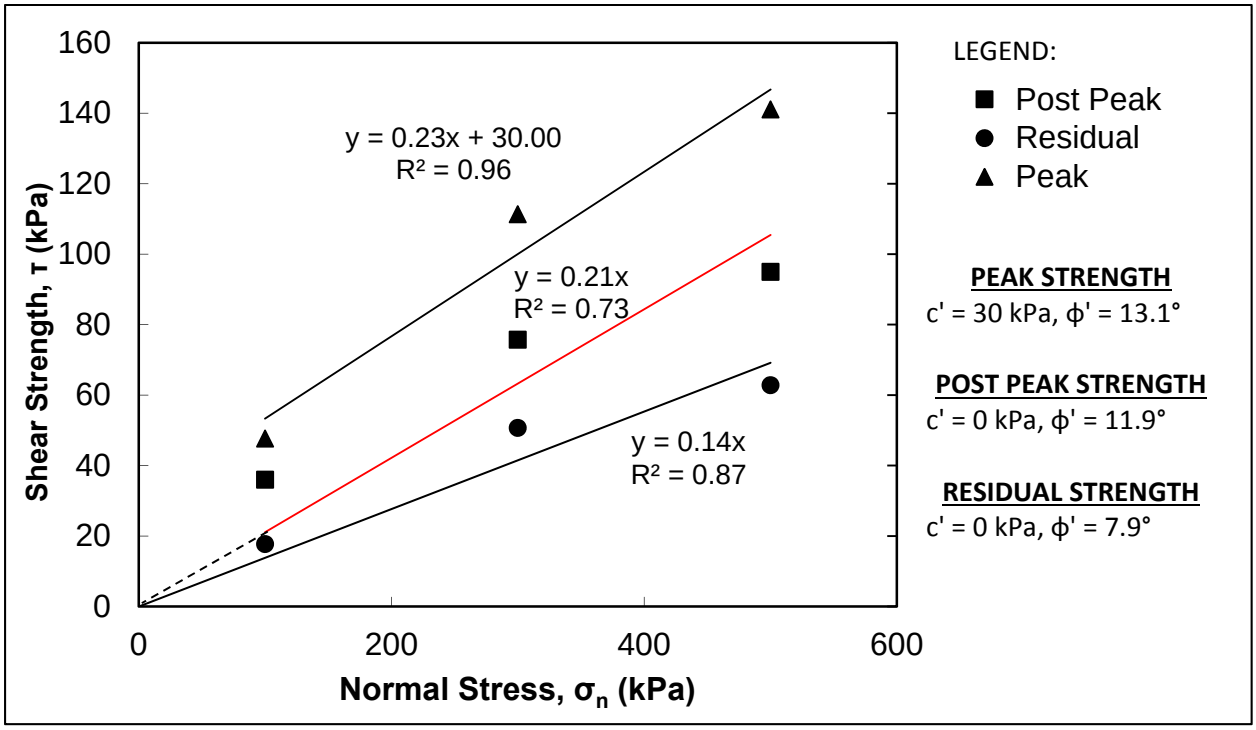

Figure 3-47. Horizontal drained shear strength envelope from clay core samples.

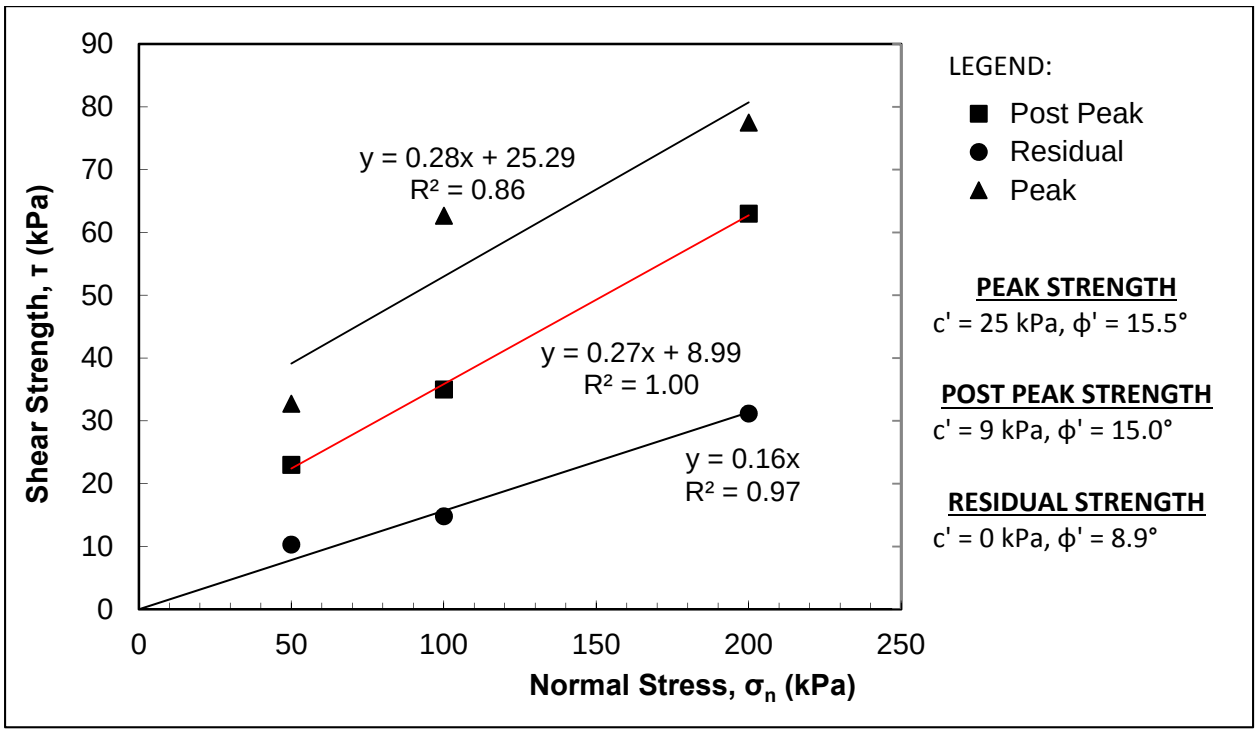

Figure 3-48. Horizontal drained shear strength envelope from clay blanket samples.

Chapter 4 Numerical Modeling

All numerical modeling was carried-out using a software developed by Geo-Slope International Ltd. (2007). Geometries of sections analyzed in modeling were extracted from the 3D model generated as discussed in Section 3.1.2. Soil parameters used in modeling are based on the laboratory test results and interpretations presented in Chapter 3. The main purpose of the numerical model is to evaluate the stability condition of two different sections in the Block Dam No.2 – Section A-A and Section B-B. The limit equilibrium method (LEM) of slope stability analysis using the SLOPE/W application was carried-out. A finite element method (FEM) of stress distribution was completed using the SIGMA/W application to eliminate the assumption of inter-slice forces in LEM analysis and more appropriately simulate the stress conditions in the field. A steady-state seepage analysis using the SEEP/W application was also done and results were incorporated in the FEM analysis in SIGMA/W to determine the location of the phreatic surface and establish an appropriate pore water pressure distribution in the model. Stress and seepage conditions were then imported to SLOPE/W program to calculate the factor of safety of the dam in a sequentially coupled approach (not mathematically coupled).

4.1 Seepage Modeling

A finite element steady-state analysis was carried-out to establish seepage conditions and to determine the location of the phreatic surface within the clay core and clay foundation. A

steady-state condition is assumed to be the typical condition of the dam during its normal operation consistent with the time of the irregular movement as well. Although the upstream head pond level seasonally fluctuates, only the critical condition was considered in the analysis. Boundary conditions applied are based on operational upstream head pond level in the upstream (wet) side of the dam, and the piezometric readings obtained from piezometers installed in the downstream (dry) side of the dam. The schematic diagram of the steady-state seepage model for section A-A and Section B-B are shown in Figure 4-1 and Figure 4-2, respectively.

The clay foundation material was assigned with a hydraulic conductivity of $1x10^{-9}$ m/s to take into account its fissured structure and the presence of silt pockets (Budhu 2010; Fell *et al*. 2015). The clay blanket and clay core on the other hand were assigned with a hydraulic conductivity in a range of $1x10^{-11}$ m/s typical for glaciolacustrine clay (Garinger *et al.* 2004). The conductivity ratio (k_v/k_h) particularly for the clay core was adjusted to be approximately 0.25 to match the location of the phreatic surface as measured in the piezometric readings of the piezometers installed in the clay core. The higher hydraulic conductivity along the horizontal direction of the clay core could be due to the contribution of silt lenses which are mostly horizontally oriented as observed during sample preparation and also potentially as a result of the horizontal placement of the core material during original construction.

Figure 4-3 and Figure 4-4 show the calculated total head contours for Section A-A and B-B, respectively. The location of the phreatic surface is approximately consistent with the piezometric readings from the installed vibrating wire piezometers. Piezometers installed in the

clay core and in the downstream foundation have positive pore pressure readings corresponding to the location of the phreatic surface. However, piezometers installed in the filter zone below the clay core register a negative reading indicative that the piezometer was installed within the unsaturated zone.

4.2 Stress and Deformation Modeling

Finite element *in-situ* and stress redistribution analyses were done using the Sigma/W program. The Modified Cam Clay (MCC) soil model was used to simulate the stress-strain behavior of all clayey materials (*i.e.* clay foundation, clay core, and clay blanket). MCC is capable of simulating the elastic, yielding and plastic behavior of soft clays. This is important since the main purpose of stress-deformation modeling is to establish an appropriate stress distribution which can be affected by yielding conditions. Due to observed structural discontinuities and being under water for over 50 years, the clay blanket may have swelled to its fully-softened condition particularly the areas of clay blanket away from the upstream toe of the dam. The clay core on the other hand has been partly submerged and is somehow affected by seasonal environmental loading, particularly the upstream face of the core. The presence of silt lenses in the clay core (Figure 3-17) together with seasonal freezing-thawing are thought to have caused fissuring in the upper portion of the clay core which facilitates softening.

The boundary conditions are another important consideration in defining any numerical model. The model was fixed in both X and Y- direction at the base, and fixed in X-direction at both ends; the upstream face of the model was assigned with constant hydrostatic pressure due to

the upstream reservoir; and the downstream side of the dam was also assigned with hydrostatic pressure due to water ponding at the toe of the dam (for section B-B). The schematic diagram of the Sigma/W models for Section A-A and B-B are shown in Figure 4-5 and Figure 4-6, respectively. Other input parameters are presented in Table 4-2. Figure 4-7 and Figure 4-8 show the calculated contours of effective vertical stress in Section A-A and Section B-B, respectively. Figure 4-9 and Figure 4-10 show the distribution of the maximum shear stress as calculated from the stress redistribution model *(contour lines are in terms of kPa).* It also shows the zones within the clay that yielded *(shaded region)*. At Section A-A, stress redistribution result shows that most of the clay foundation at the dry side of the dam had yielded. The yielding of the clay foundation at the toe of the dam (on the dry side) is partly due to the fact that it has lesser vertical effective stress as compared to that consolidated zone under the rockfill shell. Further, shear stress redistribution must have caused the soil elements beyond the toe of the dam to yield. Concentration of shear stresses on fissures increases the stress to a point where it may exceed the yield stress and result in load shedding to neighboring soil, potentially causing it to overstress, until the localized region yields and transmits the excess stresses to lower stress regions that are able to carry it. The hydrostatic pressure at the upstream side of the dam helps stabilize the soil element through applied total stresses outside the toe of the dam on the wet side. At Section B-B, results show that the clay blanket mostly has yielded particularly the upper portion and towards the toe of the dam where the vertical effective stress is lower (Figure 4-10). A localized portion of the saturated clay core had also yielded at areas closer to the filter interface, where redistributed shear stress is higher. The

contribution of pore water pressure also reduces the effective strength of the clay core in the localized area.

4.3 Slope Stability Analyses

Results from FEM stress redistribution analysis and seepage analysis were imported into LEM slope stability analyses using the SLOPE/W application. A limit equilibrium method of approach was carried out on 2 sections of the dam, Sections A-A and B-B. The location and shape of the possible slip surfaces were defined by the grid and radius method. However, for dams with sloping clay core and fissured clay foundation, a circular slip surface geometry does not always represent the shape of the critical failure plane. In the analyses done particularly on the upstream face of the dam, an additional method of defining the shape of possible slip surfaces were done *(see Appendix 13 - Appendix 18)*.

As mentioned in the previous section, the clayey materials are thought to have reached their fully-softened condition. Several cases studied and published in the literature suggested that for first-time slides, the mobilized shear strength could be as low as the average of the post peak (or fully-softened) and the residual shear strengths (Stark and Eid, 1997). Further, for soil elements, yielding usually precedes large deformation and generation of excess pore water pressure; hence, for a particular soil element that yielded, residual strength is most likely mobilized.

Input strength parameters for slope stability analyses are summarized in Table 4-3. The rockfill and the clay blanket were assigned with Mohr-Coulomb strength model for simplicity of the

analyses. An anisotropic strength model was assigned for the clay core material to simulate the difference in strength along the cross-shear direction and along the horizontal direction. It is thought that the clay core will have lower strength in the horizontal direction due to the presence of horizontally oriented fissures and silt lenses. Strength parameters used in modeling are post-peak and residual strengths. This is to represent the softened condition of the clay blanket and the tendency of the clay core materials to soften when subjected to straining under lower stress levels. The zones with yielded clays *(as shown in Figure 4-9 and Figure* 4-10*)* warrant the use of residual strength. However, to take into consideration the fact that only a portion of the clay blanket and clay core had yielded, the average of fully softened friction angle and the residual friction angle was calculated.

Three cases of slope stability analyses were carried-out and presented in this section: (a) using fully softened strength for all clay materials (*i.e*. clay foundation, clay blanket and clay core); (b) same in (a) but assuming that the mobilized shear strength in clay foundation and clay blanket is as low as the average of the fully-softened and residual shear strength due to some elements that had yielded; (c) assuming that some soil elements in all clay materials (*i.e.* clay foundation, clay blanket and clay core), had yielded and that the mobilized shear strength is the average of the fully-softened strength and the residual strength.

A summary of slope stability analyses and the calculated factors of safety are presented in Table 4-4 and Table 4-5 for Sections A-A and B-B, respectively. At Section B-B, the calculated factor of safety shows that even if both the clay blanket and the clay core had reached its fully-softened condition (as in Case A), the dam is marginally stable with a factor of safety greater than unity

(FOS = 1.13). If yielding of the clay blanket will be taken into account and assumed that some elements in the clay blanket had reached its residual strength (as in Case B), the embankment will be at incipient failure (FOS = 1.01). However, if the shape of the postulated slip surface is to be considered, where approximately 75% of the elements along the failure plane had already yielded (as in Case C), the calculated factor of safety will be less than unity (FOS = 0.90) and the embankment will have theoretically failed.

4.4 Summary and Discussion

The steady-state seepage modeling result is consistent with the field data obtained from installed piezometers. It's interesting to note that the downstream filter (*i.e.* below the clay core) registers a negative reading, however, this does not affect the results of slope stability analyses completed since the location of the critical slip surface is away from the downstream filter region. The stress redistribution analysis is satisfactory enough in simulating the stress conditions in the field. The shear stress distribution shows yielding in regions with lower vertical effective stress (lower strength) and with observed structural discontinuities. The calculated factor of safety based on the fully softened conditions of the clayey materials show a factor of safety above unity. If yielding of the clay foundation and clay blanket are to be considered, both sections of the dam (*i.e.* Section A-A and Section B-B) will be at incipient failure. The mobilized strength at failure can be as low as the average of the fully-softened and the residual strength.

Table 4-1. Summary of input parameters for steady-state analysis in Seep/W.

	Clay foundation	Clay core	Clay blanket
Vertical Hydraulic Conductivity, k_v	$1x10^{-9}$ m/s	$1x10^{-11}$ m/s	$1x10^{-11}$ m/s
Conductivity Ratio, k_v/k_h	1.0	0.25	1.0

Table 4-2. Input parameters for stress-deformation modeling.

	Rockfill	Clay foundation	Clay core	Clay blanket
Constitutive Model	Linear Elastic	Modified Cam Clay	Modified Cam Clay	Modified Cam Clay
E (MPa)	300	n/a	n/a	n/a
υ	0.35	0.35	0.35	0.45
γ (kN/m^3)	18	17	17	17
$OCR_{apparent}$	n/a	4.6	2	1.5
λ	n/a	0.1235	0.1252	0.1448
κ	n/a	0.0275	0.0243	0.0420
M	n/a	0.647	0.739	0.567

Table 4-3. Input parameters for slope-stability modeling.

	Rockfill	Clay Core	Clay Blanket	Clay Foundation
Material strength model	Mohr-Coulomb	Anisotropic Strength	Mohr-Coulomb	Bilinear Strength
γ (kN/m^3)	18	17	17	17
$c'_{post\ peak}$ (kPa)	n/a	0	0	0
Φ'_{peak} (°)	45	n/a	n/a	n/a
$\Phi'_{horizontal\ post\ peak}$ (°)	n/a	12	15	29 , 16
$\Phi'_{cross\text{-}shear\ post\ peak}$ (°)	n/a	19	n/a	n/a
$\Phi'_{residual}$ (°)	n/a	8	9	7
$^{\dagger}\Phi'_{average\ horizontal}$ (°)	n/a	10	12	18 , 12
$^{\dagger}\Phi'_{average\ cross\text{-}shear}$ (°)	n/a	14	n/a	n/a

†*average of post peak and residual angles of friction*

Table 4-4. Results from slope-stability analyses for Section A-A.

Case	Clay foundation , Φ' (*low stress, high stress*)	Clay core , Φ' (*cross-shear, horizontal shear*)	Factor of Safety (FOS) Upstream[1,2]	Downstream[1]
Case A	29,16	19,12	1.30, 1.34	1.30
Case B	18,12	19,12	1.08, 0.98	1.17
Case C	18,12	14,10	0.97, 0.88	1.17

[1]*circular slip surface,* [2]*user defined slip surface*

Table 4-5. Results from slope-stability analyses for Section B-B.

Case	Clay blanket , Φ' (*horizontal*)	Clay core , Φ' (*cross-shear, horizontal shear*)	Factor of Safety (FOS) Upstream[1,2]	Downstream[1]
Case A	15	19,12	1.13, 1.12	1.43
Case B	12	19,12	1.01, 0.98	1.43
Case C	12	14,10	0.90, 0.88	1.43

[1]*circular slip surface,* [2]*user defined slip surface*

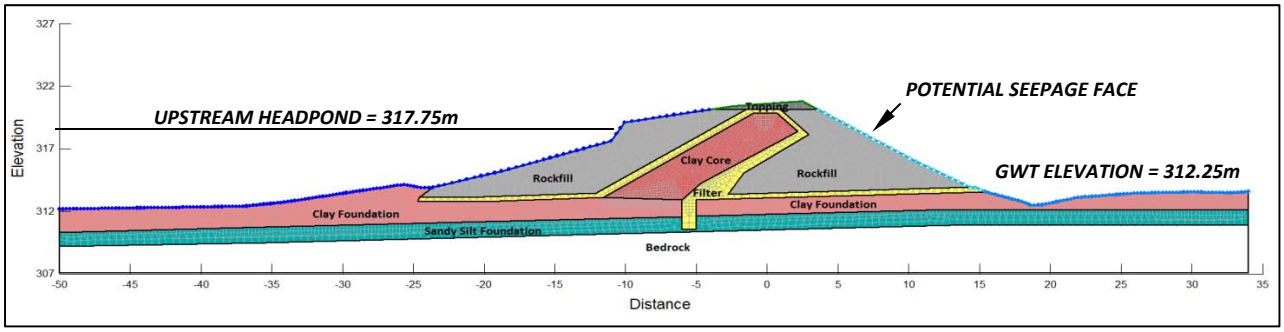

Figure 4-1. Schematic of Steady-State Seepage Model in Seep/W (Section A-A).

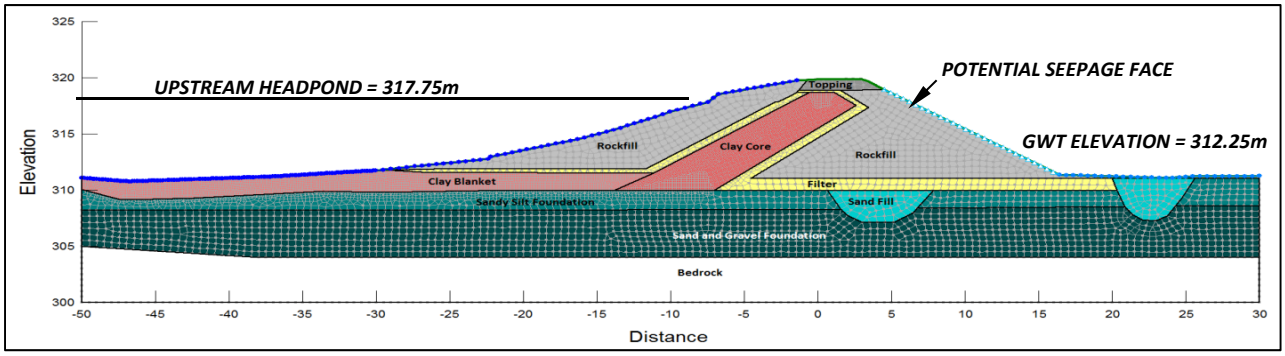

Figure 4-2. Schematic of Steady-State Seepage Model in Seep/W (Section B-B).

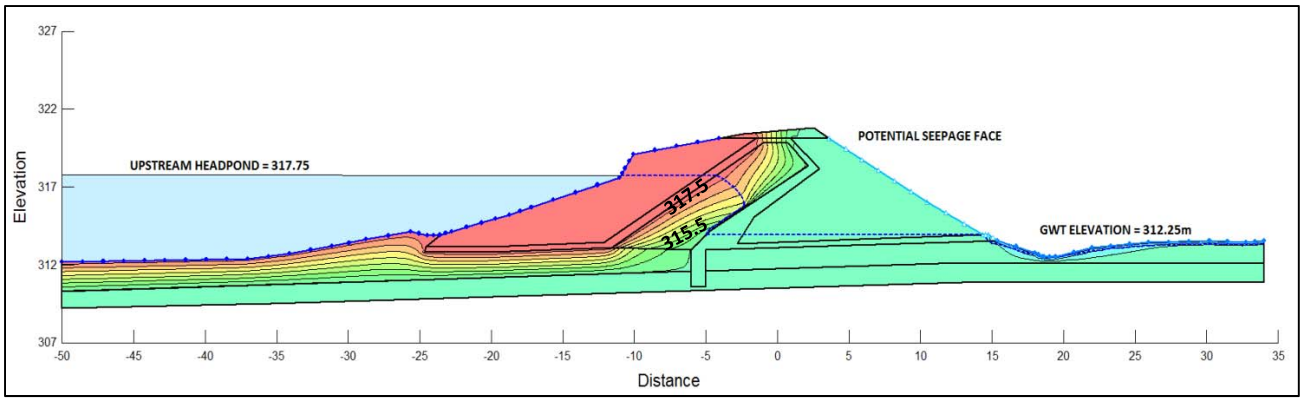

Figure 4-3. Contours of calculated total head (Section A-A).

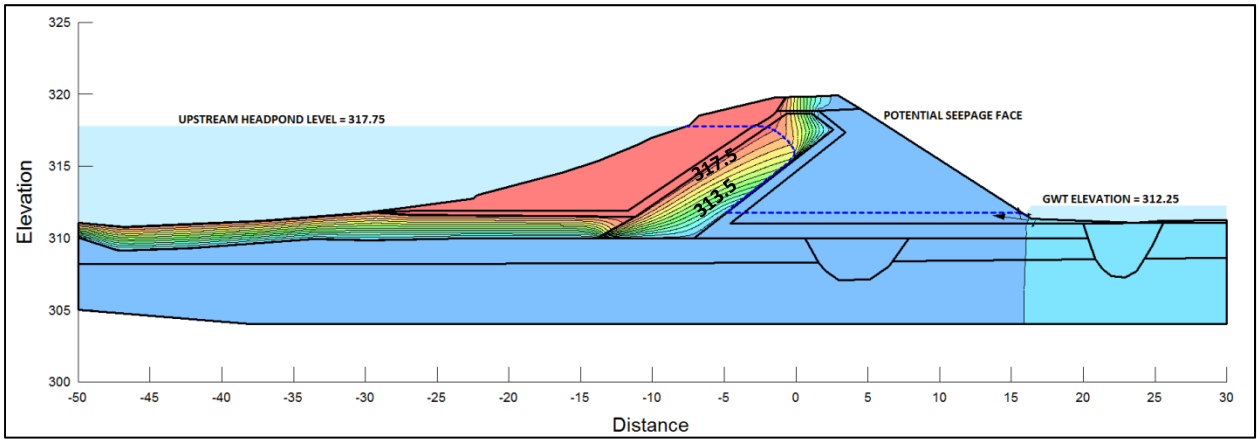

Figure 4-4. Contours of calculated total head (Section B-B).

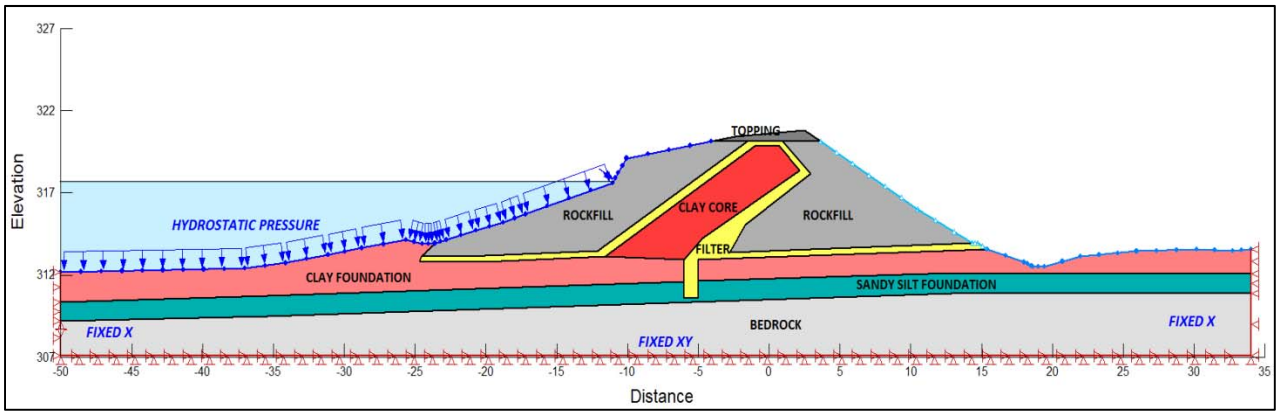

Figure 4-5. Schematic of Stress Redistribution Model in Sigma/W (Section A-A).

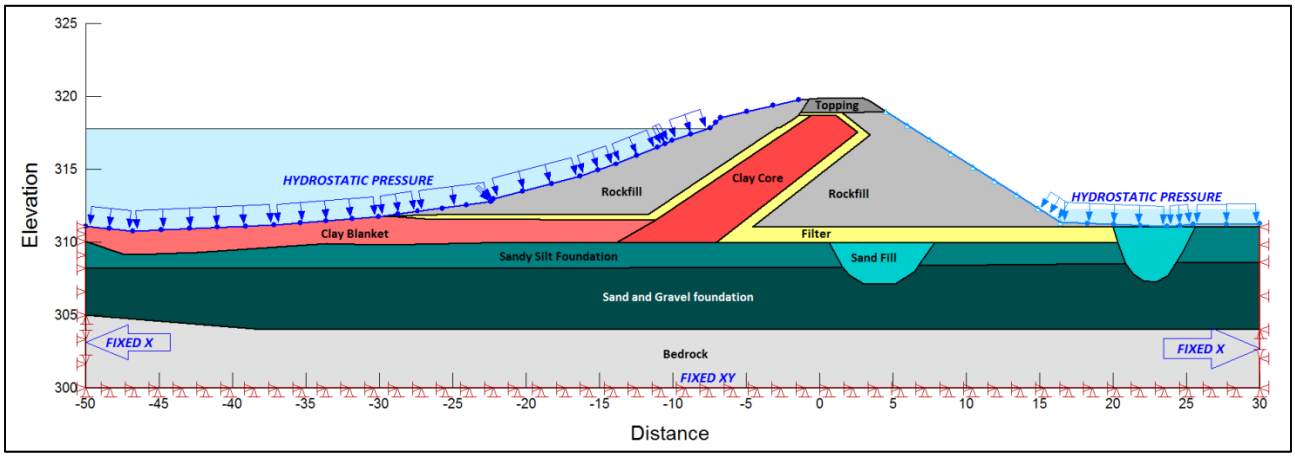

Figure 4-6. Schematic of Stress Redistribution Model in Sigma/W (Section B-B).

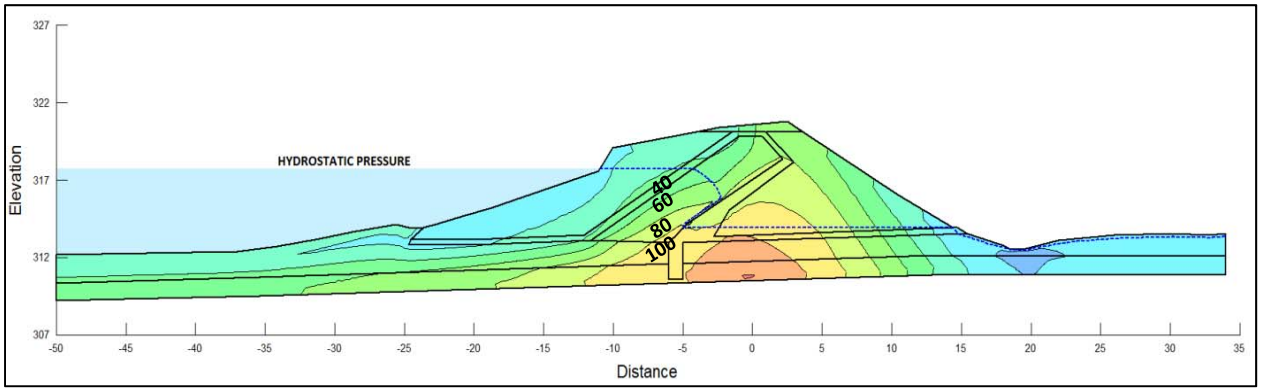

Figure 4-7. Contours of calculated effective vertical stress in stress redistribution model (Section A-A).

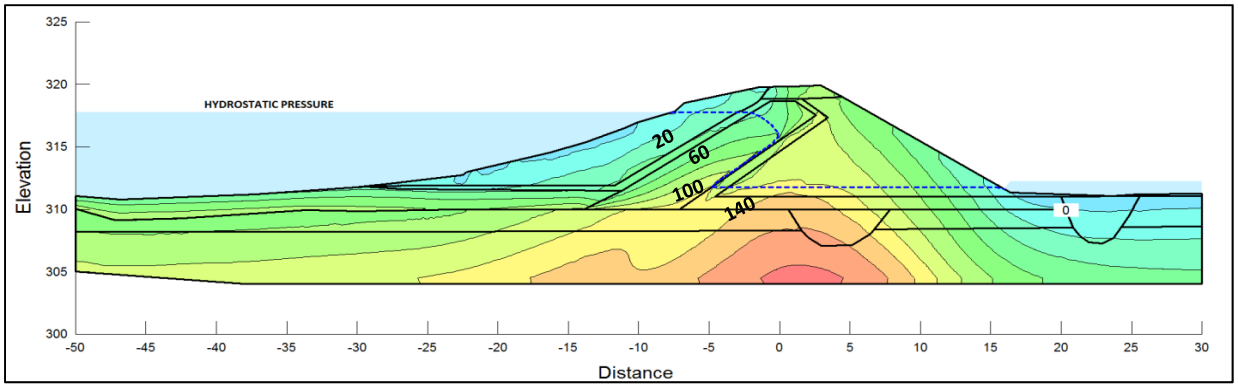

Figure 4-8. Contours of calculated effective vertical stress in stress redistribution model (Section B-B).

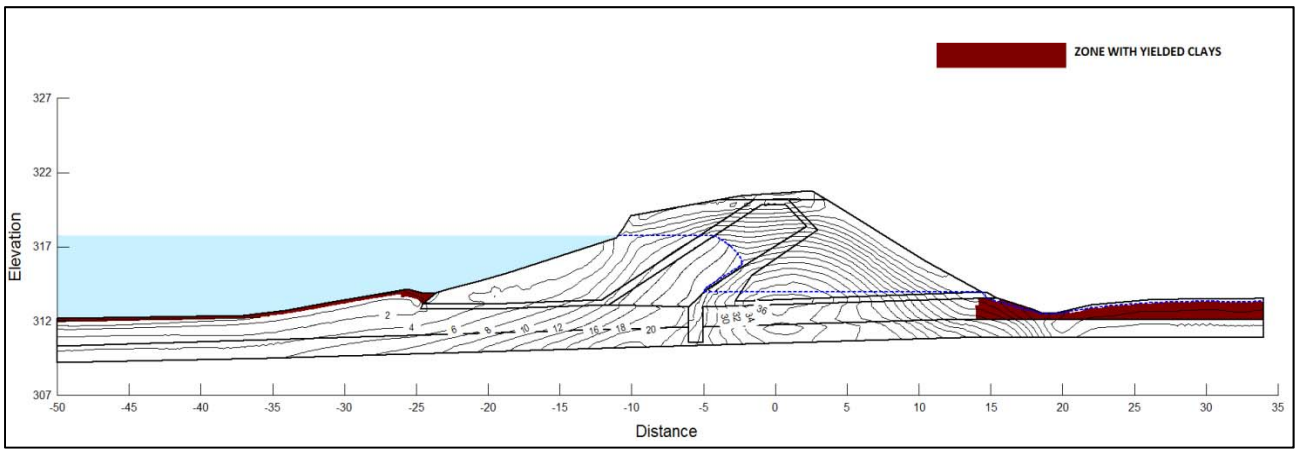

Figure 4-9. Shear stress distribution and zones of yielded clays based on stress redistribution analysis (Section A-A).

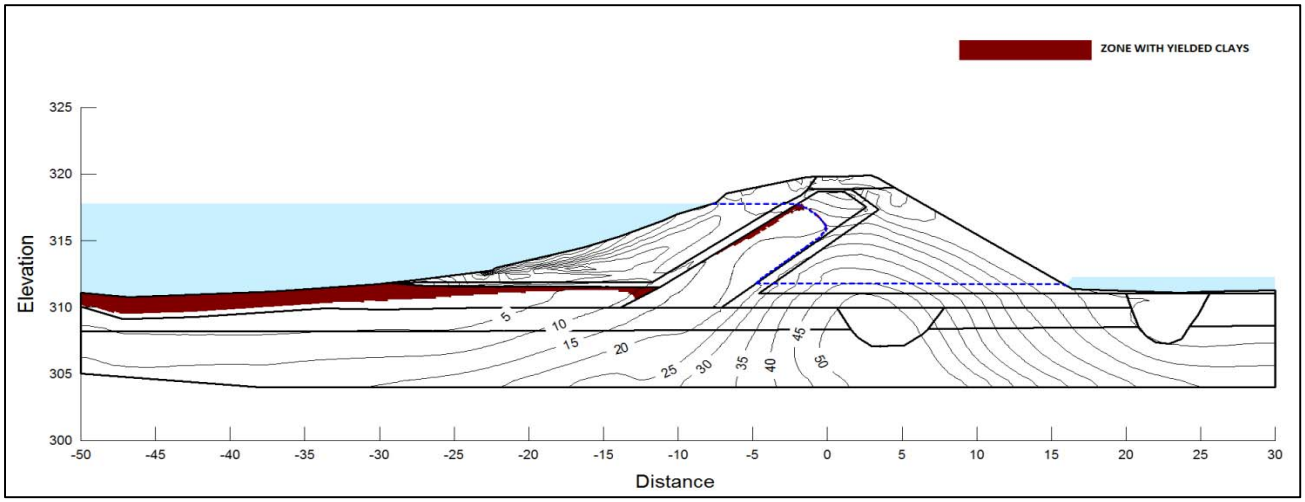

Figure 4-10. Shear stress distribution and zones of yielded clays based on stress redistribution analysis (Section B-B).

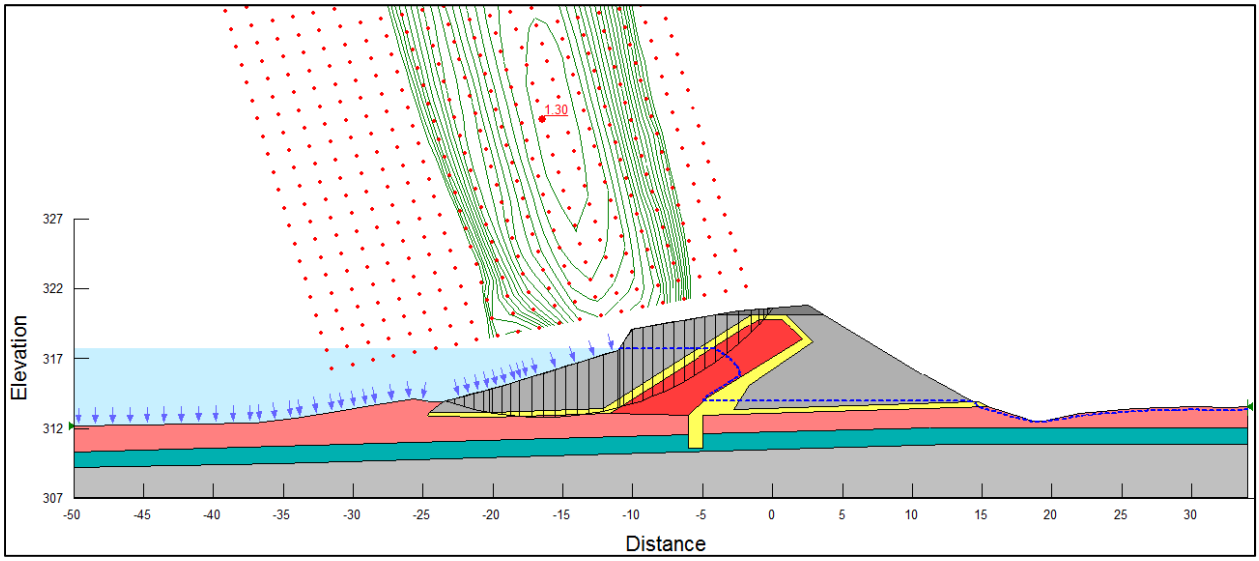

Figure 4-11. Slope-stability analysis of Section A-A upstream slope, Case A.

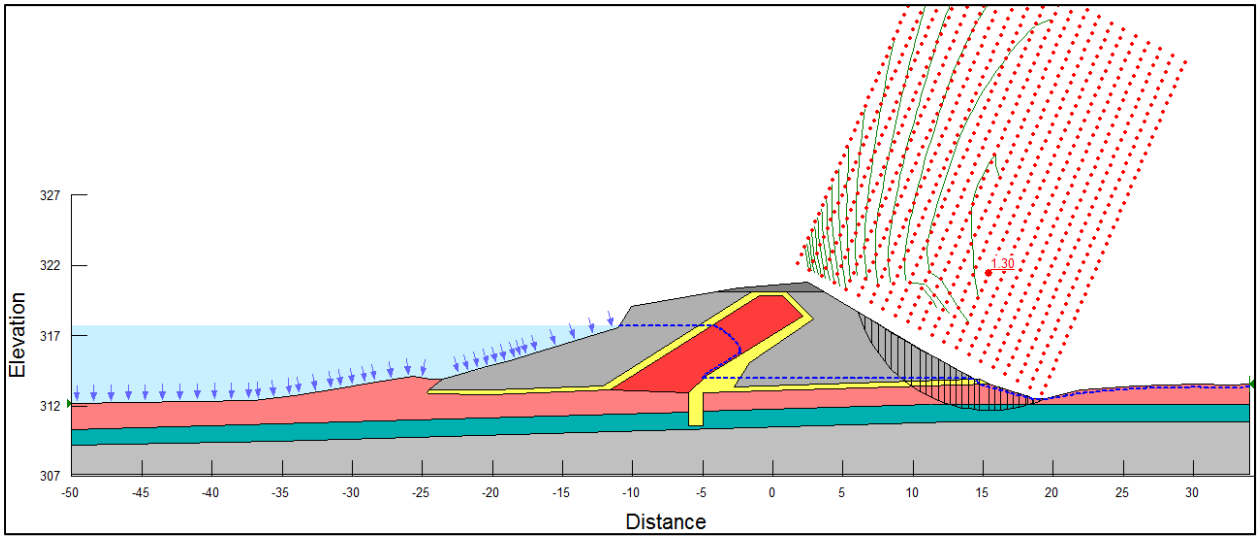

Figure 4-12. Slope-stability analysis of Section A-A downstream slope, Case A.

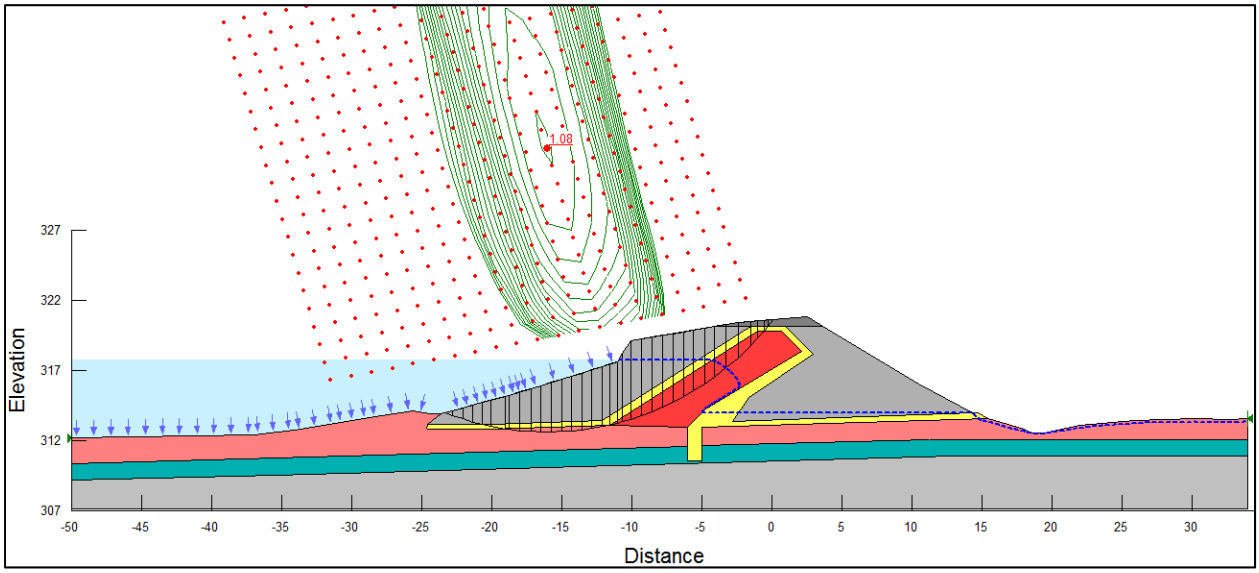

Figure 4-13. Slope-stability analysis of Section A-A upstream slope, Case B.

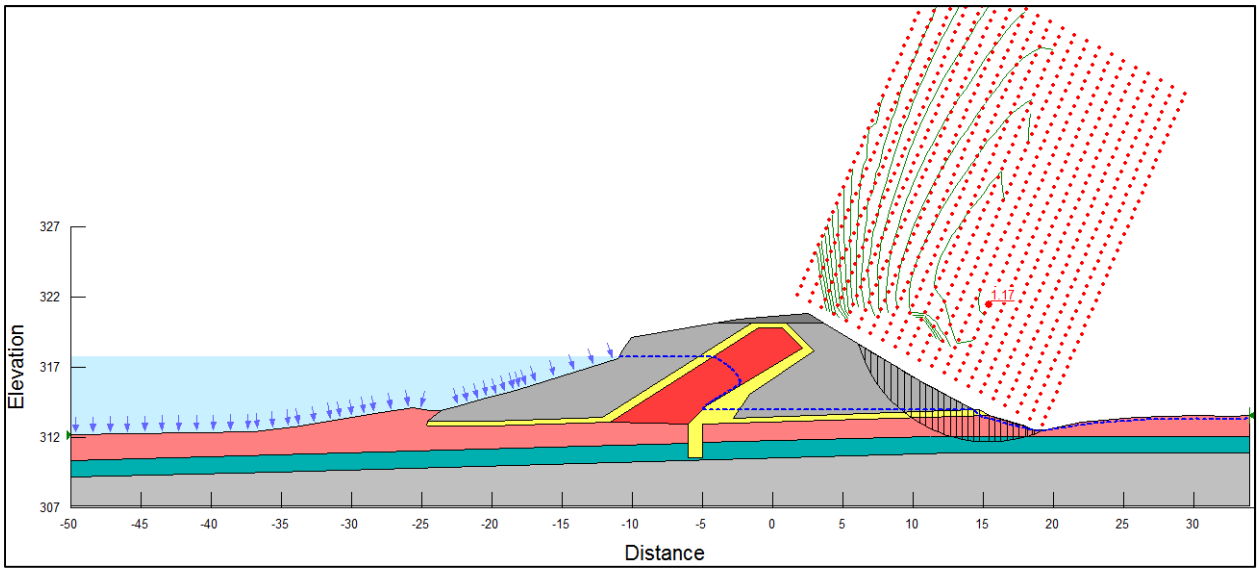

Figure 4-14. Slope-stability analysis of Section A-A downstream slope, Case B.

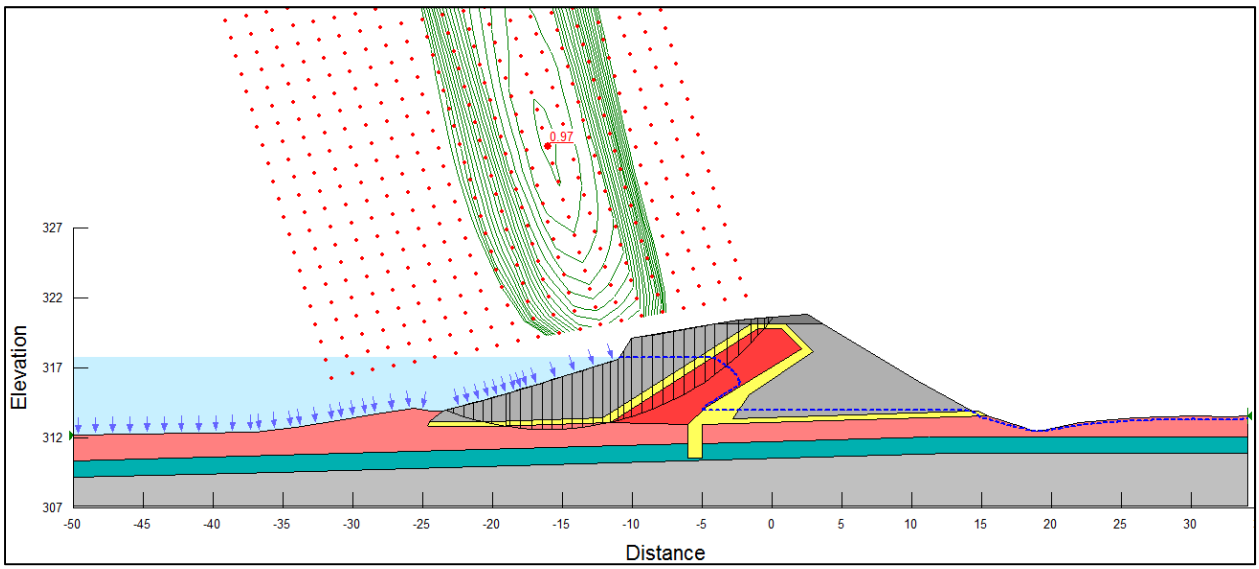

Figure 4-15. Slope-stability analysis of Section A-A upstream slope, Case C.

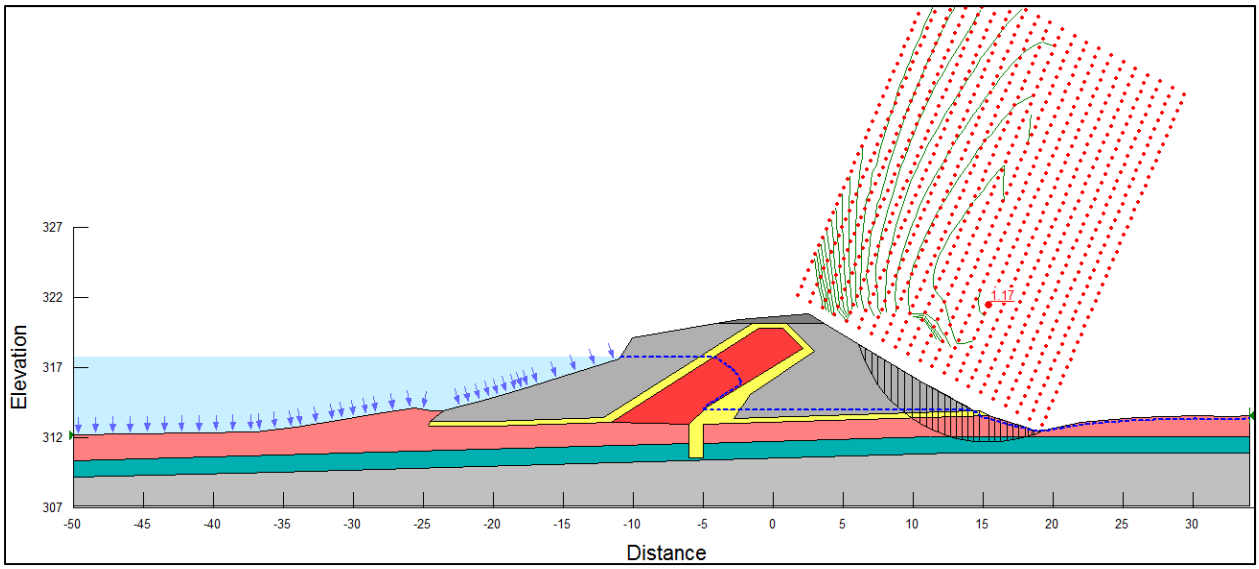

Figure 4-16. Slope-stability analysis of Section A-A downstream slope, Case C.

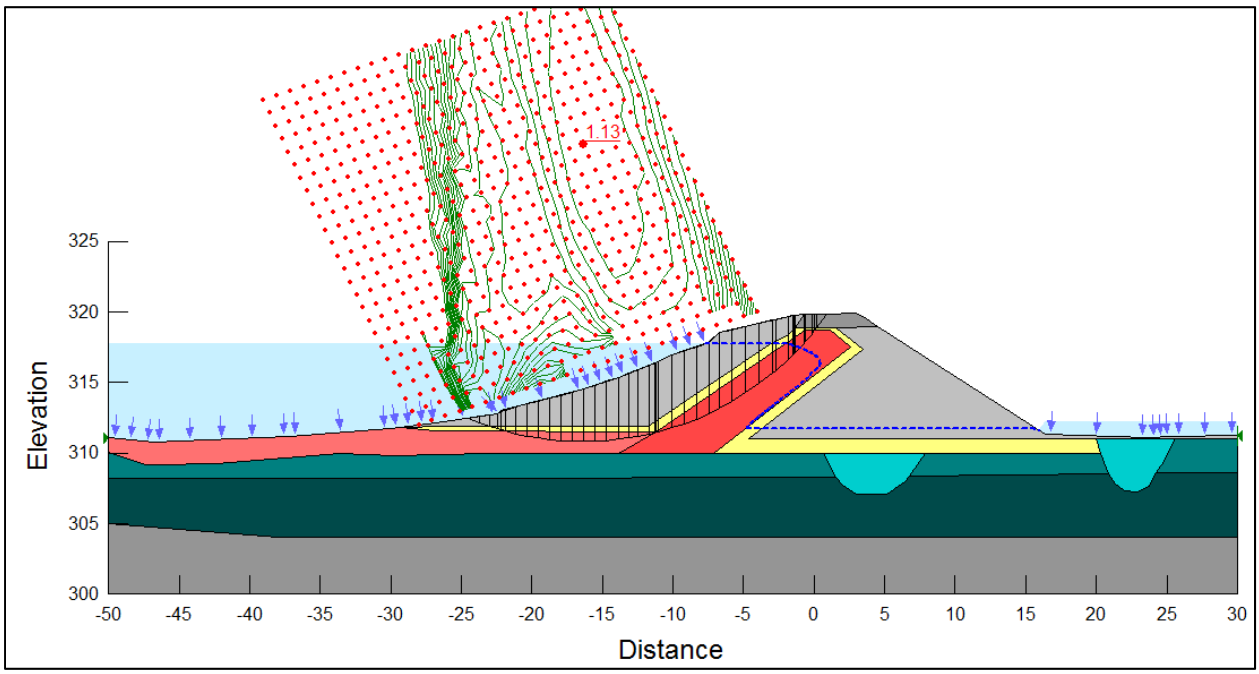

Figure 4-17. Slope-stability analysis of Section B-B upstream slope, Case A.

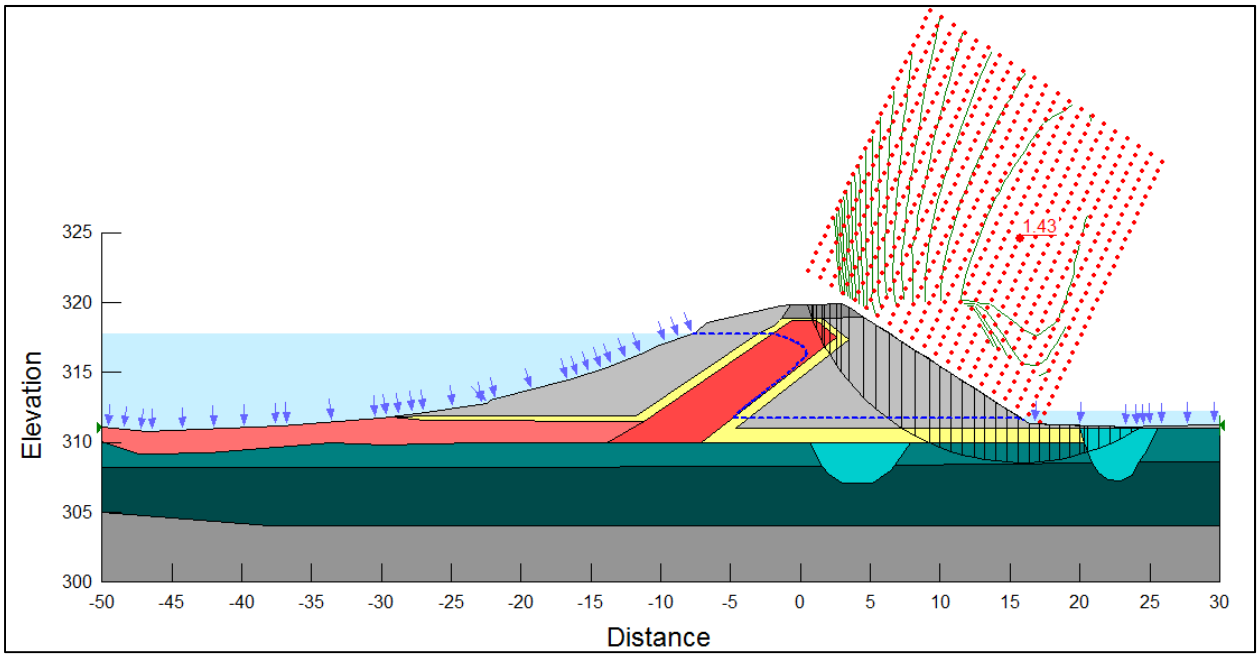

Figure 4-18. Slope-stability analysis of Section B-B downstream slope, Case A.

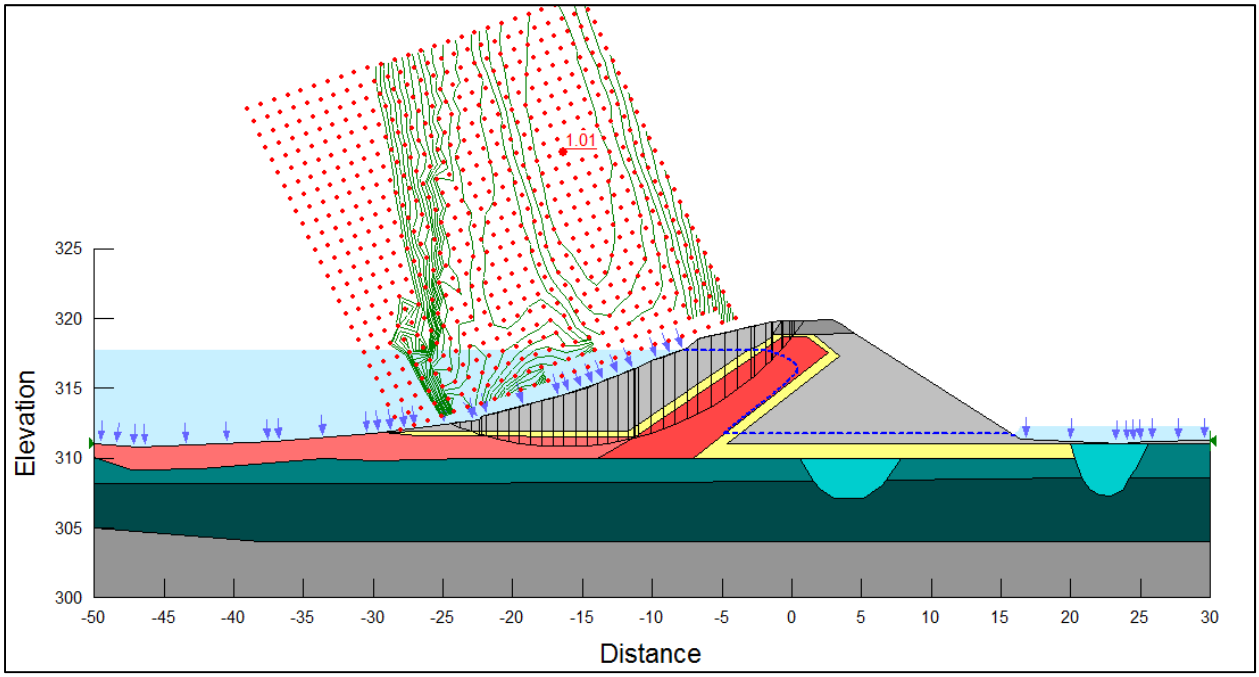

Figure 4-19. Slope-stability analysis of Section B-B upstream slope, Case B.

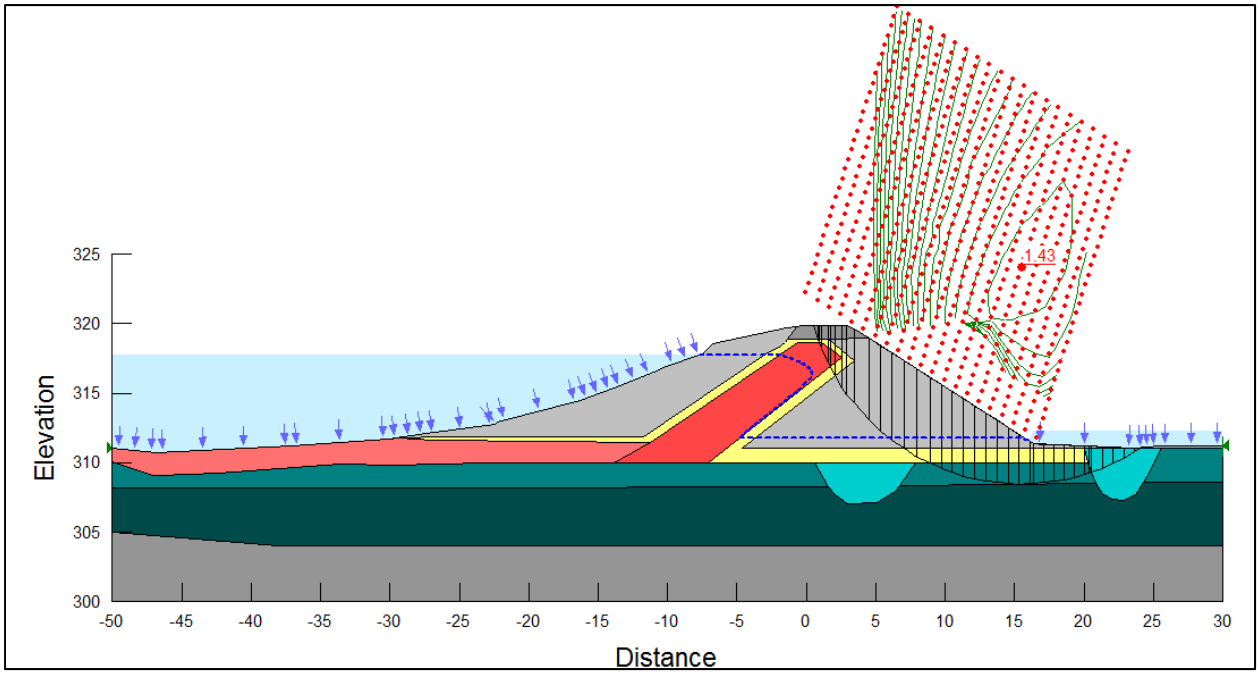

Figure 4-20. Slope-stability analysis of Section B-B downstream slope, Case B.

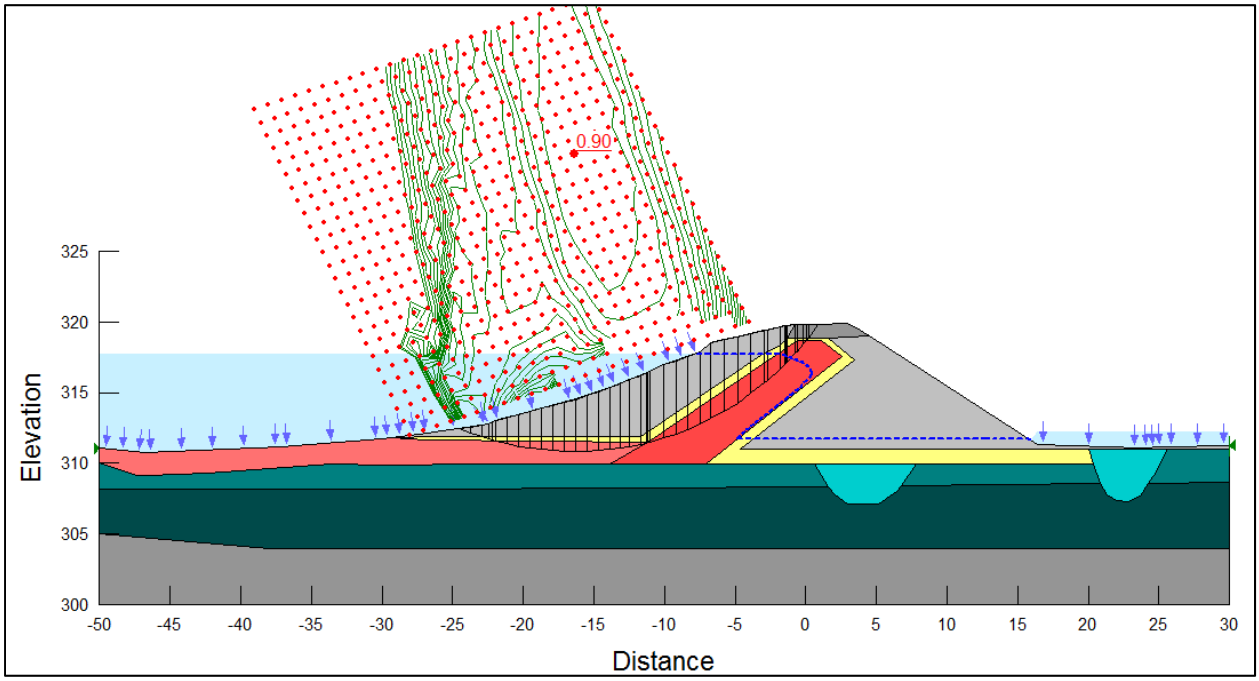

Figure 4-21. Slope-stability analysis of Section B-B upstream slope, Case C.

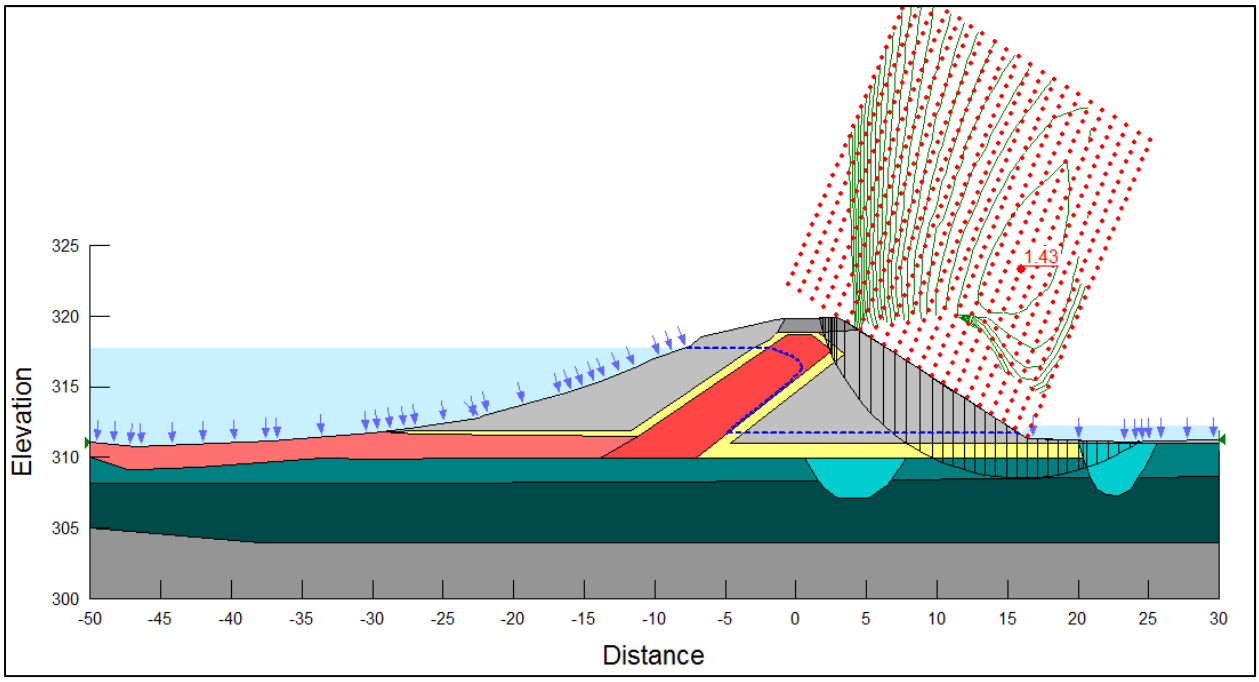

Figure 4-22. Slope-stability analysis of Section B-B downstream slope, Case C.

Chapter 5 Conclusions and Recommendations

This research was undertaken as part of slope stability assessment of old earth fill dams founded on glaciolacustrine clays. Extensive field work was conducted to assess the *in-situ* condition of Block Dam 2. Vibrating wire piezometers were installed to monitor the pore water pressure in the clay core and clay foundation. A laboratory testing program was undertaken to determine the soil properties and soil parameters needed for remedial design and numerical modeling. A correlation between cone tip resistance and undrained strength was established. Interpretation of CPTu cone tip resistance in terms of drained parameters was also attempted. Further, numerical modelling was carried-out using parameters determined from the laboratory tests to assess the stability condition of Block Dam 2.

5.1 CONCLUSIONS

Environmental loading like seasonal freezing-thawing and wetting-drying can cause fissures, even to mechanically engineered clays. In addition to softening effects facilitated by fissures, shear stress concentrations may also be formed along structural discontinuities and could lead to progressive failure. Based on the research done, the following conclusions can be drawn:

1) Laboratory test results show that the clay foundation, clay core, and clay blanket in Block Dam 2 are similar materials. The clay materials can be described as highly plastic, smectite-rich and fissured. Presence of fissures were observed in different levels:

macrostructure fissures in clay foundation are visible with the naked eye during the field investigation; fissures in the clay blanket and clay core were noticed during sample preparation; microstructural fissures in a form of gaps between flocs were observed under scanning electron microscope.

2) The clay materials used in Block Dam 2 may be part of Lake Agassiz clay deposits with slight variation in terms of its mineralogical components (*i.e*. with different cementing agents between clay particles).
3) The clay foundation and clay core have anisotropic strength with higher cross-shear strength and lower horizontal shear strength. The failure envelope is bilinear for the fissured clay foundation and linear for the clay core materials.
4) Local cone factor, Nkt value of 35 was found to have the best fit line for undrained shear strength and cone tip resistance correlation.
5) Numerical modeling shows that the clay blanket (on the wet side) and clay foundation (on the dry side) of Block Dam 2 has yielded. Yielding of clays can be attributed to overstressing of intact soil due to shear stress concentrations in structural discontinuities. Further, the analyses demonstrate that for embankments with fissured clays, the mobilized strength can be as low as the average of its fully softened strength and its residual strength.

5.2 RECOMMENDATIONS

This thesis constitutes initial work done as part of assessing the stability of aging earth fill dams. Tests done are preliminary and require further testing to confirm the obtained parameters and

to understand further the cause of observed movement in one of the sections in Block Dam 2. However, in no case there was a breach of water from the fore bay. Engineers have undertaken design of remedial measures to prevent further movements. Instrumentation was added to monitor that section of the dam. Site personnel were trained in monitoring and surveillance.

The following works are recommended:

1) Highly plastic materials are prone to creep. Additional laboratory tests are required to understand the creep behavior of the *in-situ* materials.
2) Although gypsum is not the main cementing agent of the clayey materials in Block Dam 2, it would still be interesting to investigate the possible effects on strength of strain softening due to leaching of cementing agents in the clay blanket.
3) 2D plane strain numerical analyses using a coupled FEM stress analyses and LEM of slope stability analyses gives reasonable results. However, full FEM slope stability analysis may give better results, using a constitutive model that takes into account swelling, softening, and progressive yielding of the clay materials.

References

Acres International Limited. 2001. *Unpublished Report.*

Baracos, A. 1977. “Compositional and Structural Anisotropy of Winnipeg Soils - a Study Based on Scanning Electron Microscopy and X-Ray Diffraction Analyses.” *Canadian Geotechnical Journal* 14: 125–37.

Budhu, M. 2010. Soil Mechanics and Foundations 3rd ed. *Soil Mechanics and Foundations*.

Deer, W.A., Howie, R.A., Zusman, J. (1966). An Introduction to the Rock-Forming Minerals. *Mineralogy and Rocks.* Longmans. London.

Eid, Hisham T, and Timothy D Stark. 1998. “Undrained Shear Strength from Cone Penetration Test.” : 1021–25.

Fell, Robin; et al. 2015. CRC Press *Geotechnical Engineering of Dams, 2nd Ed*.

Freeman, W.S., and H.B. Sutherland. 1974. “Slope Stability Analysis in Anisotropic Winnipeg Clays.”

Garinger, Blair et al. 2004. 41 Canadian Geotechnical Journal *Instability of Dykes at Seven Sisters Generating Station*.

Graham, J. 1979. “Embankment Stability on Anisotropic Soft Clays.” *Canadian Geotechnical Journal* 16(1968): 295–308.

Graham, J, and V.C.S. Au. 1985. “Effects of Freeze-Thaw and Softening on a Natural Clay at Low Stresses.” *Canadian Geotechnical Journal* 22: 69–78.

Graham, J., and G.T. Houlsby. 1983. “(O-06) Anisotrophic Elasticity of a Natural Clay (Graham 1983).pdf.” *Geotechnique*.

Graham, J., and D.H. Shields. 1985. “(34) Influence of Geology and Geological Process on the Geotechnical Properties of a Plastic Clay (Graham and Shields, 1985).pdf.”

Hatch Ltd. 2010. *Unpublished report*.

Larsson, Rolf, and Helen Åhnberg. 2005. “On the Evaluation of Undrained Shear Strength and Preconsolidation Pressure from Common Field Tests in Clay.” *Canadian Geotechnical Journal* 42(4): 1221–31. http://www.nrcresearchpress.com/doi/abs/10.1139/t05-031 (January 10, 2015).

Loh, K.A., and R T Holt. 1974. “Directional Variation in Undrained Shear Strength and Fabric of Winnipeg Upper Brown Clay.” *Canadian Geotechnical Journal* 11(1974).

MacDonald, D.H., J. de Ruiter, and T.C. Kenney. 1961. “The Geotechnical Properties of Impervious Fill Materials in Some Canadian Dams.” In *Proceedings of the 5th International Conference on Soil Mechanics and Foundation Engineering*, , 657–62.

Man, Alex, and Jim Graham. 2010. “Pore Fluid Chemistry, Stress-Strain Behaviour, and Yielding

in Reconstituted Highly Plastic Clay." *Engineering Geology* 116(3-4): 296–310. http://linkinghub.elsevier.com/retrieve/pii/S0013795210001870 (May 30, 2014).

Man, Alex, Jim Graham, and James Blatz. 2011. "Seepage, Leaching, and Embankment Instability." *Canadian Geotechnical Journal* 48(3): 473–92. http://www.nrcresearchpress.com/doi/abs/10.1139/T10-083 (January 12, 2015).

McGown, Alan, and Amr M. Radwan. 1975. "The Presence and Influence of Fissures in the Boulder Clays of West Central Scotland." *Canadian Geotechnical Journal* 12: 84–97.

Mitchell, J. (1993). Fundamentals of Soil Behavior 2nd Ed. *Soil Mechanics.* Wiley. New York.

Rémai, Zsolt. 2013. "Correlation of Undrained Shear Strength and CPT Resistance." *Periodica Polytechnica Civil Engineering* 57(1): 39. http://www.pp.bme.hu/ci/2013_1/ci2013_1_05.html.

Rivard, P.J., and Y. Lu. 1978. "Shear Strength of Soft Fissured Clays'." *Canadian Geotechnical Journal* 15: 382–90.

Robertson, P. K. 2009. "Interpretation of Cone Penetration Tests — a Unified Approach." *Canadian Geotechnical Journal* 46(11): 1337–55. http://www.nrcresearchpress.com/doi/abs/10.1139/T09-065 (December 16, 2014).

Robertson, P.K. 1990. "Soil Classification Using the Cone Penetration Test." *Canadian*

Geotechnical Journal 27: 151–58.

Sellountou, E A, C Vipulanandan, and M W O Neill. 2000. *Estimation of Drained Shear Strength Parameters (c ' and φ ') of Beaumont Over-Consolidated Clay from Piezocone Data (CPTU).*

Shin, Young Jin, and Daehyeon Kim. 2011. "Assessment of Undrained Shear Strength Based on Cone Penetration Test (CPT) for Clayey Soils." *KSCE Journal of Civil Engineering* 15(7): 1161–66. http://link.springer.com/10.1007/s12205-011-0808-6 (May 30, 2014).

Skempton, A.W., F.R.S., and D.J. Petley. 1968. "(17) The Strength along Structural Discontinuities in Stiff Clays (Skempton and Petley).pdf." In *Proc. of Geotechnical Conference, Oslo*, , 29–46.

Skempton, A.W., F.R.S., R.L. Schuster, and D.J. Petley. 1969. "Joints and Fissures in the London Clay at Wraysbury and Edgware." *Geotechnique* 19(2): 205–17.

Stark, Timothy D., and Hisham T. Eid. 1997. "(5) Slope Stability Analysis in Stiff Fissured Clays." *Journal of Geotechnical and Geoenvironmental Engineering*.

Tan, K.H. (2005). Soil Sampling, Preparation, and Analysis. *Taylor and Francis.Boca raton, Florida.*

Tavenas, F., B. Trak, and S. Leroueil. 1980. "Remarks on the Validity of Stability Analyses."

Canadian Geotechnical Journal 17(1): 61–73. http://www.nrcresearchpress.com/doi/abs/10.1139/t80-006.

Vitone, C., F. Coetecchia, J. Desrues, and G. Viggiani. 2009. "An Approach to the Interpretation of the Mechanical Behaviour of Intensely Fissured Clays." *Soils and foundations* 49(3): 355–68.

Welton, E.J.. (1984). SEM Petrology Atlas. *American Association of Petroleum Geologists. Tusla, Okla.*

Yoshida, N, R Morgenstern, and D H Chan. 1991. "Finite-Element Analysis of Softening Effects in Fissured , Overconshlidatid Ckays and Mudstones." *Canadian Geotechnical Journal* 28(1977): 51–61.

Appendix A ***Drilling and Sampling Program.***

LOCATION		NO. OF BOREHOLES	BOREHOLE	SAMPLING DEPTH (m)	SAMPLING TYPE	NOTES
Block Dam No.2	Crest: U/S side	2	BH1/8	4	4" Shelby samples	*Clay core at 0.9 – 5.0m below grade;* ***VW piezometers to be installed in the clay core.***
	Crest: U/S side	1	BH2	4	4" Shelby samples	*Clay core at 0.9 – 5.0m below grade*
	U/S side slope	1	BH3	4	4" Shelby samples	*Clay core at 1.0 - 5.0m below grade;* ***VW piezometers to be installed in the clay core.***
	U/S side slope	1	BH7	4	4" Shelby samples	*Clay core at 1.0 - 5.0m below grade;* ***nested piezometers to be installed in the clay core and in the filter zone.***
	Upstream	18	PS1 – PS18	≈ 1	Piston samples	*Off-shore piston sampling (forebay)*
	Toe of the dam	1	BH4	-	Split spoon	*Overburden is typically 0.5-1.5m thick;* ***VW piezometer to be installed at 2.5m depth***
	Toe of the dam	1	BH5	≈ 2.2	4" Shelby samples	*Overburden is typically 0.5-1.5m thick*
	Toe of the dam	1	BH6	≈ 2.6	4" Shelby samples	*Clay foundation up to 2.2m depth;* ***nested piezometers to be installed at ≈1.5m and ≈2.3 m depths***
	2 - D/S, 1 - Crest	(3)	TP1 – TP3	1 - 3	test pit[2]	*Shelby tube samples will be obtained in each TP*
	5 – D/S, 7 - Crest	12	CP1 – CP12	-	n/a	*Profiles to be located next to borehole locations.*

FIELD TESTING/SAMPLING	TOTAL NO. OF BOREHOLES / TESTPITS
Boreholes: 4" Shelby Tube/Split spoon sampling	**8**
Boreholes: 3" Piston Tube/Split spoon sampling	**18**
Test Pits: 4" Shelby Tube[2] and Block sampling	**3**
Cone Penetration Testing	**12**

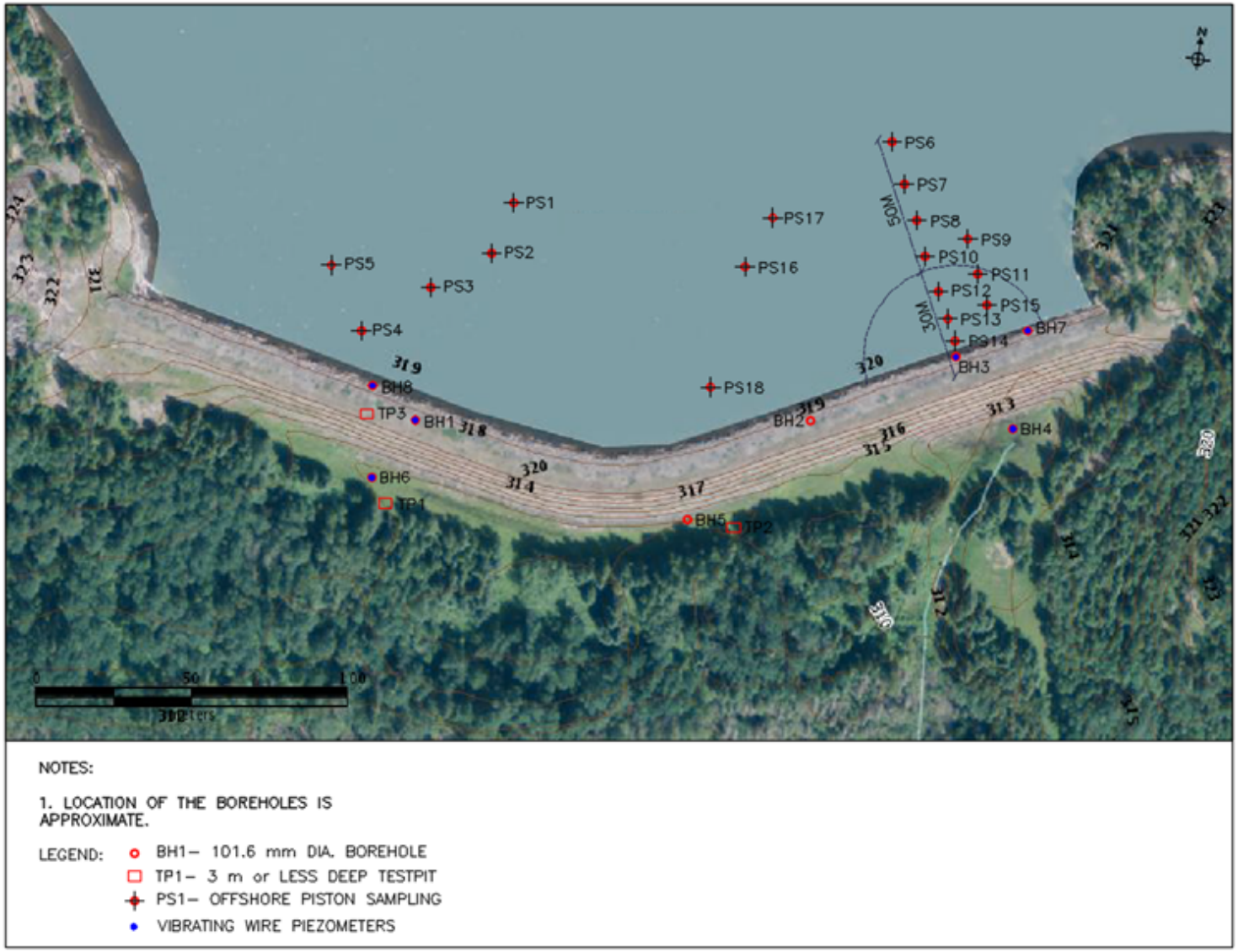

Appendix 1. Borehole and test pit location plan.

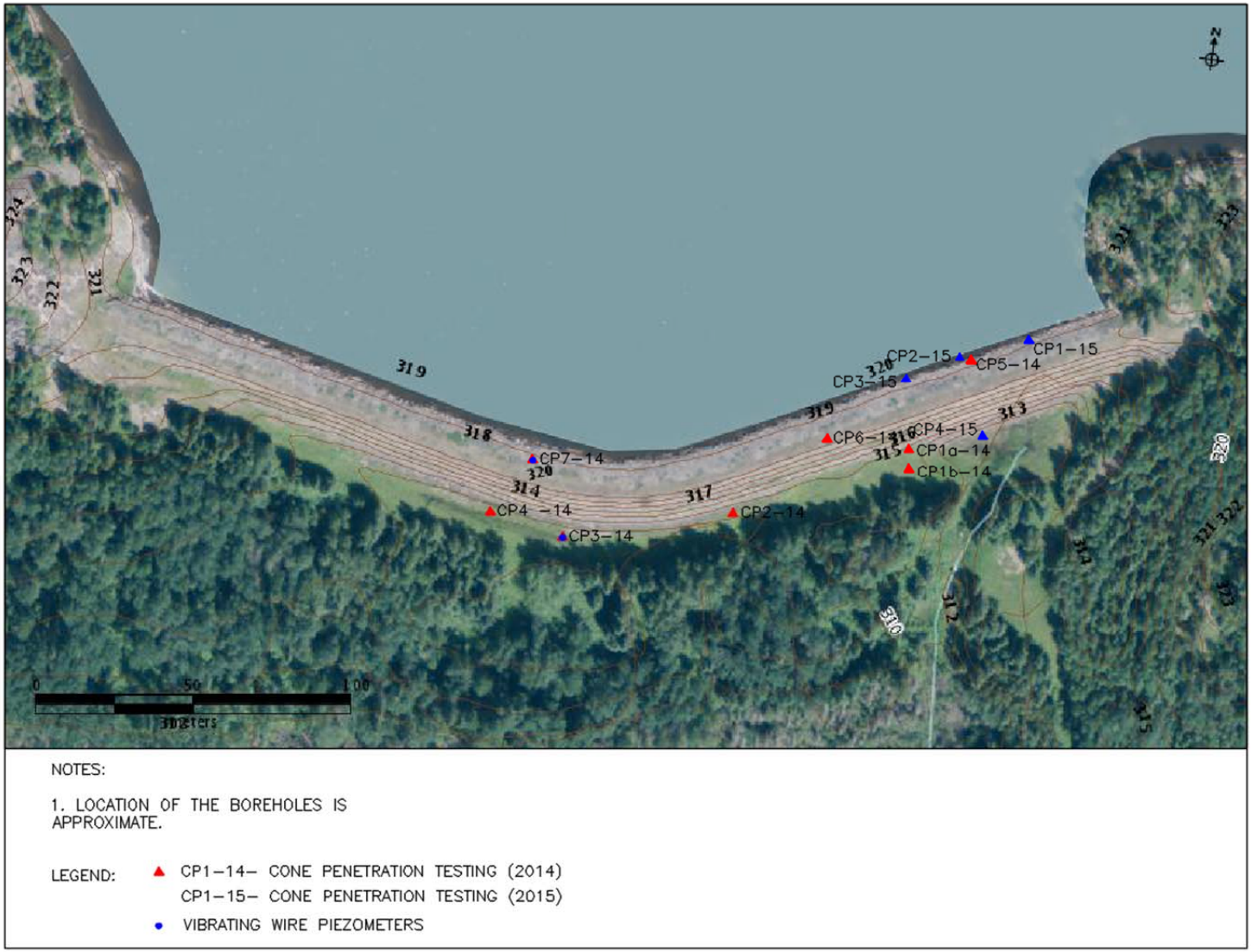

Appendix 2. CPTu borehole locations plan.

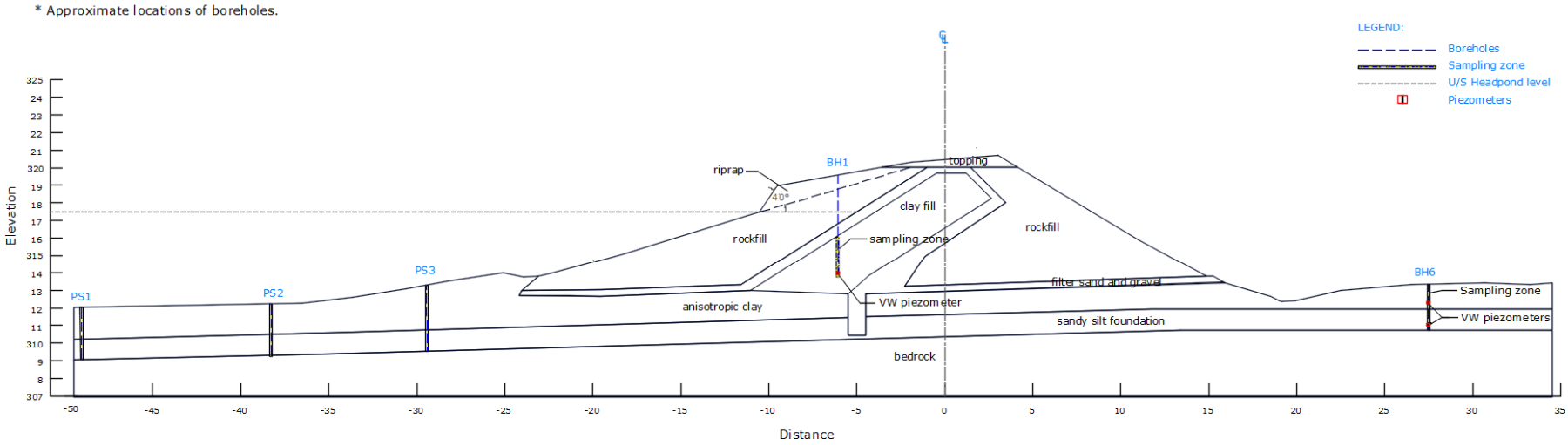

BLOCK DAM NO.2 SECTION A-A (Western section).

Appendix 3. Section A-A sampling and instrumentation profile.

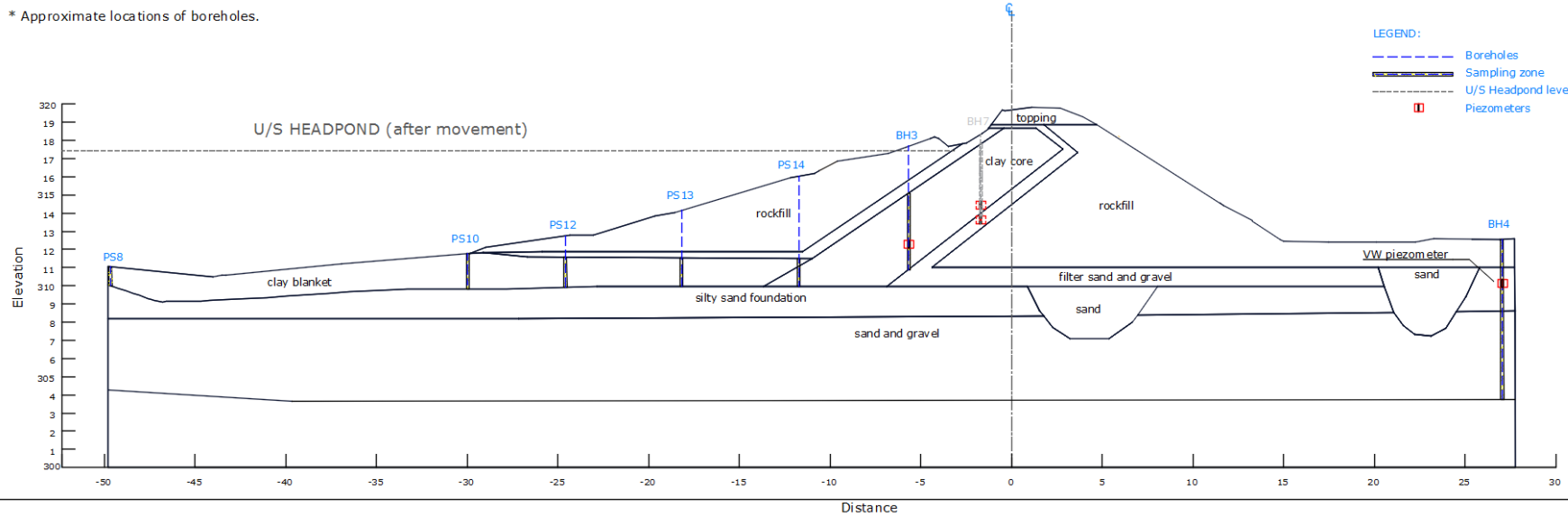

BLOCK DAM NO.2 SECTION B-B (Eastern section).

Appendix 4. Section B-B sampling and instrumentation profile.

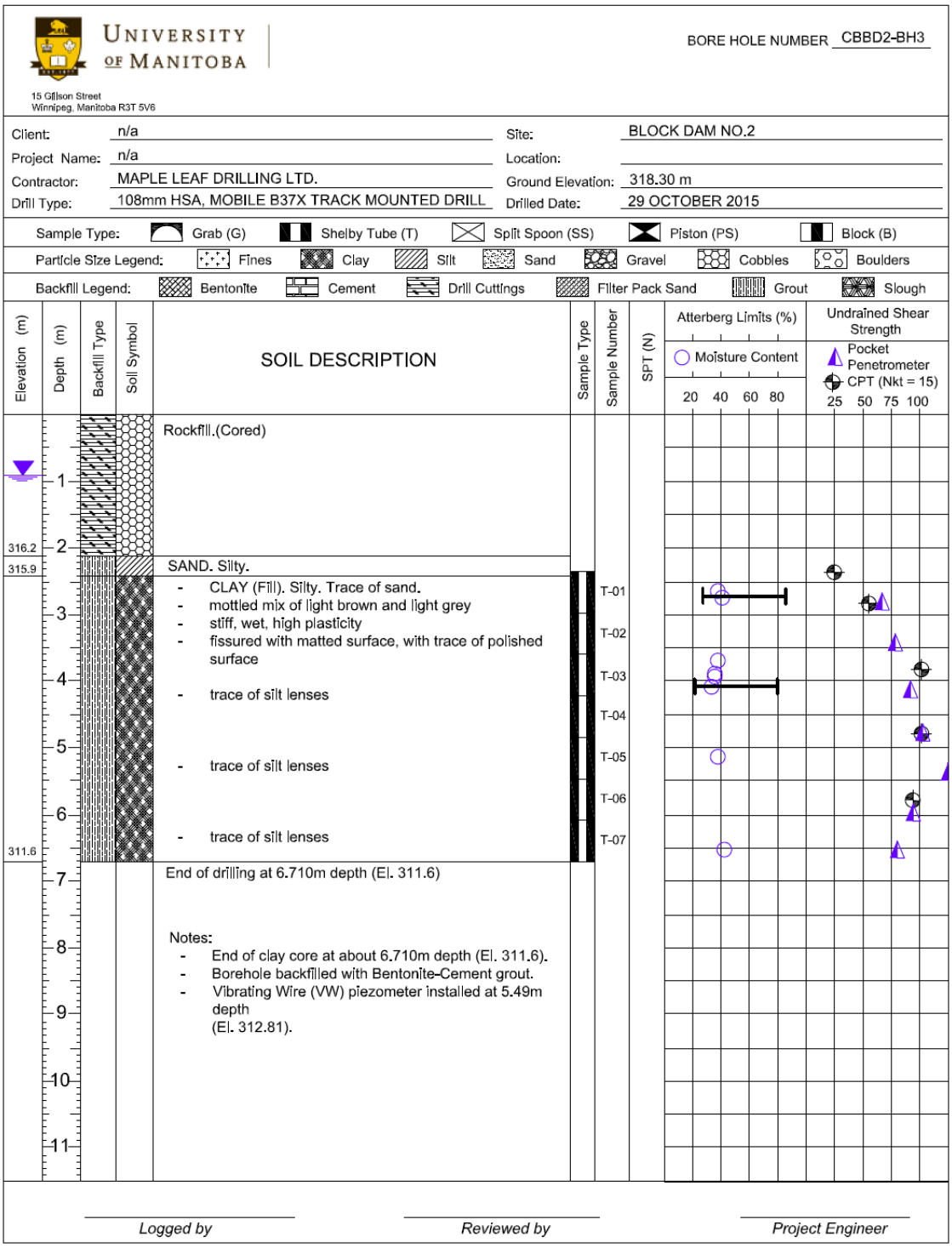

Appendix 5. Borehole log from clay core (BH3).

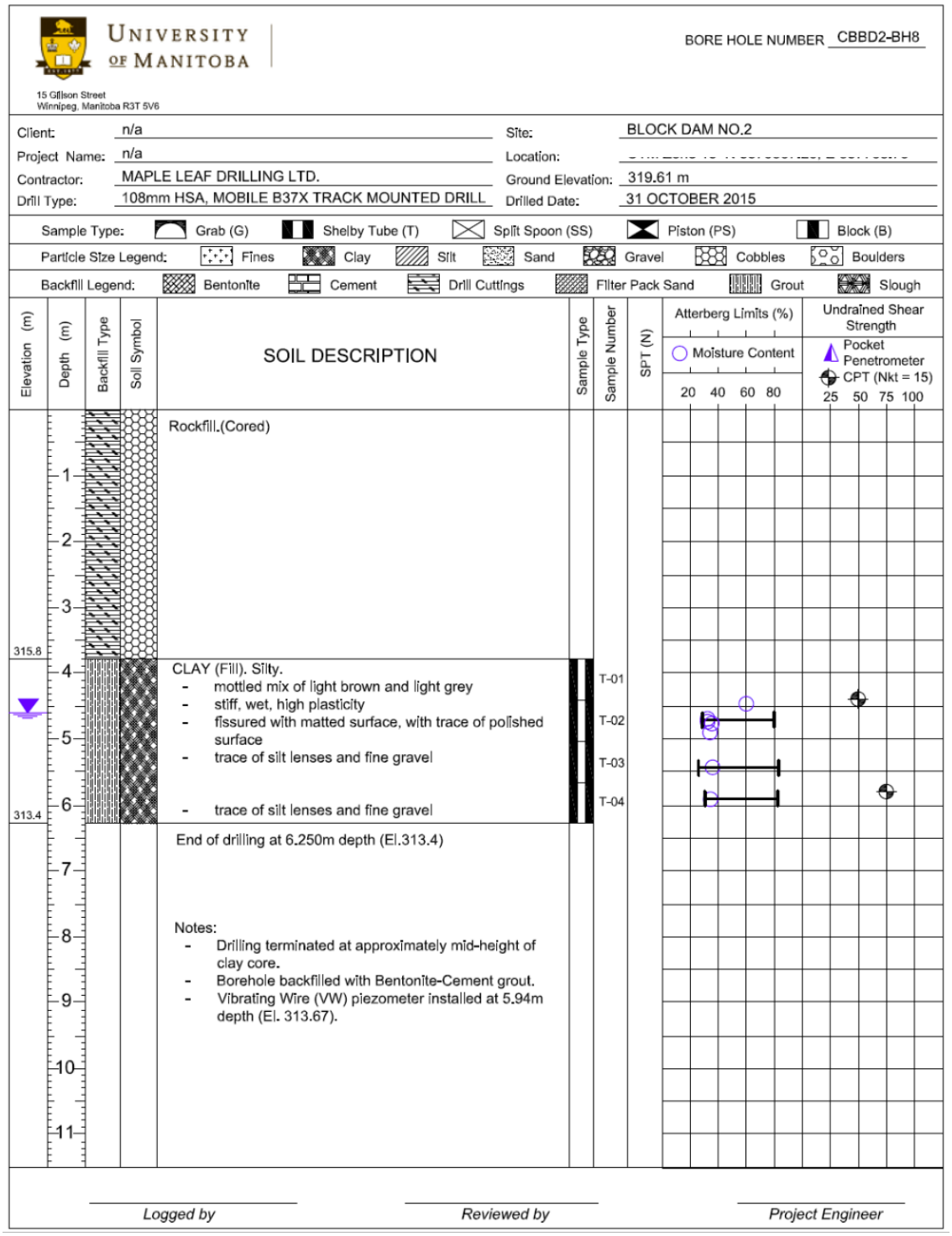

Appendix 6. Borehole log from clay core (BH8).

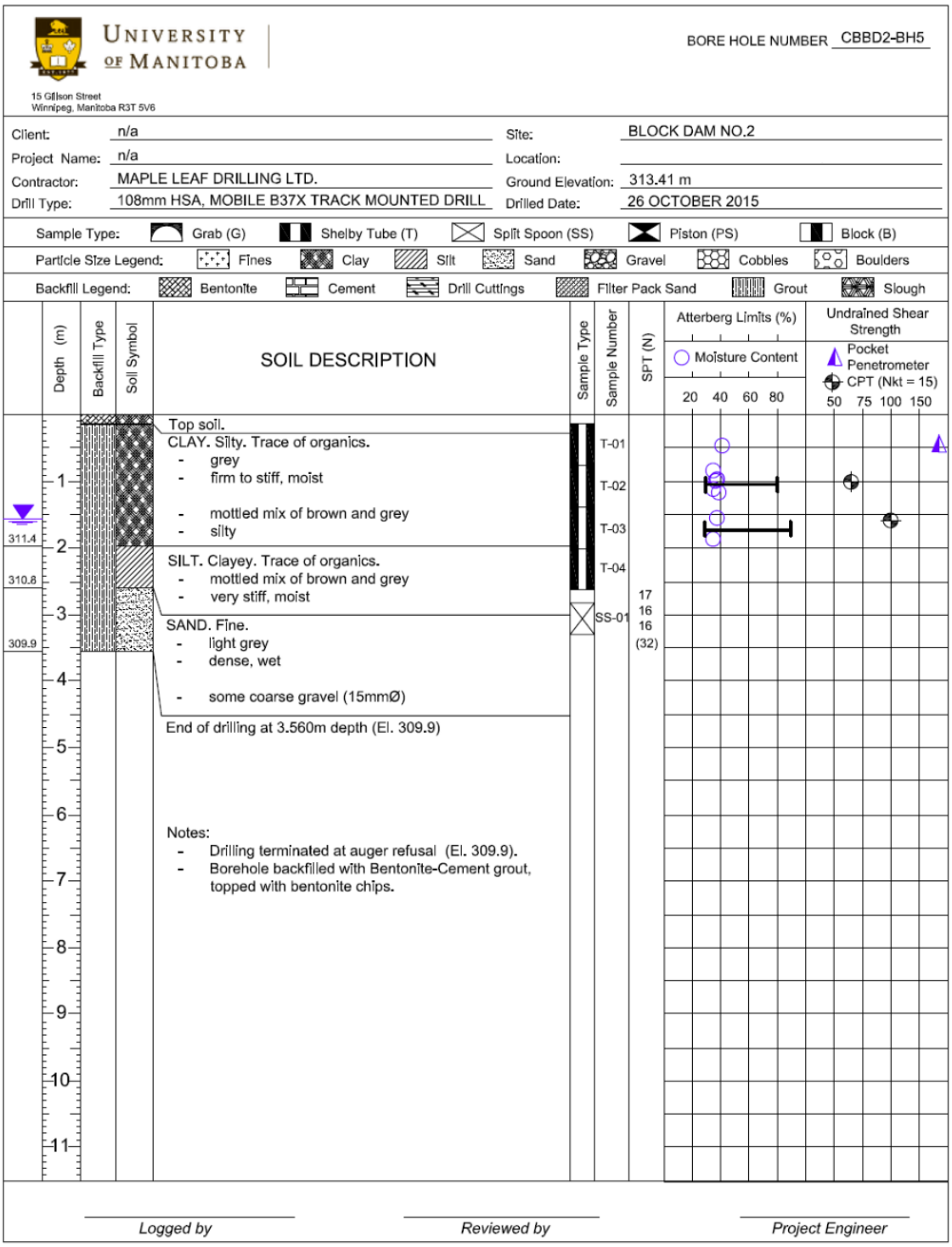

Appendix 7. Borehole log from clay foundation (BH5).

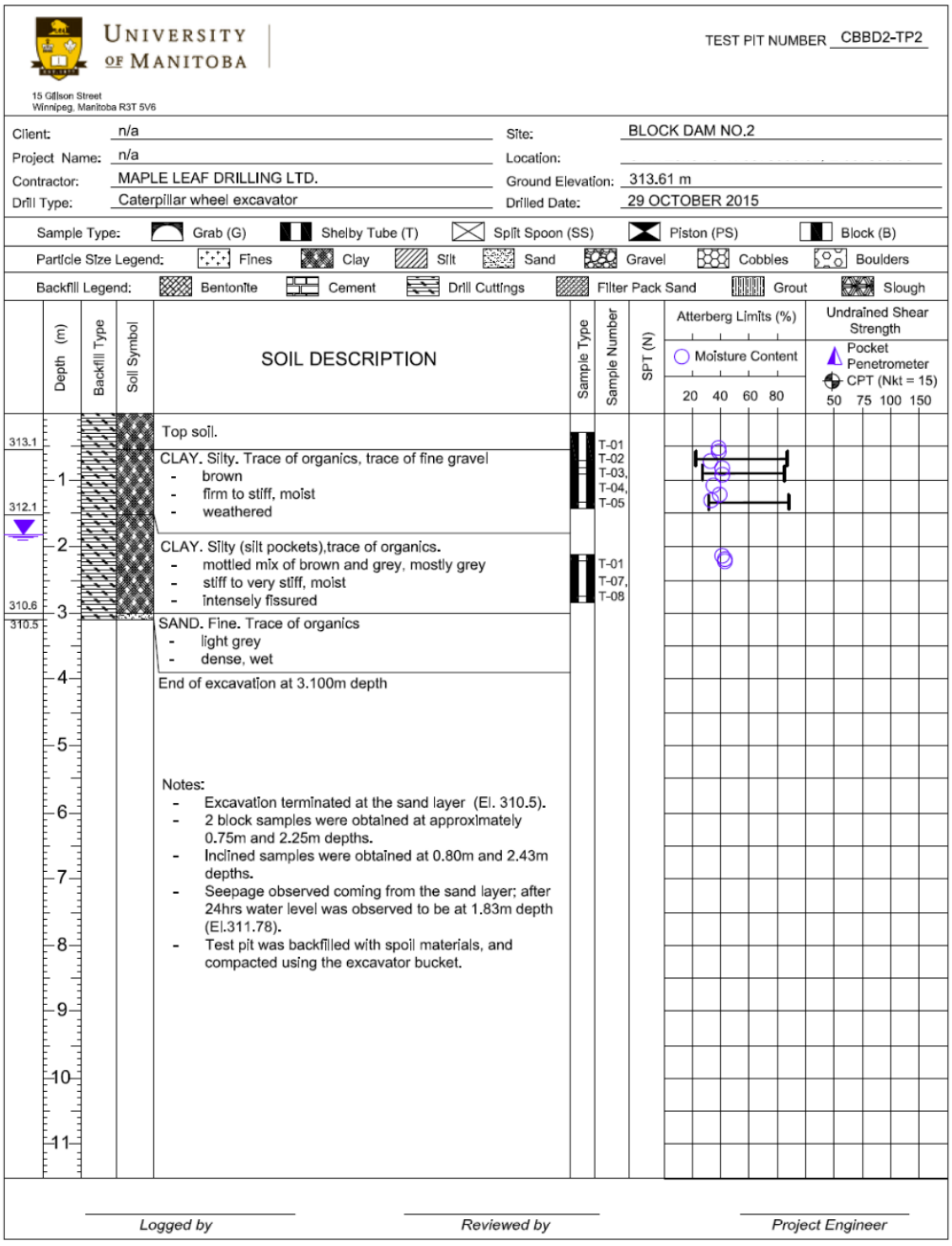

Appendix 8. Test pit log from clay foundation (TP2).

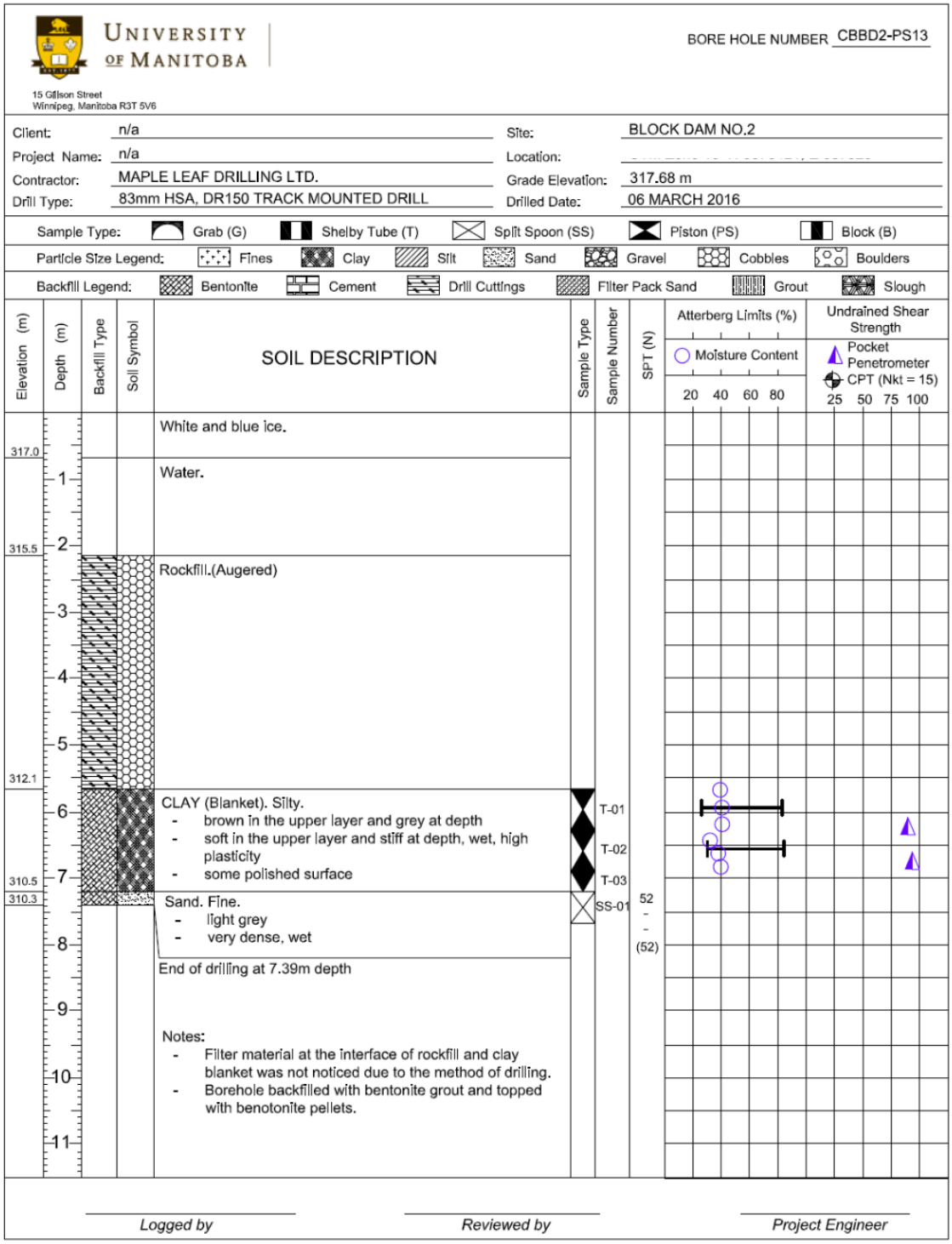

Appendix 9. Borehole log from clay blanket (PS13).

Appendix C ***X-Ray Diffraction Charts***

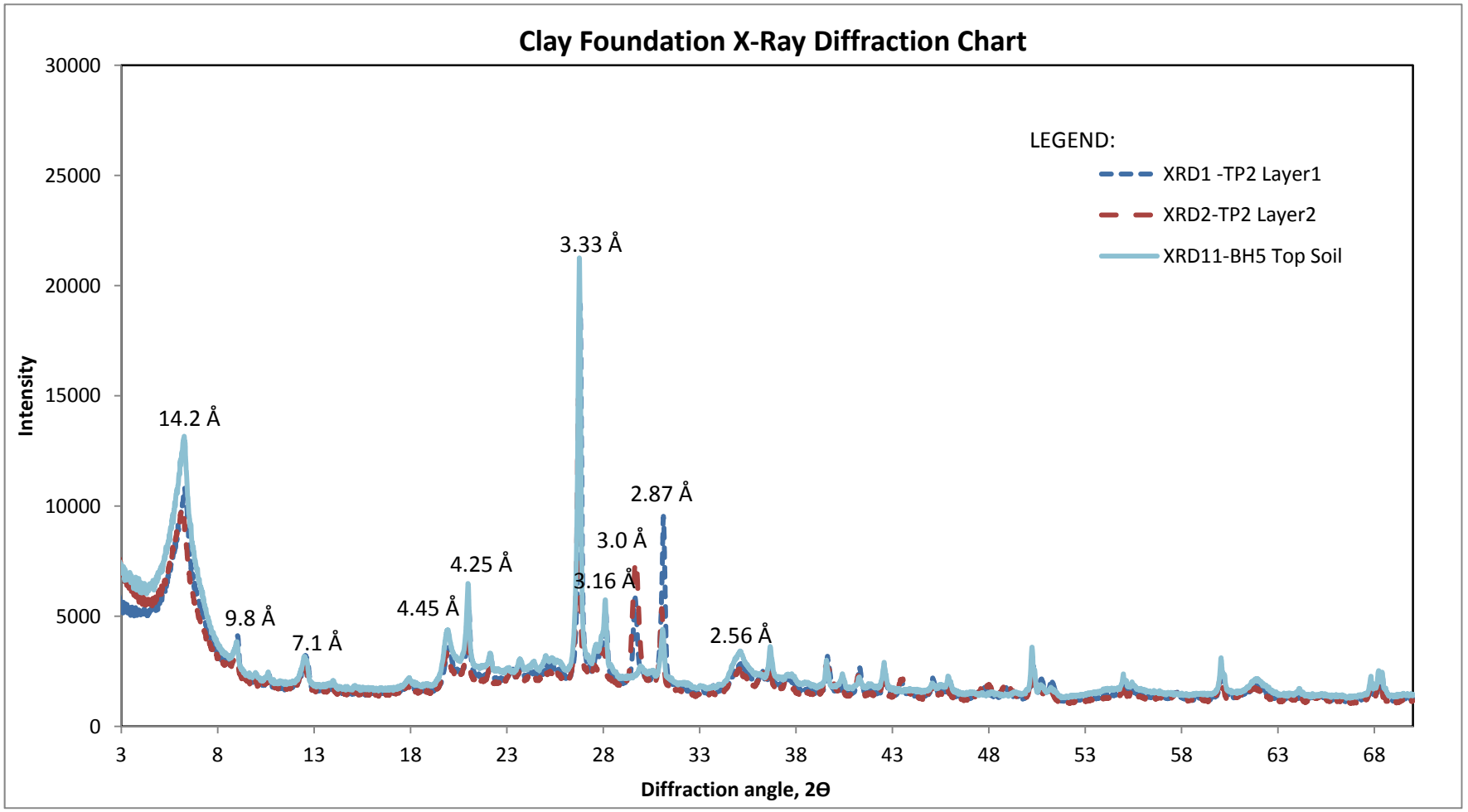

Appendix 10. X-ray diffraction chart of clay foundation samples.

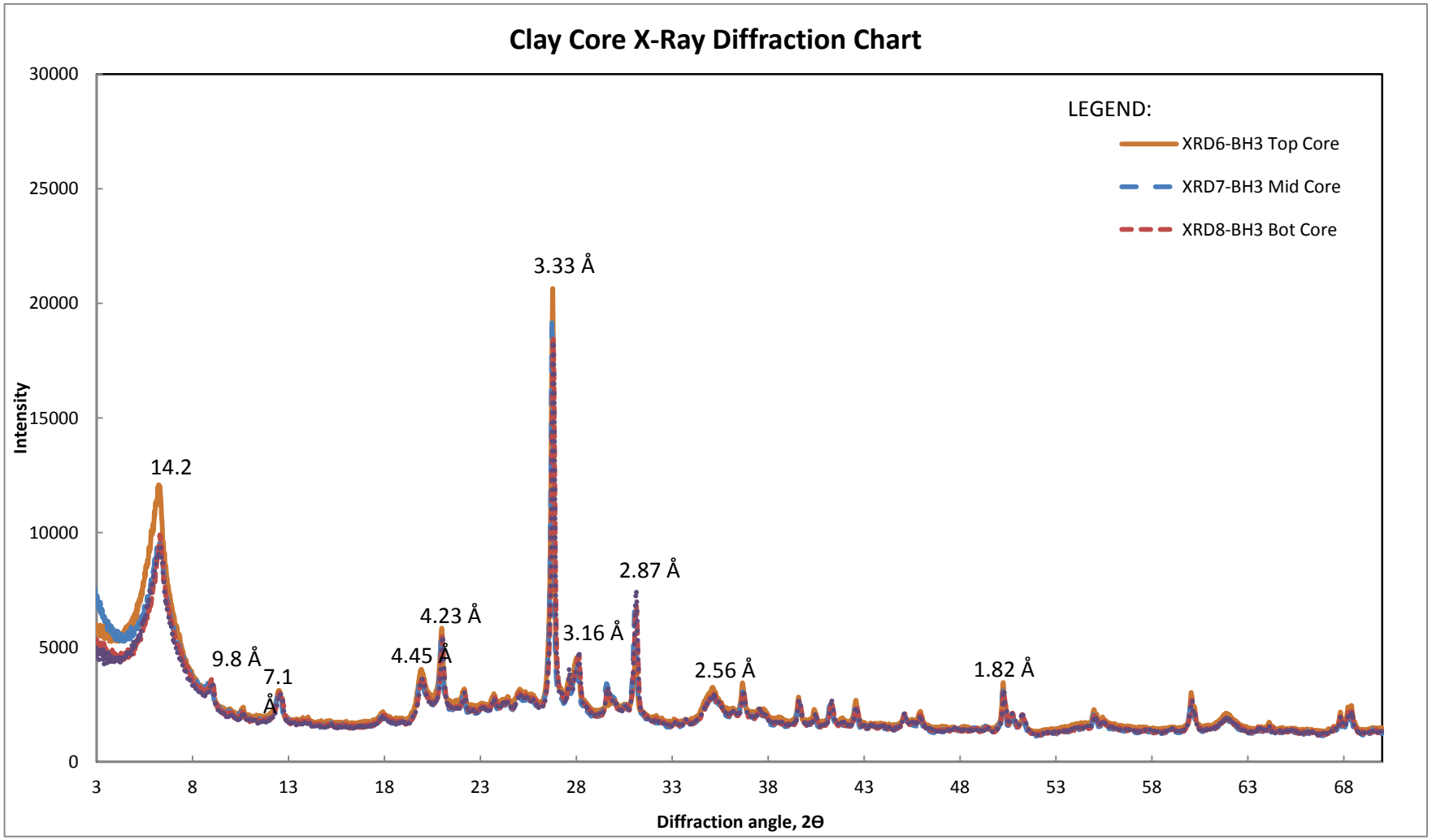

Appendix 11. X-ray diffraction chart of clay core samples.

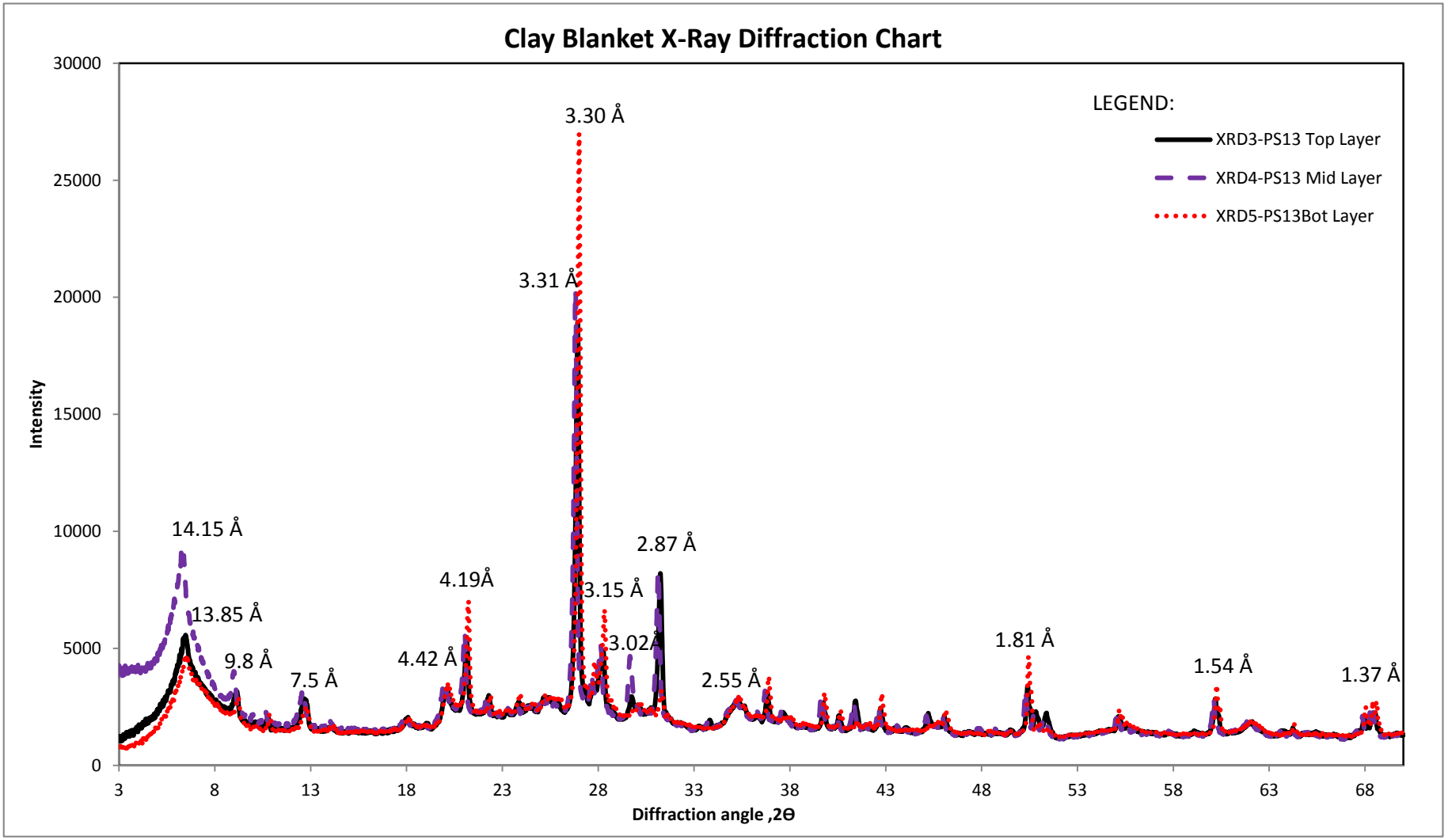

Appendix 12. X-ray diffraction chart of clay blanket samples.

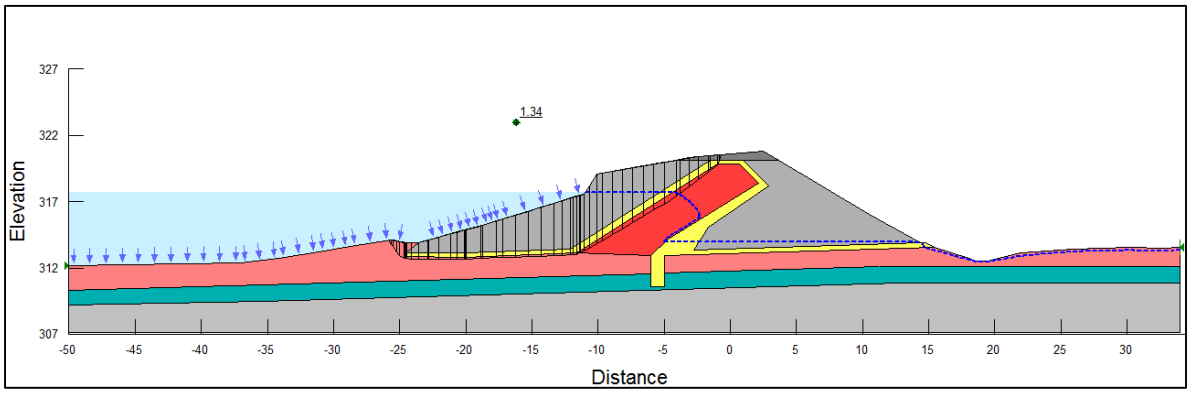

Appendix 13. Slope-stability analysis of Section A-A upstream slope, Case A.

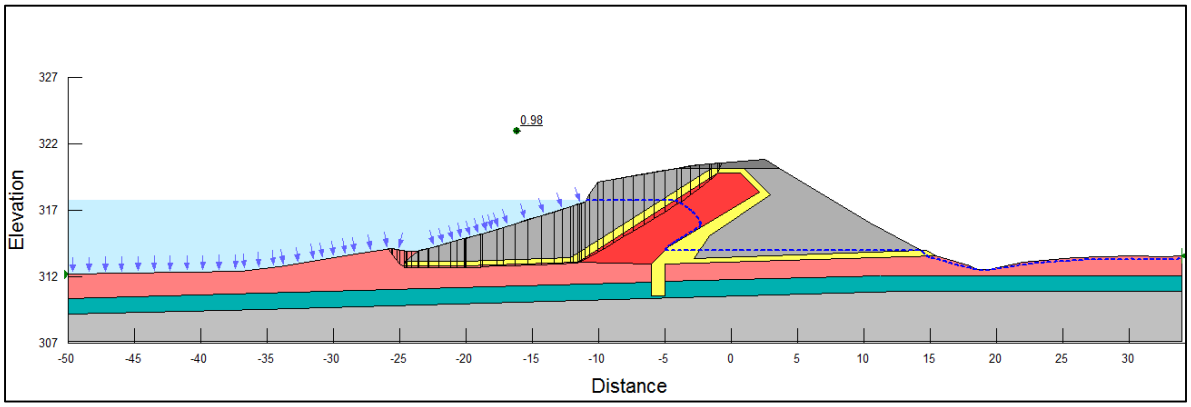

Appendix 14. Slope-stability analysis of Section A-A upstream slope, Case B.

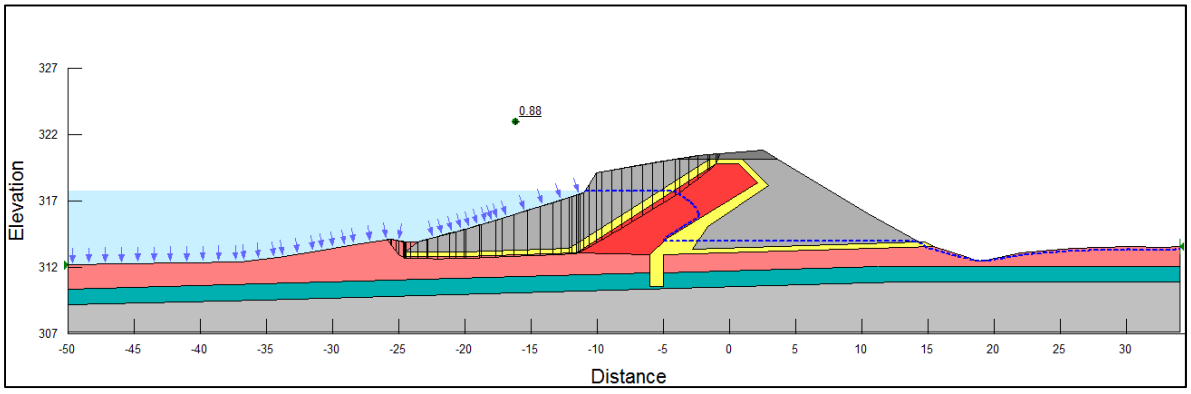

Appendix 15. Slope-stability analysis of Section A-A upstream slope, Case C.

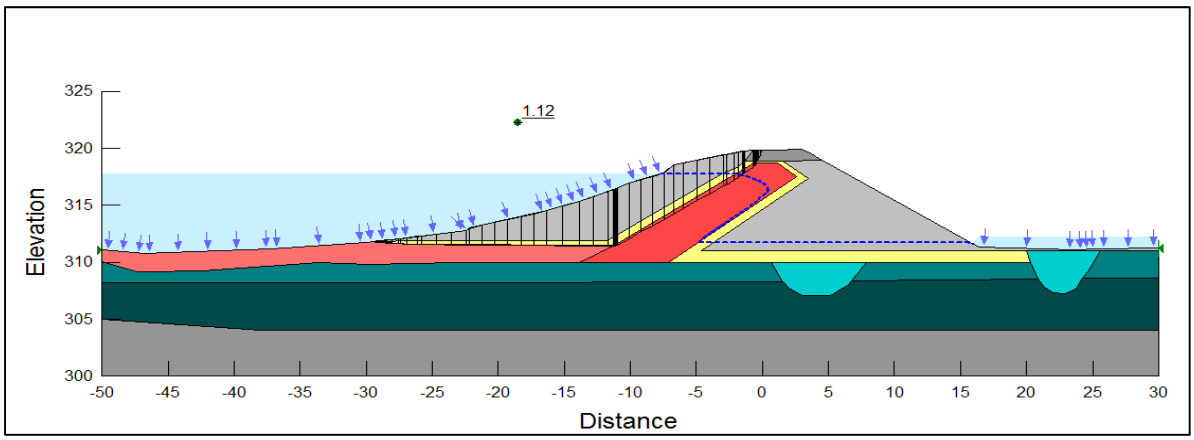

Appendix 16. Slope-stability analysis of Section B-B upstream slope, Case A.

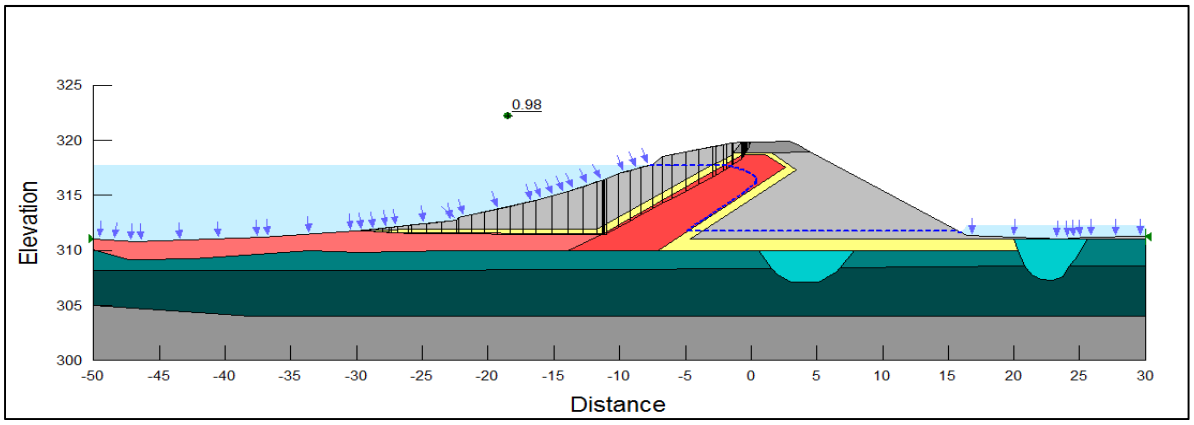

Appendix 17. Slope-stability analysis of Section B-B upstream slope, Case B.

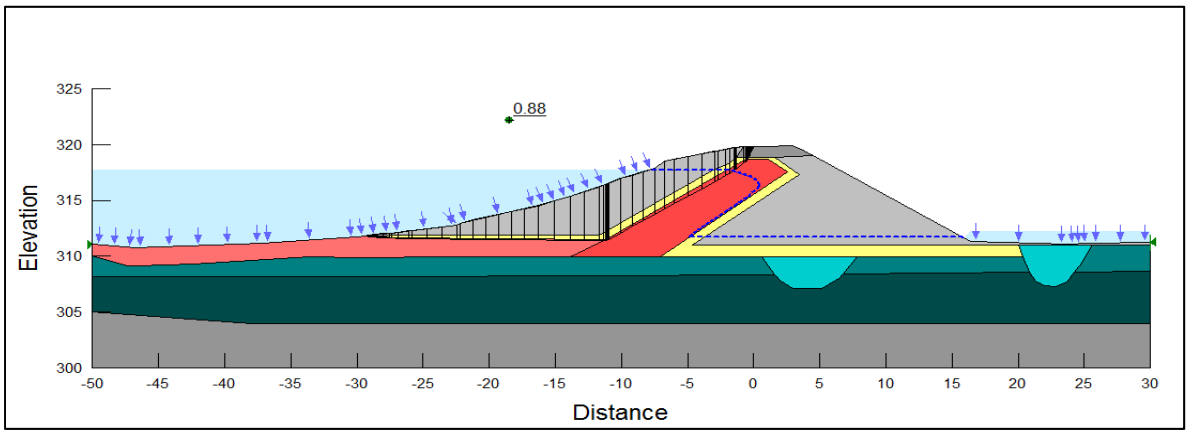

Appendix 18. Slope-stability analysis of Section B-B upstream slope, Case C.